Toblerols, Cyclopropanol-Containing Modulators of Methylobacterial Antibiosis Generated by an Unusual Polyketide Synthase

Supporting Information

Toblerols, Cyclopropanol-Containing Modulators of Methylobacterial Antibiosis Generated by an Unusual Polyketide Synthase

Reiko Ueoka, Miriam Bortfeld-Miller, Brandon I. Morinaka, Julia Vorholt, and Jörn Piel

Abstract *Trans*-AT polyketide synthases (PKSs) are a family of biosynthetically versatile modular type I PKSs that generate bioactive polyketides of impressive structural diversity. In this study, we detected in the genome of several bacteria a cryptic, architecturally unusual *trans*-AT PKS gene cluster that eluded automated PKS prediction. Genomic mining of one of these strains, the model methylotroph *Methylobacterium extorquens* AM1, revealed unique epoxide- and cyclopropanol-containing polyketides named toblerols. Relative and absolute stereochemistry were determined by NMR experiments, chemical derivatization, and the comparison of CD data between derivatized natural product and a synthesized model compound. Biosynthetic data suggest that the cyclopropanol moiety is generated by carbon-carbon shortening of a more extended precursor. Surprisingly, a knock-out strain impaired in polyketide production showed strong inhibitory activity against other methylobacteria in contrast to the wild-type producer. The activity was inhibited by complementation with toblerols, suggesting that these compounds modulate an as-yet unknown methylobacterial antibiotic.

Table of Contents

Experimental Procedures

General. LC-ESI mass spectrometry was performed on a Thermo Scientific Q Exactive mass spectrometer coupled to a Dionex Ultimate 3000 UPLC system. NMR spectra were recorded on a Bruker Avance III spectrometer equipped with a cold probe at 500 MHz and 600 MHz for ^{1}H NMR and 125 MHz and 150 MHz for ^{13}C NMR at 298K. Chemical shifts were referenced to the solvent peaks at δ_H 2.50 and δ_C 39.51 for DMSO-*d*$_6$, and δ_H 7.27 and δ_C 77.23 for chloroform-*d*.

Plasmid and strain construction. *E. coli* DH5α was used for cloning purposes and cultivated aerobically in LB-Lennox (1% tryptone, 0.5% yeast extract, 0.5% NaCl) at 37 °C. Experiments involving *Methylobacterium extorquens* AM1 were performed at 28 °C in minimal medium[1] supplemented with 5 ml methanol per liter (MM-Methanol medium). When appropriate, kanamycin was used at a concentration of 50 ug ml^{-1}.

For the generation of in-frame deletion mutants in *M. extorquens* AM1, a *sacB*-based allelic exchange method using pK18 mobsacB[2] was employed using the primers listed in Table S3. All DNA manipulations were performed according to standard protocols[3]. The genome sequence of *M. extorquens* AM1 is available[4].

Bacterial interaction screen. For the interaction screen, the strain to be tested for inhibition (*M. extorquens* AM1 WT and mutants) was grown for 10 to 14 days on solid MM-Methanol medium at room temperature. The sensitive strain to be tested (*Methylobacterium* sp. Leaf97 and Leaf101[5]) was grown at 28 °C over-night in liquid MM-Methanol medium to reach exponential phase. An aliquot of this culture (20 µl) was added to 20 ml MM-Methanol agar at 45 °C and poured into round Petri-dishes (8.5 cm). After 15 minutes, a full inoculating loop of the inhibitory strains was added on top of the solidified agar containing the sensitive strain. Zones of inhibition were determined after an incubation period of two to three days at 28 °C. To test if the inhibition zones can be complemented, pure compound from AM1 WT or extracts from AM1 WT and ΔtobC mutant strains were applied on top of the inhibitory strain (2 µl and 5 µl). Extracts for the assay were prepared from 350 mL cultures. After centrifugation, the supernatants were extracted with EtOAc, and dried. 200 µL of MeOH was added right before the assay.

Extraction and Isolation. 2 L of *M. extorquens* AM1 were cultured in default minimal medium with MeOH as a carbon source at 30 °C overnight on the shaker. The culture was centrifuged and the supernatant was extracted 3 times with EtOAc. The organic layer was dried and separated by RP-HPLC (Phenomenex Luna 5µ C18, ϕ 10 x 250 mm, 2.0 mL/min, 200 nm) with a gradient elution from 5% MeCN to 100% MeCN to afford 13 fractions (Fr.1-13). Fr.4 was further separated by RP-HPLC (Phenomenex Luna 5µ Phenyl-Hexyl, ϕ 10 x 250 mm, 1.0 mL/min, 200 nm) with 20% MeCN to obtain toblerol D (1.1 mg). Fr.5 was separated by RP-HPLC (Phenomenex Luna 5µ Phenyl-Hexyl, ϕ 10 x 250 mm, 2.0 mL/min, 200 nm) with 18% MeCN to obtain a mixture of toblerol E and F (0.7 mg) and the mixture of toblerol G and H (0.6 mg). Fr.6 was separated by RP-HPLC (Phenomenex Luna 5µ Phenyl-Hexyl, ϕ 10 x 250 mm, 2.0 mL/min, 200 nm) with 30% MeCN to afford toblerol A (0.8 mg) and toblerol B (1.0 mg). Fr.10 was separated by RP-HPLC (Phenomenex Luna 5µ C18, ϕ 10 x 250 mm, 2.0 mL/min, 200 nm) with 65% MeCN to obtain toblerol C (0.7 mg).

Toblerol A (1): colorless oil; ^{1}H NMR (DMSO-*d*$_6$) and ^{13}C NMR (DMSO-*d*$_6$) data, see Table S4; HRESIMS *m/z* 251.1251 (calcd for $C_{12}H_{20}O_4Na$, 251.1254).

Toblerol B (2): colorless oil; ^{1}H NMR (DMSO-d_6) and ^{13}C NMR (DMSO-d_6) data, see Table S4; HRESIMS *m/z* 279.1198 (calcd for $C_{13}H_{20}O_5Na$, 279.1203).

Toblerol C (3): colorless oil; ^{1}H NMR (DMSO-d_6) and ^{13}C NMR (DMSO-d_6) data, see Table S5; HRESIMS *m/z* 211.1678 (calcd for $C_{13}H_{23}O_2$, 211.1693).

Toblerol D (4): colorless oil; ^{1}H NMR (DMSO-d_6) and ^{13}C NMR (DMSO-d_6) data, see Table S5; HRESIMS *m/z* 267.1187 (calcd for $C_{12}H_{20}O_5Na$, 267.1203).

The mixture of toblerol E (5) and F (6): colorless oil; ^{1}H NMR (DMSO-d_6) and ^{13}C NMR (DMSO-d_6) data, see Table S6; HRESIMS *m/z* 303.0952 (calcd for $C_{12}H_{21}O_5ClNa$, 303.0970) for toblerol E (**5**); HRESIMS *m/z* 251.1248 (calcd for $C_{12}H_{20}O_4Na$, 251.1254) for toblerol F (**6**).

The mixture of toblerol G (7) and H (8): colorless oil; ^{1}H NMR (DMSO-d_6) and ^{13}C NMR (DMSO-d_6) data, see Table S7; HRESIMS *m/z* 303.0953 (calcd for $C_{12}H_{21}O_5ClNa$, 303.0970) for toblerol G (**7**); HRESIMS *m/z* 253.1408 (calcd for $C_{12}H_{22}O_4Na$, 253.1410) for toblerol H (**8**).

Structure elucidation of toblerol A (1). Toblerol A (**1**) had a predicted molecular formula of $C_{12}H_{20}O_4$, as determined by HR-ESIMS spectroscopy (Figure S2). The ^{1}H NMR and HSQC spectra suggested that there were two epoxides and one cyclopropane ring (Figure S3-4). COSY correlations showed three units **a-c** (Figure S5). HMBC correlations from H-1 to C-3, from H-2 to C-3 and C-4, and from H-3 to C-2 deduced the connection between unit **a** and unit **b** (Figure S6). Unit **b** and unit **c** were connected because of HMBC cross peaks from H-6 to C-4 and C-5. The cyclopropanol moiety in unit **c** was determined by HMBC correlations from H-9 to C-12, from H-10 to C-12, from H-12 to C-9, and from OH-12 to C-10, C-11 and C-12. 5,6- and 7,8-epoxides were determined by their typical chemical shifts and remaining atoms according to the molecular formula. The small coupling constant of H-5 and H-6 ($^{3}J_{H5,H6}$ = 2.2 Hz) and the large coupling constant of H-7 and H-8 ($^{3}J_{H7,H8}$ = 4.4 Hz) suggested a *trans*- and *cis*-epoxide, respectively (Table S4). NOESY correlation between H-3 and H-5, between H-4 and H-6, between H-5 and H-7, and between H-6 and H-9 also supported the relative stereochemistry of epoxides (Figure S7). The relative stereochemistry of cyclopropanol was determined to be *trans* based on NOESY correlations between H-9 and H-11a, between H-9 and H-12, between H-10 and H-11b, and between H-11a and H-12.

Structure elucidation of toblerol B (2). Toblerol B (**2**) had a predicted molecular formula of $C_{13}H_{20}O_5$, as determined by HR-ESIMS spectroscopy (Figure S9). The ^{1}H NMR and HSQC spectra suggested that **2** had an additional formyl group compared to **1** (Figure S10-11). COSY correlations showed three units **a-c** (Figure S12). HMBC correlations from H-1 to C-3 and from H-2 to C-3 and C-4 revealed the connection between unit **a** and unit **b** (Figure S13). Unit **b** and unit **c** were connected because of HMBC cross peaks from H-5 to C-6 and C-7, and from H-6 to C-4 and C-5. The formyl group was attached to unit **c**, which was determined by HMBC correlations from H-12 to C-13 and from H-13 to C-12. 5,6- and 7,8-epoxides were determined by their typical chemical shifts and remaining atoms according to the molecular formula. The small coupling constant of H-5 and H-6 ($^{3}J_{H5,H6}$ = 2.3 Hz) and the large coupling constant of H-7 and H-8 ($^{3}J_{H7,H8}$ = 4.4 Hz) suggested a *trans*- and *cis*-epoxide, respectively (Table S4). NOESY correlations between H-4 and H-6, between H-5 and H-7, between H-6 and H-9, and between H-7 and H-8 also supported the relative stereochemistry of epoxides (Figure S14). The relative stereochemistry of the cyclopropane ring was determined to be *trans* based on strong NOESY

correlations between H-9 and H-11a, between H-9 and H-12, between H-10 and H-11b, and between H-11a and H-12, as well as the small coupling constant of H-10 and H-12 ($^3J_{H10,H12}$ = 2.8 Hz).

Structure elucidation of toblerol C (3). Toblerol C (**3**) had a predicted molecular formula of $C_{13}H_{22}O_2$, as determined by HR-ESIMS spectroscopy (Figure S15). The ^{1}H NMR and HSQC spectra suggested that **3** had a double bond and a cyclopropane ring (Figure S16-17). COSY correlations showed two units **a** and **b** (Figure S18). The cyclopropanoic acid moiety was determined by HMBC cross peaks from H-9 to C-12, and from H-11 to C-13 (Figure S19). The length of the CH_2 chain between unit **a** and unit **b** was determined by its molecular formula. The small coupling constant of H-7 and H-8 ($^3J_{H7,H8}$ = 11.4 Hz) suggested *Z* geometry (Table S5). The relative stereochemistry of the cyclopropane ring was determined to be *trans* based on strong NOESY correlations between H-9 and H-11a, between H-9 and H-12, between H-10 and H-11b, and between H-11a and H-12 (Figure S21).

Structure elucidation of toblerol D (4). Toblerol D (**4**) had a predicted molecular formula of $C_{12}H_{20}O_5$, as determined by HR-ESIMS spectroscopy (Figure S22). The ^{1}H NMR and HSQC spectra suggested that **4** had one epoxide unit (Figure S23-24). COSY correlations showed three units **a-c** (Figure S25). HMBC correlations from H-1 to C-3, from H-2 to C-3 and C-4, from H-3 to C-2, and from H-4 to C-2 revealed the connection between unit **a** and unit **b** (Figure S26). Unit **b** and unit **c** were connected because of HMBC cross peaks from H-5 to C-6 and C-7, and from H-6 to C-4 and C-5. The presence of the epoxide between unit **b** and unit **c** was determined by the typical chemical shifts for epoxides. The carboxyl group was attached to C-10 in unit **c** based on the HMBC correlations from H-9 to C-12, from H-10 to C-12, and from H-11 to C-12. Finally, the molecular formula suggested the connection of C-8 and C-12 to form a lactone ring. The small coupling constant of H-5 and H-6 ($^3J_{H5,H6}$ = 2.4 Hz) suggested a *trans*-epoxide (Table S5). NOESY correlations between H-4 and H-6, between OH-4 and H-6, between H-5 and OH-7 also supported the relative stereochemistry of the epoxide (Figure S28). The relative stereochemistry of the lactone ring was determined based on NOESY correlations between H-7 and H-9a, between OH-7 and H-9a, between H-8, H-9b and H-10, and between H-9a and H-11.

Structure elucidation of toblerol E (5). Toblerol E (**5**) had a predicted molecular formula of $C_{12}H_{21}O_5Cl$, as determined by HR-ESIMS spectroscopy (Figure S29). COSY correlations showed three units **a-c** (Figure S33). HMBC correlations from H-1 to C-3, from H-2 to C-3, and from H-3 to C-2 revealed the connection between unit **a** and unit **b** (Figure S34). Unit **b** and unit **c** were connected because of HMBC cross peaks from OH-6 to C-7, and from OH-7 to C-6. The carboxyl group was attached to C-10 in unit **c** based on the HMBC correlations from H-9 to C-12, from H-10 to C-12, and from H-11 to C-12. The molecular formula and the chemical shifts suggested the connection of C-8 and C-12 to form a lactone ring, and the position of the remaining chloride to be C-5. The relative stereochemistry of the lactone ring was determined based on NOESY correlations between H-7 and H-9a, and between H-8, H-9b and H-10 (Figure S35).

Structure elucidation of toblerol F (6). Toblerol F (**6**) had a predicted molecular formula of $C_{12}H_{20}O_4$, as determined by HR-ESIMS spectroscopy (Figure S41). The ^{1}H NMR and HSQC spectra suggested the presence of one double bond (Figure S31-32). COSY correlations showed three units **a-c** (Figure S33). Unit **a** and unit **c** were connected via one methylene and unit **b** by HMBC correlations from H-1 to C-3, from H-2 to C-3, from H-3 to C-2 and C-4, from OH-4 to C-3, from H-5 to C-3 and C-4, and from OH-5 to C-4 (Figure S34). The carboxyl group was attached to C-10 in unit **c** based on the HMBC correlations from H-9 to C-12, from H-10 to C-12, and from H-11 to C-12. The molecular formula suggested the connection of C-8 and C-12 to form a lactone ring. The *E* geometry of the double bond in unit **c** was determined by the large coupling constants ($^3J_{H6,H7}$ = 15.8 Hz) (Table S6). The relative

stereochemistry of lactone ring was determined based on NOESY correlations between H-7 and H-9a, and between H-8, H-9b and H-10 (Figure S35).

Structure elucidation of toblerol G (7). Toblerol G (**7**) had a predicted molecular formula of $C_{12}H_{21}O_5Cl_1$, as determined by HR-ESIMS spectroscopy (Figure S30). COSY correlations showed three units **a-c** (Figure S38). HMBC correlations from H-1 to C-3, from H-2 to C-3, from H-3 to C-2, and from H-4 to C-2 revealed the connection between unit **a** and unit **b** (Figure S39). Unit **b** and unit **c** were connected because of HMBC cross peaks from H-4 to C-5, from OH-4 to C-5, from H-5 to C-3, from OH-5 to C-4, and from H-6 to C-4. The carboxyl group was attached to C-10 in unit **c** based on the HMBC correlations from H-9 to C-12, from H-10 to C-12, and from H-11 to C-12. The molecular formula and the chemical shifts suggested the connection of C-8 and C-12 to form a lactone ring, and the position of the remaining chloride to be C-6. The relative stereochemistry of the lactone ring was determined based on NOESY correlations between H-7 and H-9a, between H-8, H-9b and H-10, and between H-9a and H-11 (Figure S40).

Structure elucidation of toblerol H (8). Toblerol H (**8**) had a predicted molecular formula of $C_{12}H_{22}O_4$, as determined by HR-ESIMS spectroscopy (Figure S42). The ^{1}H NMR and HSQC spectra suggested that there was one cyclopropane ring (Figure S36-37). COSY correlations showed three units **a-c** (Figure S38). HMBC correlations from H-1 to C-3, from H-2 to C-3, from H-3 to C-2, and from H-4 to C-2 revealed the connection between unit **a** and unit **b** (Figure S39). Unit **b** and unit **c** were connected because of HMBC cross peaks from H-5 to C-7, from OH-6 to C-7, from H-7 to C-6, from H-8 to C-6, from OH-8 to C-7, and from H-9 to C-7. The cyclopropanol moiety in unit **c** was determined by HMBC correlations from H-9 to C-12, and from OH-12 to C-10. An ether ring in unit **b** was determined by chemical shifts and remaining atoms according to molecular formula. The relative stereochemistry of the cyclopropanol moiety was determined to be *trans* based on the small coupling constant of H-10 and H-12 ($^3J_{H10,H12}$ = 2.6 Hz) and the strong NOESY correlations between H-9 and H-11a, between H-9 and H-12, between H-10 and H-11b, between H-10 and OH-12, between H-11a and H-12, and between H-11b and OH-12 (Table S7 and Figure S40). The relative stereochemistry of the ether ring was also determined by the NOESY cross peaks between H-4 and H-5b, between H-4 and H-7, between H-5a and H-6, between H-5b and OH-6, and between H-6 and H-8.

Preparation of MTPA esters 2b and 2c. Toblerol B (**2**; 0.2 mg each) was reacted with *R*-(-)- or *S*-(+)-MTPACl (5 μL) in 100 μL of CH_2Cl_2 containing 1 mg of DMAP for 1 h. The mixture was partitioned between 0.1 M $NaHCO_3$ and CH_2Cl_2. The CH_2Cl_2 layer was washed with 0.1 M HCl and H_2O, then the CH_2Cl_2 layer was concentrated and separated by RP-HPLC (Phenomenex Luna 5μ C18, ϕ 10 x 250 mm, 2.0 mL/min, 200 nm) with a gradient elution from 5% MeCN to 100% MeCN to afford *S*-(-)-MTPA ester **2b** and *R*-(+)-MTPA ester **2c**, respectively (Figure S43-51).

^{13}C-feeding experiment of toblerol D (4). MM-medium (without MeOH) was supplemented with 10 mM sodium acetate and 2 mM 2-^{13}C or 1,2-$^{13}C_2$ sodium acetate respectively. 600 mL of *M. extorquens* AM1 WT strain was cultured at 30 °C 2 days on the shaker. Each culture was extracted and separated as described in extraction and isolation section.

Derivatization of toblerol A (1) to toblerol H (8). Toblerol A (**1**; 0.6 mg) was reacted with 80 μL of Red-Al in 0.5 mL of dry THF and stirred at -20 °C for 3 days. After the mixture was poured into sodium potassium tartrate solution, it was extracted with Et_2O.The extract was measured by LCMS (Figure S52) and NMR (Figure S53-55).

Extraction and Isolation of 13 and 14. 5L of the Δ*tobL* strain was cultured in default minimal medium with MeOH as a carbon source at 30 °C overnight on the shaker. Culture was centrifuged and supernatant was extracted 3 times with EtOAc. The organic layer was dried and separated by RP-HPLC (Phenomenex Luna 5μ C18, ϕ 10 x 250 mm, 2.0 mL/min, 200 nm) with a gradient elution from 5% MeCN to 100% MeCN to afford 13 fractions (Fr.1-13). Fr.10 was separated by RP-HPLC (Phenomenex Kinetex 5μ C18, ϕ 10 x 250 mm, 2.0 mL/min, 200 nm) with 60% MeCN + 0.1% formic acid to obtain **13**. Fr.6 was further separated by RP-HPLC (Phenomenex Luna 5μ Phenyl-Hexyl, ϕ 10 x 250 mm, 1.0 mL/min, 200 nm) with 30% MeCN to obtain **14**.

Structure elucidation of 13. 13 had a predicted molecular formula of $C_{12}H_{22}O_2$, as determined by HR-ESIMS spectroscopy (*m*/*z* 199.1695 $[M+H]^+$) (Figure S78). The ^{1}H NMR and HSQC spectra suggested that **11** had a double bond (Figure S79-80). COSY correlations showed two units **a** and **b** (Figure S81). The carboxyl group was connected to unit **b** based on HMBC cross peaks from H-9, H-10 and H-11 to C-12 (Figure S82). The length of CH_2 chain between unit **a** and unit **b** was determined by its molecular formula. The small coupling constant of H-7 and H-8 ($^3J_{H7,H8}$ = 11.0 Hz) suggested *Z* geometry (Table S8).

Structure elucidation of 14. 14 had a predicted molecular formula of $C_{12}H_{24}O_3$, as determined by HR-ESIMS spectroscopy (*m*/*z* 239.1625 $[M+Na]^+$) (Figure S83). The ^{1}H NMR and HSQC spectra suggested that there was one cyclopropane ring (Figure S84-85). COSY correlations showed two units **a** and **b** (Figure S86). HMBC correlations from H-1 to C-3 and from H-2 to C-3 elongated one methylene from unit **a** (Figure S87). Strong HSQC-TOCSY correlations from H-1 to C-2, C-3 and C-4, and a weak correlation from H-1 to C-5 elongated two more methylenes from it (Figure S88). The cyclopropanol moiety in unit **b** was determined by HMBC correlations from OH-12 to C-10, C-11 and C-12. HSQC-TOCSY correlations from OH-8 to C-7 showed that one methylene was attached to unit **b**. Finally HMBC cross peaks from OH-6 to C-7 and HSQC-TOCSY correlations from H-6 to C-4, C-5 and C-7, and from OH-6 to C-5, C-6 and C-7 showed that two units were connected via one oxygenated methane C-6. The relative stereochemistry of cyclopropanol was determined to be *trans* based on the strong NOESY correlations between H-9 and H-11a, between H-9 and H-12, between H-10 and H-11b, between H-10 and OH-12, between H-11a and H-12, and between H-11b and OH-12 (Figure S89).

Conversion of toblerol A (1) to the corresponding mono-napthoate ester (9).

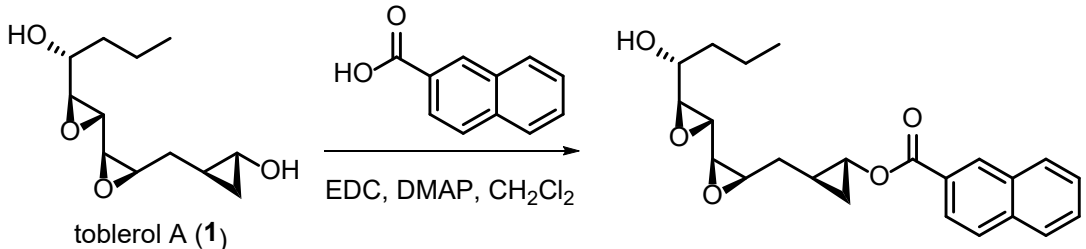

toblerol A (**1**) toblerol A mono-naphthoate ester (**9**)

Toblerol A (100 μg) was dissolved in CH_2Cl_2 (100 μL). To this solution was added 2-naphthoic acid (80 μg in 80 μL CH_2Cl_2), DMAP (62.6 μg in 62.6 μL CH_2Cl_2), and EDC (111.5 μg in 111.5 μL CH_2Cl_2) and the mixture was stirred overnight at room temperature. The mixture was subjected to two rounds of HPLC. First using HPLC conditions: column: Phenomenex, Synergi-Hydro RP, 4μ, 250 x 10 mm; flow rate: 3 mL/min; mobile phase/gradient: 10% CH_3CN/H_2O for 5 minutes then ramped to 100% CH_3CN

over 40 minutes. The fraction containing the mono-naphthoate ester was dried under reduced pressure and subjected to a second round of HPLC (column: Phenomenex, Synergi-Hydro RP, 4μ, 250 x 10 mm; flow rate: 3 mL/min; mobile phase: 68.5% CH_3CN/H_2O) the purified fraction was evaporated to give the purified mono-naphthoate ester (~ 25 μg). The position of the naphthoate was assigned by 2D NMR analysis which showed a downfield shift in the carbinol proton H-13 from δ 3.03 ppm in toblerol A to δ 4.15 ppm in the mono-naphthoate ester (**9**) (Figure S57-58). ^{1}H NMR (600 MHz, CD_3CN) δ 0.88 (t, *J* = 7.2 Hz, H-1), 1.48 – 1.31 (m, H-2ab), 1.51 – 1.45 (m, H-3), 3.38 (p, *J* = 6.0 Hz, H-4), 2.87 (d, *J* = 6.0 Hz, OH-4), 2.95 (dd, *J* = 6.0, 2.3 Hz, H-5), 2.86 (dd, *J* = 6.9, 2.3 Hz, H-6), 2.73 (dd, *J* = 6.9, 4.4 Hz, H-7), 3.24 (m, H-8), 1.75 – 1.64 (m, H-9ab), 1.39 – 1.32 (m, H-10), 0.84 (ddd, *J* = 6.5, 6.5, 6.5 Hz, H-11a), 1.15 (ddd, *J* = 10.0, 6.5, 2.8 Hz, H-11b), 4.15 (ddd, *J* = 6.5, 2.8, 2.8 Hz, H-12), 8.59 (brs, 1H-Np), 8.04-7.96 (m, 4H-Np), 7.67-7.59 (m, 2H-Np). HR-ESIMS $[M+Na]^+$ *m/z* 405.1675 (calc'd for $C_{23}H_{26}NaO_5$, 405.1672).

Synthesis of model compound 10.

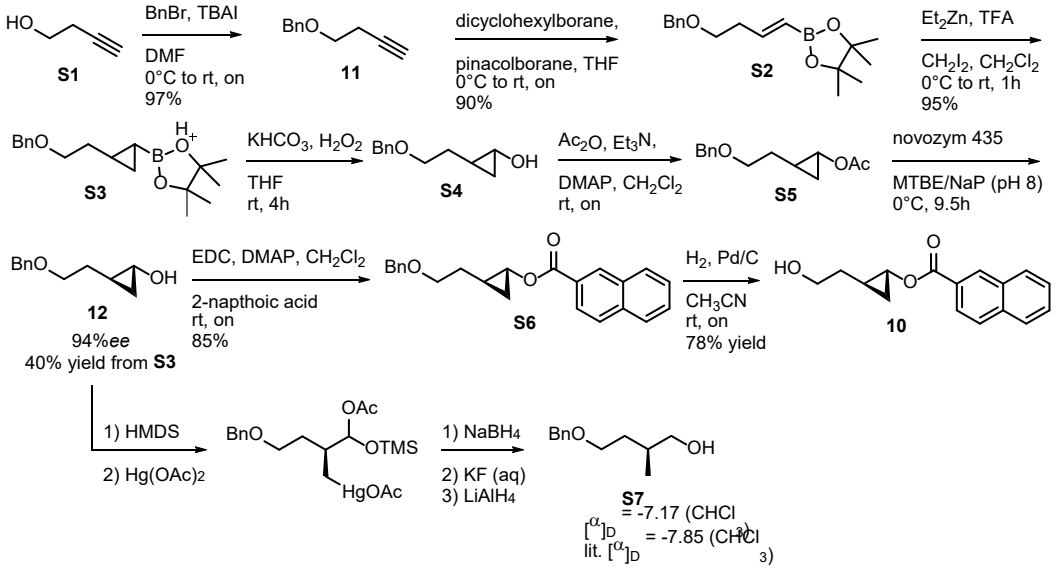

Benzyl alkynyl ether (11). A 2-necked round-bottom flask was charged with sodium hydride (1.2 g, dispersion in mineral oil) and a stir bar was added. The flask was purged with argon and DMF (100 mL) was added. The mixture was cooled to 0 °C and 3-butyn-1-ol (**S1**) (2 mL, 26 mmol) was added dropwise and the mixture stirred for 20 minutes. Tetrabutylammonium iodide (0.96 g, 2.6 mmol) was added in one portion, followed by benzyl bromide (3.5 mL, 29 mmol). The ice bath was removed and the reaction was gradually warmed to room temperature and stirred overnight. The reaction was quenched with brine (150 mL) and extracted with ethyl acetate (3 x 100 mL). The combined organic layers were dried (sodium sulfate), filtered, and the solvent evaporated. The crude material was chromatographed on silica gel (0.5% ethyl acetate/hexane) to give the protected alkyne **11** (4.04 g, 97% yield). ^{1}H and ^{13}C NMR were consistent with those of literature values.[6] HR-ESIMS $[M+H]^+$ *m/z* 161.0956 (calc'd for $C_{11}H_{13}O$, 161.0961).

Boronic ester (S2). We followed a procedure similar to Shirakawa and co-workers.[7] The dicyclohexylborane was used immediately after preparation. A dry 25 mL 2-necked round-bottom flask, with a gas inlet for argon, a sample inlet with a serum cap, and a magnetic stirring bar, was flushed with argon. The flask was charged with borane·THF complex (1M, 2.52 mmol) in THF (0.4 M solution) and then to the stirred solution was added cyclohexene (5.04 mmol, 0.510 mL) at 0 °C. After stirring for 1.5 h at 0 °C, the THF was removed under reduced pressure to give a white solid composed of dicyclohexylborane. The flask was cooled to 0 °C, pinacolborane (3.55g, 27.7 mmol) was added followed by the alkyne **11** (4.04 g, 25.2 mmol). The mixture was allowed to warm to room tem perature and stirred

for 4 hours. Air was bubbled through the reaction mixture for 2 hours to oxidize the the dicyclohexylborane. The mixture was diluted with hexane, washed with water, dried with sodium sulfate, and the solvent evaporated to give the boronic ester **S2** as a slightly yellow oil (6.54 g, 90% yield) (Figure S59-60). The crude material was used in the next step without further purification. ^{1}H NMR (400 MHz, $CDCl_3$) δ 7.40 – 7.22 (m, 5H), 6.63 (dt, *J* = 18.1, 6.4 Hz, 1H), 5.53 (dt, *J* = 18.0, 1.6 Hz, 1H), 4.51 (s, 2H), 3.56 (t, *J* = 6.8 Hz, 2H), 2.49 (qd, *J* = 6.8, 1.6 Hz, 2H), 1.26 (s, 12H). ^{13}C NMR (100 MHz, $CDCl_3$) δ 150.4 (CH), 138.4 (C), 128.3 (2 x CH), 127.7 (2 x CH), 127.5 (CH), 83.1 (2 x C), 72.9 (CH_2), 68.9 (CH_2), 36.1 (CH_2), 24.8 (4 x CH_3).[i] HR-ESIMS $[M+H]^+$ *m/z* 289.1956 (calc'd for $C_{17}H_{26}BO_3$, 289.1970).

Cylopropylboronic ester (S3). We followed the procedure reported by Yang and coworkers.[8] A dry 2-necked round-bottom flask, with a gas inlet for argon, a sample inlet with a serum cap, and a magnetic stirring bar, was flushed with argon. The flask was cooled to 0 °C and charged with dichloromethane (80 mL) and diethyl zinc (1M in hexane, 90 mL). Trifluoroacetic acid (90 mmol, 6.89 mL) in dichloromethane (40 mL) was added dropwise and the mixture stirred for 20 minutes at 0 °C. Diiodomethane (90 mmol, 7.23 mL) in dichloromethane (40 mL) was added dropwise and stirred for 20 minutes at 0 °C. The alkene **S2** (45 mmol, 12.97 g) in diclorometh ane (40 mL) was added dropwise and the ice bath was removed and stirred an additional 45 minutes. The reaction was quenched with saturated ammonium chloride (500 mL) and the mixture extracted with hexane (3 x 500 mL), The organic layers were washed with saturated sodium bicarbonate (250 mL), water (250 mL), brine (250 mL), dried with sodium sulfate, and the solvent evaporated to give the crude cyclopropylboronic ester **S3** (12.92 g, 95% yield) which was used in the next step without further purification (Figure S61-62). ^{1}H NMR (400 MHz, $CDCl_3$) δ 7.38 – 7.24 (m, 5H), 4.51 (d, *J* = 0.9 Hz, 2H), 3.55 (t, *J* = 6.8 Hz, 2H), 1.65 (dddd, *J* = 13.6, 6.8, 6.8, 6.8 Hz, 1H), 1.51 (dddd, 13.6, 6.8, 6.8, 6.8 Hz, 1H), 1.21 (s, 12H), 1.07 – 0.99 (m, 1H), 0.70 (ddd, *J* = 7.7, 6.0, 3.4 Hz, 1H), 0.44 (ddd, *J* = 9.2, 5.2, 3.4 Hz, 1H), -0.37 (dt, *J* = 9.2, 6.0 Hz, 1H). ^{13}C NMR (100 MHz, $CDCl_3$) δ 138.7 (C), 128.3 (2 x CH), 127.6 (2 x CH), 127.4 (CH), 82.8 (C), 73.0 (CH_2), 70.5 (CH_2), 35.4 (CH_2), 24.70 (2 x CH_3), 24.66 (2 x CH_3), 15.1 (CH), 11.1 (CH_2).[1] HR-ESIMS $[M+H]^+$ *m/z* 303.2131 (calc'd for $C_{18}H_{28}BO_3$, 303.2126).

(1*R*, 2*S*)-cyclopropylalcohol (12). The optically enriched cyclopropanol was prepared in a similar manner as that of Pietruszka and coworkers.[9] The cyclopropylboronic ester **S3** (11.6 g, 38.48 mmol) was dissolved in THF (160 mL), and a mixture of 2N potassium bicarbonate (45 mL) and 30% hydrogen peroxide (13.5 mL) were added and the mixture was stirred for 4 hours. Additional 2N potassium bicarbonate (20 mL) and 30% hydrogen peroxide (6 mL) were added and stirred an additional 2 hours. The mixture was poured into water (1 L) and extracted with ether (3 x 500 mL). The organic layers were washed with saturated ammonium chloride (500 mL), water (500 mL), brine (500 mL), dried with magnesium sulfate, and the solvent evaporated to give the crude alcohol **S4**, which was used in the next step without further purification (Figure S63-64). ^{1}H NMR (400 MHz, $CDCl_3$) δ 7.37 – 7.27 (m, 5H), 4.52 (s, 2H), 3.53 (t, *J* = 6.6 Hz, 2H), 3.23 (ddd, *J* = 6.2, 2.7, 2.7 Hz, 1H), 1.57 (dddd, *J* = 14.0, 7.0, 7.0, 7.0 Hz, 1H), 1.41 (dddd, J = 14.0, 7.0, 7.0, 7.0 Hz, 1H), 1.00 (m, 1H), 0.71 (ddd, *J* = 9.9, 6.2, 2.7 Hz, 1H), 0.35 (ddd, *J* = 6.2, 6.2, 6.2 Hz, 1H). ^{13}C NMR (100 MHz, $CDCl_3$) δ 138.5 (C), 128.4 (2 x CH), 127.6 (2 x CH), 127.5 (CH), 72.9 (CH_2), 69.7 (CH_2), 52.4 (CH), 31.8 (CH_2), 18.0 (CH), 14.1 (CH_2). HR-ESIMS $[M+H]^+$ *m/z* 215.1048 (calc'd for $C_{12}H_{16}NaO_2$, 215.1043). The alcohol **S4** and dimethylaminopyridine (274.9 mg, 2.25 mmol) were dissolved in dichloromethane (45 mL) and the mixture cooled to 0 °C. Acetic anhydride (12.74 mL, 135 mmol) was added dropwise followed by triethylamine (18.81 mL, 135 mmol). The reaction was warmed to room temperature and stirred overnight. The mixture was poured into saturated ammonium chloride (150 mL) and extracted with ether (3 x 100 mL). The organic layers were combined and washed with saturated sodium bicarbonate (100 mL), water (100 mL), brine (100 mL), dried with magnesium sulfate, and the solvent evaporated to give the crude acetate (**S5**), which was used in the next step without further purification (Figure S65-66). ^{1}H NMR (400 MHz, $CDCl_3$) δ 7.37 – 7.25 (m, 5H), 4.52 (s, 2H), 3.85 (ddd, *J* = 6.7, 2.8, 2.8 Hz, 1H), 3.57 (t, *J* = 6.6 Hz, 2H), 1.61 (dddd, *J* = 14.0, 7.0, 7.0, 7.0 Hz, 1H), 1.53 (dddd, *J* = 14.0, 7.0, 7.0, 6.3 Hz, 1H), 1.36 (m, 1H), 0.85 (ddd, *J* = 10.1,

6.3, 3.1 Hz, 1H), 0.58 (ddd, *J* = 6.3, 6.3, 6.3 Hz, 1H). ^{13}C NMR (100 MHz, $CDCl_3$) δ 171.7 (C), 138.5 (C), 128.3 (2 x CH), 127.6 (2 x CH), 127.5 (CH), 72.9 (CH_2), 69.3 (CH_2), 52.2 (CH), 31.6 (CH_2), 20.9 (CH_3), 15.6 (CH), 11.7 (CH_2). HR-ESIMS [M+H]+ *m/z* 235.1320 (calc'd for $C_{14}H_{19}O_3$, 235.1329). A 1 L round bottom flask containing the acetate (**S5**) and a large magnetic stir bar was charged with *tert*-butyl methyl ether (200 mL) that had been saturated with 100 mM aqueous sodium phosphate (pH 8). The mixture was cooled in as ice bath and Novozym 435 (208 mg) was added and the mixture stirred for 9.5 h at 0 °C. The mixture was filtered through a pad of silica gel and rinsed with ether. The solvent was evaporated and the mixture chromatographed on silica gel using a stepwise gradient from 0% to 60% ethyl acetate/hexane to give the alcohol **12** (2.94 g, 40 % yield from **S4**) (Figure S67-68). $[\alpha]^{25}_D$ = –20.0 (*c* 0.66, $CHCl_3$) ^{1}H NMR (400 MHz, $CDCl_3$) δ 7.37 – 7.27 (m, 5H), 4.52 (s, 2H), 3.53 (t, *J* = 6.6 Hz, 2H), 3.23 (ddd, *J* = 6.2, 2.7, 2.7 Hz, 1H), 1.57 (dddd, *J* = 14.0, 7.0, 7.0, 7.0 Hz, 1H), 1.41 (dddd, *J* = 14.0, 7.0, 7.0, 7.0 Hz, 1H), 1.00 (m, 1H), 0.71 (ddd, *J* = 9.9, 6.2, 2.7 Hz, 1H), 0.35 (ddd, *J* = 6.2, 6.2, 6.2 Hz, 1H). ^{13}C NMR (100 MHz, $CDCl_3$) δ 138.5 (C), 128.4 (2 x CH), 127.6 (2 x CH), 127.5 (CH), 72.9 (CH_2), 69.7 (CH_2), 52.4 (CH), 31.8 (CH_2), 18.0 (CH), 14.1 (CH_2). HR-ESIMS $[M+H]^+$ *m/z* 215.1040 (calc'd for $C_{12}H_{16}NaO_2$, 215.1043). The % ee was determined by conversion to the corresponding naphthoate ester (**S6**) and chiral HPLC (see below).

Primary alcohol (S7). The absolute configuration of **12** was established by reductive conversion to the corresponding primary alcohol **S7** as described by Imai and coworkers[10] and comparison of the measure specific rotation with literature values.[11] The cyclopropanol **12** (22.3 mg, 116 µmol) was stirred with hexamethyldisalizane (100 µL) for 4 hours at 55 °C and placed under high vacuum. The crude ether was treated with mercury acetate (37 mg, 116.0 µmol) in acetic acid (500 µL) and stirred at room temperature for 1 hour and placed under high vacuum. The residue was dissolved in dichloromethane (0.75 mL) and treated with sodium borohydride (8.8 mg, 233 µmol) and stirred at room temperature for 20 minutes and the solvent removed under high vacuum. To the mixture was added 20% aqueous potassium fluoride (0.5 mL) in acetone (1 mL) and stirred for 30 minutes at room temperature. The organic layer was removed and the aqueous layer washed with ether (2 x 1 mL). The organic layers were dried with magnesium sulfate and solvent evaporated under reduced pressure. The mixture was dissolved in ether and lithium aluminum hydride (18.5 mg, 487 µmol) was carefully added and stirred for 20 minutes at room temperature. The reaction was quenched with water, acidified with 2N hydrochloric acid, the organic layer was removed and the aqueous layer extracted with ether (2 x 5 mL). The organic layers were combined, dried with magnesium sulfate, and the solvent evaporated under reduced pressure. The mixture was chromatographed on silica gel to give the alcohol **S7** (14.6 mg, 65 % yield) as a colorless oil (Figure S69-70). $[\alpha]^{25}_D$ = –7.17 ($CHCl_3$); ^{1}H NMR (400 MHz, $CDCl_3$) δ 7.37 – 7.26 (m, 5H), 4.52 (s, 2H), 3.59 (ddd, *J* = 9.4, 6.1, 2.2 Hz, 1H), 3.52 (ddd, *J* = 9.4, 7.9, 4.7 Hz, 1H), 3.53-3.47 (m, 1H), 3.47 – 3.40 (m, 1H), 1.86 – 1.78 (m, 1H), 1.74 – 1.65 (m, 1H), 1.62 – 1.54 (m, 1H), 0.92 (d, *J* = 6.8 Hz, 3H). ^{13}C NMR (100 MHz, $CDCl_3$) δ 138.0 (C), 128.4 (2 x CH), 127.74 (2 x CH), 127.70 (CH), 73.1 (CH_2), 68.7 (CH_2), 68.1 (CH_2), 34.2 (CH_2), 34.1 (CH), 17.2 (CH_3); HR-ESIMS $[M+H]^+$ *m/z* 195.1375 (calc'd for $C_{12}H_{19}O_2$, 195.1380).

Benzyl protected naphthoate ester (S6). To a solution of alcohol **12** (52.3 mg, 0.272 mmol) in CH_2Cl_2 (2 mL) was added the acid (56.2 mg, 0.326 mmol) and DMAP (3.3 mg, 0.027 mmol). The mixture was cooled in an ice bath and EDCI (50.6 mg, 0.326 mmol) in CH_2Cl_2 was added dropwise and the mixture allowed to warm to room temperature and stirred overnight. The mixture was evaporated and chromatographed on Silica gel (5% EtOAc in hexane to give the corresponding naphthoate ester **S6** (50 mg, 85% yield) (Figure S71-72). $[\alpha]^{25}_D$ = –45.1 (*c* 0.67, $CHCl_3$); ^{1}H NMR (400 MHz, $CDCl_3$) δ 8.56 (brs, 1H), 8.02 (dd, J = 8.6, 1.7 Hz, 1H), 7.95 (dd, J = 8.2, 1.4 Hz, 1H). 7.91 – 7.85 (m, 2H), 7.60 (m, 1H), 7.54 (m, 1H), 7.39 – 7.25 (m, 5H), 4.57 (s, 2H), 4.17 (dt, J = 6.7, 2.9 Hz, 1H), 3.67 (t, J = 6.5 Hz, 2H), 1.74 (dddd, J = 13.8, 6.7, 6.7, 6.7 Hz, 1H), 1.65 (dddd, J = 13.8, 6.7, 6.7, 6.7 Hz, 1H), 1.37 (ddddd, J = 9.9, 6.7, 6.7, 6.7, 2.9Hz 1H), 1.07 (ddd, J = 9.9, 6.7, 2.9 Hz, 1H) 0.75 (ddd, J = 6.7, 6.7, 6.7 Hz, 1H). ^{13}C NMR (100 MHz, $CDCl_3$) δ 167.5 (C), 138.5 (C), 132.4 (C), 131.0 (C), 129.3 (CH), 128.3 (2 x CH), 128.2 (CH), 128.1 (CH), 127.7 (CH), 127.6 (2 x CH), 127.5 (CH), 127.2 (C), 126.6 (CH), 125.1 (CH), 73.0 (CH_2), 69.4 (CH_2), 54.8 (CH), 31.7 (CH), 16.0 (CH2), 12.1 (CH). HR-ESIMS $[M+H]^+$ *m/z* 347.1626 (calc'd for $C_{23}H_{23}O_3$, 347.1642). Chiral HPLC (column: Phenomenex, Lux-amylose, 5µ, 250 x 4.6 mm; flow rate:

1.5 mL/min; mobile phase: 10% *i*-PrOH/hexane) T_r = 5.41 min (minor, peak area = 17.27 mAU/sec) and 5.95 (major, peak area = 579.02 mAU/sec).

Model compound (10). The naphthoate ester **S6** (25 mg, 72.2 μmol) in a glass vial with a screw cap septum was dissolved in ethyl acetate (1 mL). Pd on carbon (10 wt. % loading, 7.7 mg) and a stir bar were added and the vial was purged with an H_2 filled balloon and vigorously stirred overnight. The material was passed through a syringe filter and subjected to reversed phase HPLC (column: Phenomenex, Luna, C18 (2), 5μ, 250 x 10 mm; flow rate: 3 mL/min; mobile phase: 59.5 % CH_3CN/H_2O) to give the corresponding model compound **10** (9.9 mg, 53% yield) (Figure S73-74). $[\alpha]^{23}_D$ = +13.4 (*c* 0.33, $CHCl_3$); ^{1}H NMR (400 MHz, $CDCl_3$) δ 8.56 (brs, 1H), 8.02 (dd, *J* = 8.4, 1.7 Hz, 1H). 7.95 (dd, *J* = 8.4, 1.4 Hz, 1H). 7.88 (brd, *J* = 8.4 Hz, 2H), 7.61 (m, 1H), 7.55 (m, 1H), 4.16 (dd, *J* = 9.4, 4.2 Hz, 1H), 4.06 (ddd, *J* = 6.8, 2.8, 2.8 Hz, 1H), 3.89-3.75 (m, 2H), 2.02-1.96 (m, 1H), 1.27-1.02 (m, 3H), 0.68 (ddd. *J* = 6.8, 6.8, 6.8 Hz, 1H); ^{13}C NMR (100 MHz, $CDCl_3$) δ 169.1 (C), 132.4 (C), 131.4 (CH), 129.4 (CH), 129.0 (CH), 128.5 (CH), 128.3 (CH), 127.8 (CH), 126.8 (CH), 126.6 (C), 125.1 (CH), 62.6 (CH_2), 55.0 (CH), 34.6 (CH_2), 17.7 (CH), 10.0 (CH_2); HR-ESIMS $[M+H]^+$ *m/z* 257.1162 (calc'd for $C_{16}H_{17}O_3$, 257.1172).

Supplementary Figures and Tables

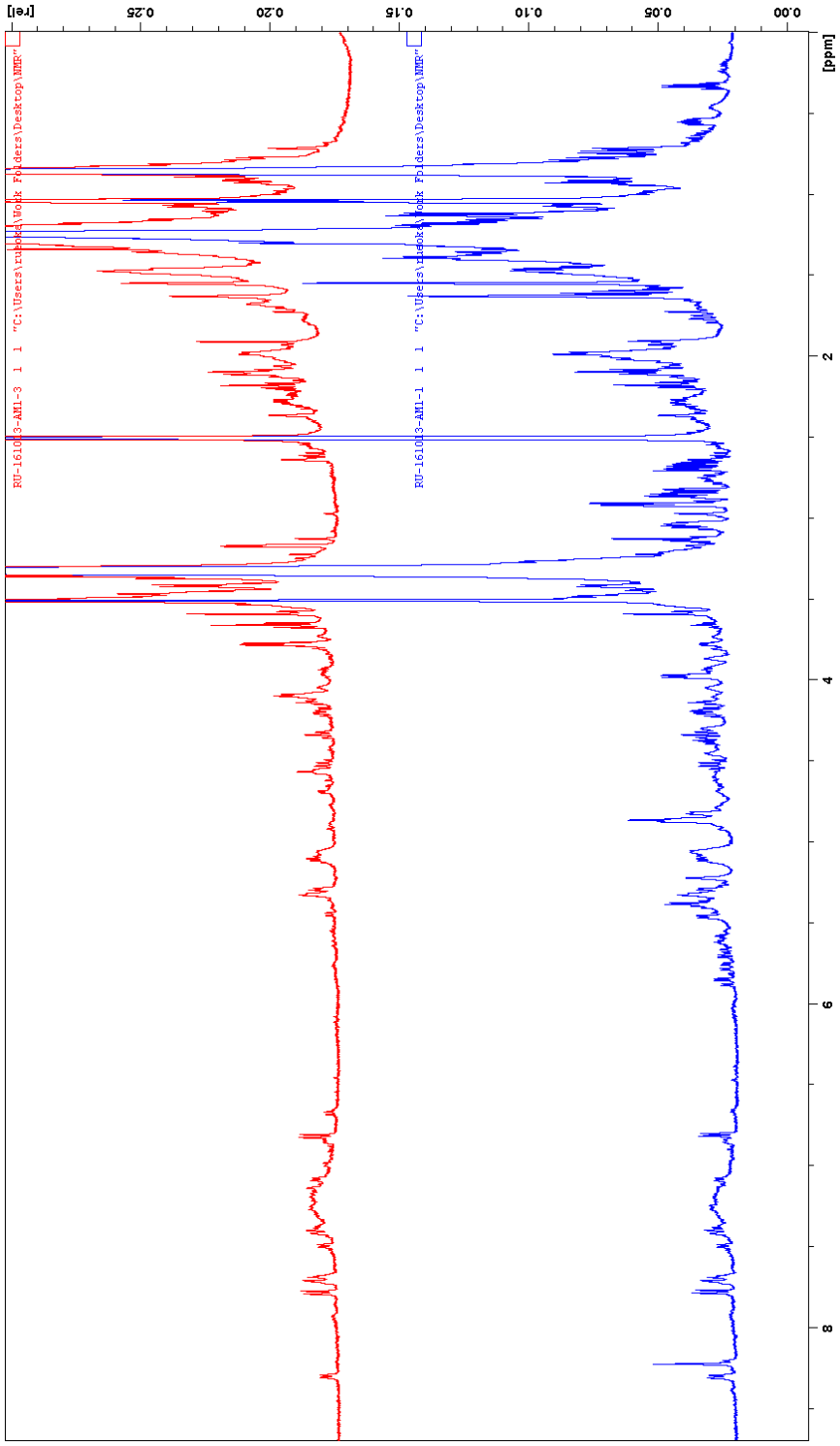

Figure S1. ^{1}H NMR spectrum of supernatant extracts from *M. extorquens* AM1 WT strain (lower) and Δ*tobC* strain (upper) in DMSO-d_6.

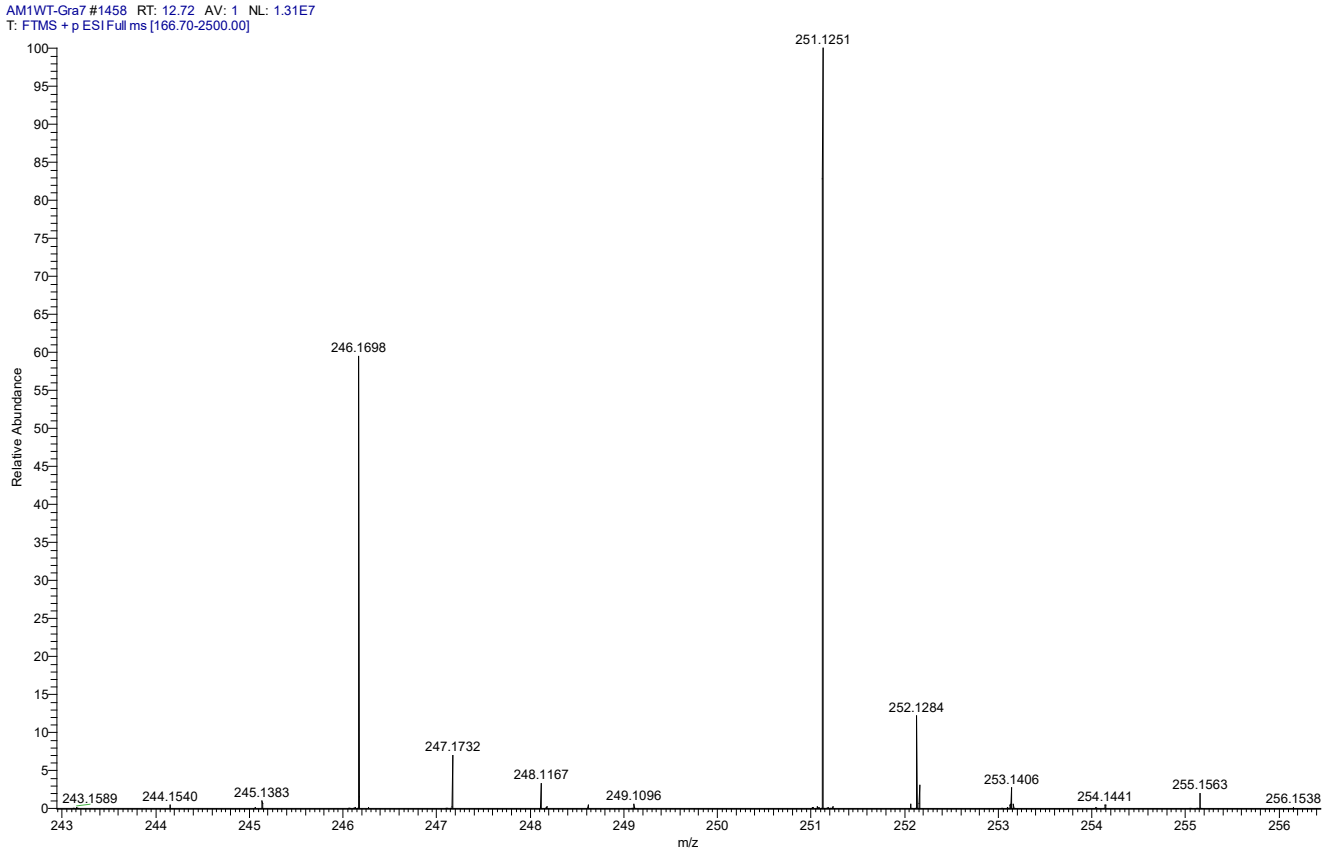

Figure S2: HR-LC-ESIMS data of toblerol A (1). Mass spectrum of the peak at 12.72 min (*m/z* 246.1698 $[M+NH_4]^+$ and *m/z* 251.1251 $[M+Na]^+$).

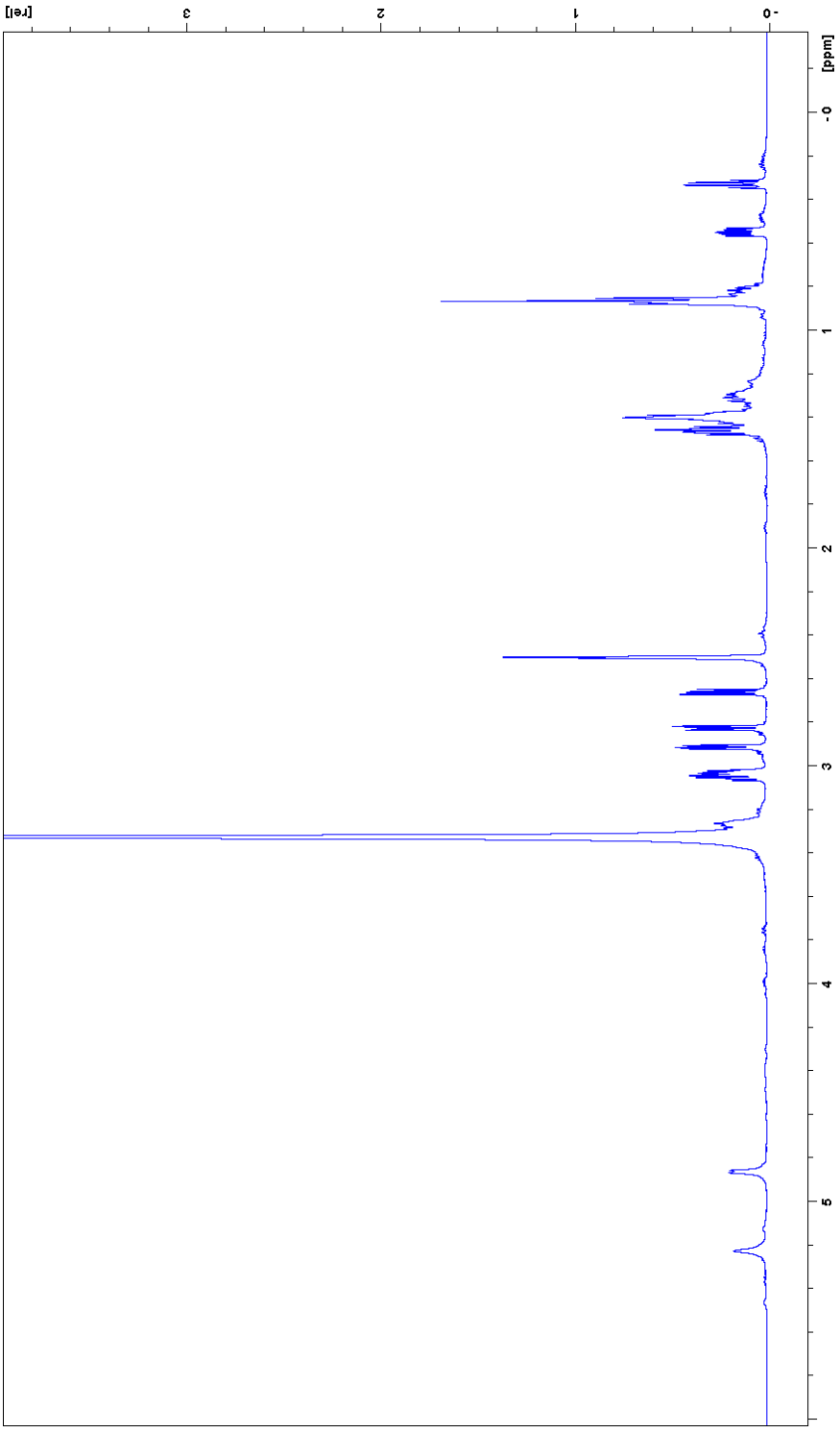

Figure S3. ^{1}H NMR spectrum of toblerol A (1) in DMSO-d_6.

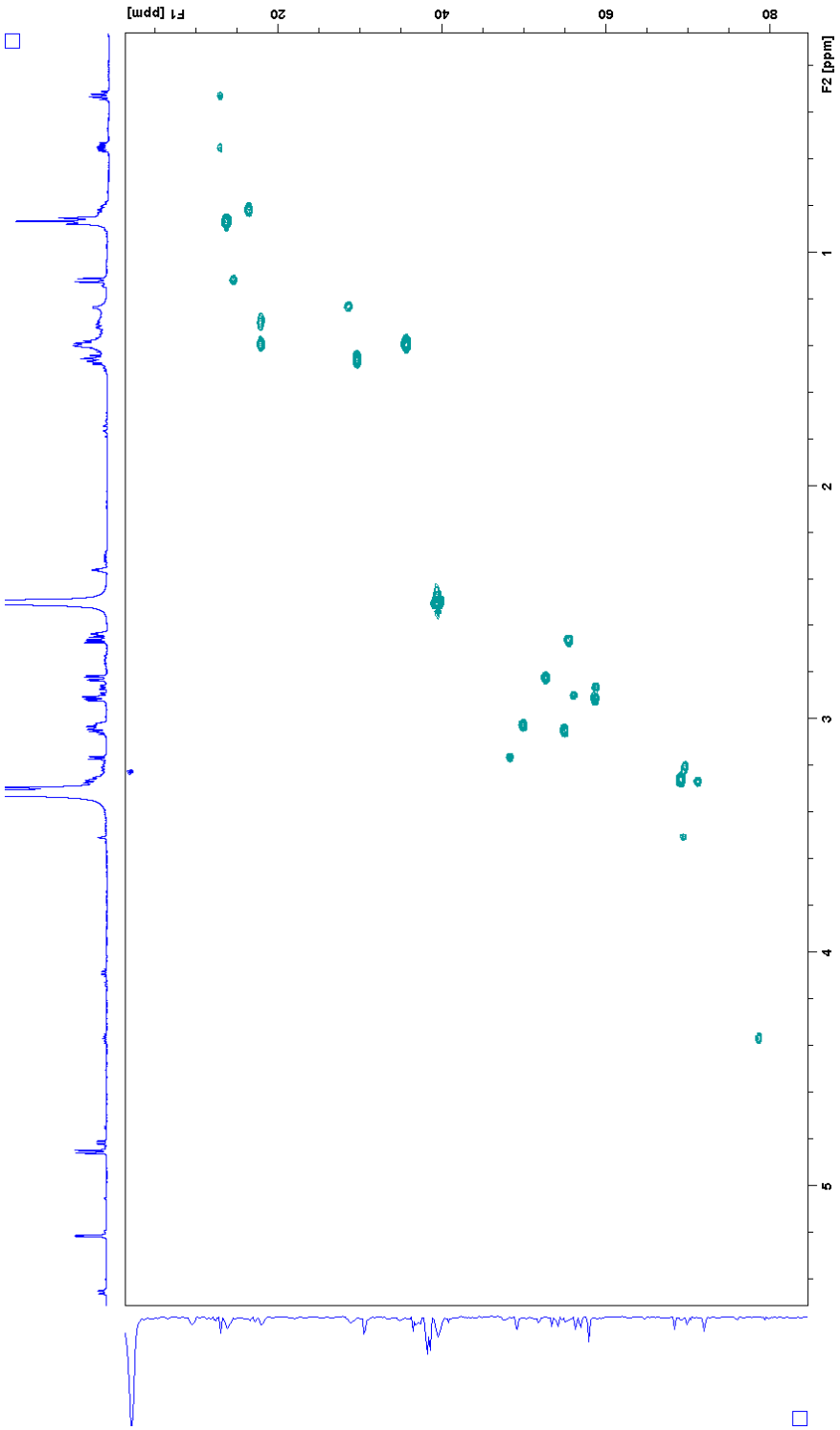

Figure S4. HSQC spectrum of toblerol A (1) in DMSO-d_6.

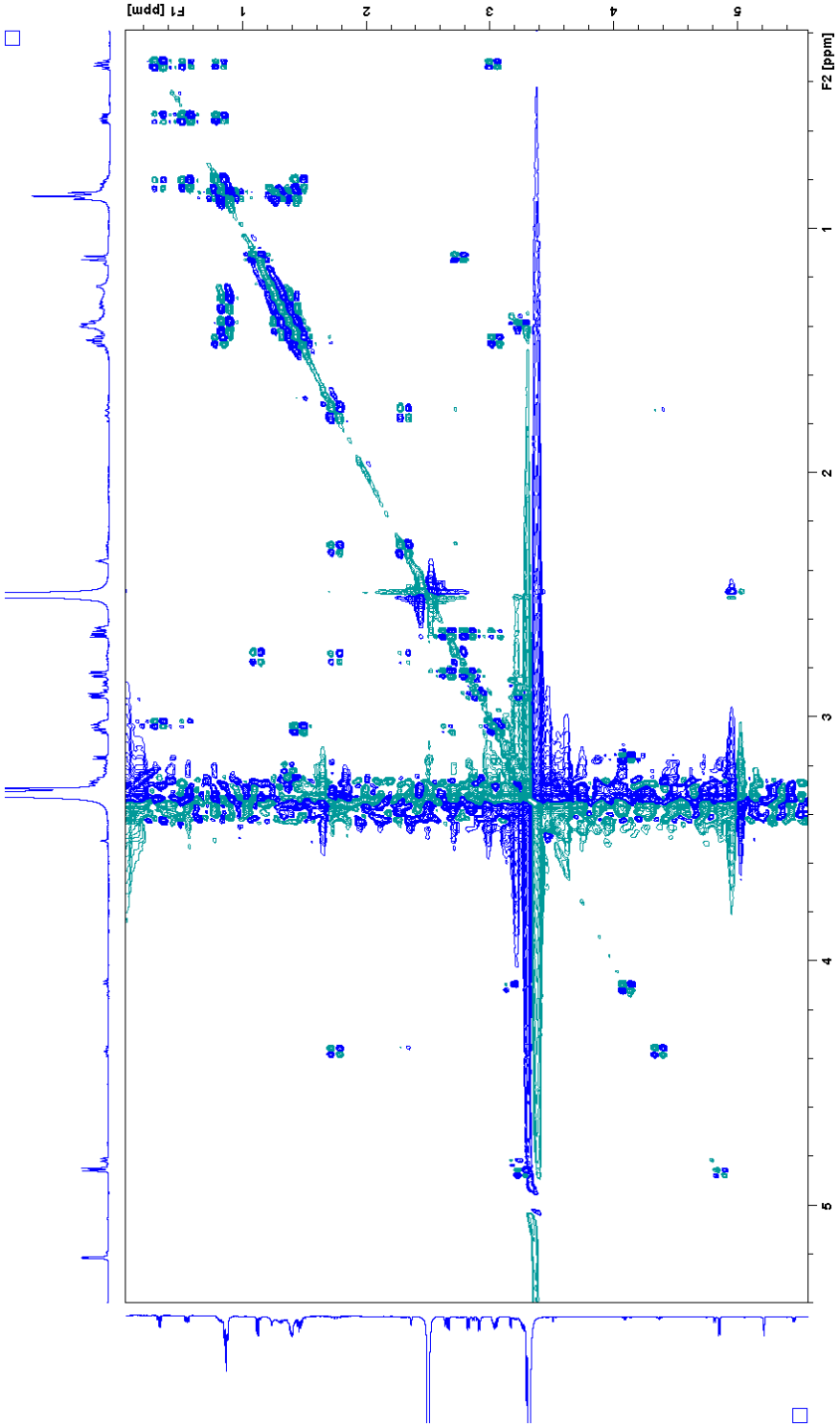

Figure S5. COSY spectrum of toblerol A (1) in DMSO-d_6.

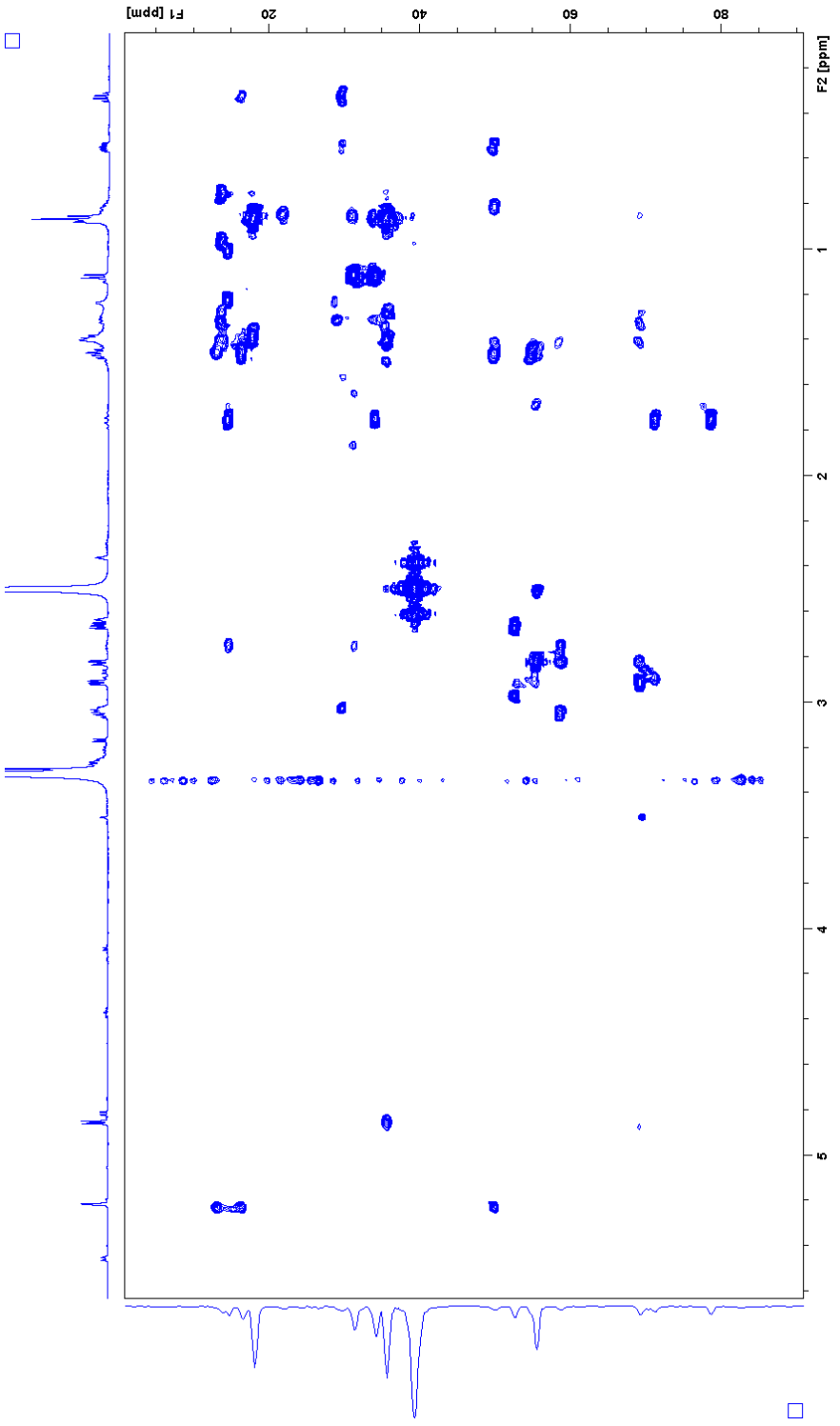

Figure S6. HMBC spectrum of toblerol A (1) in DMSO-d_6.

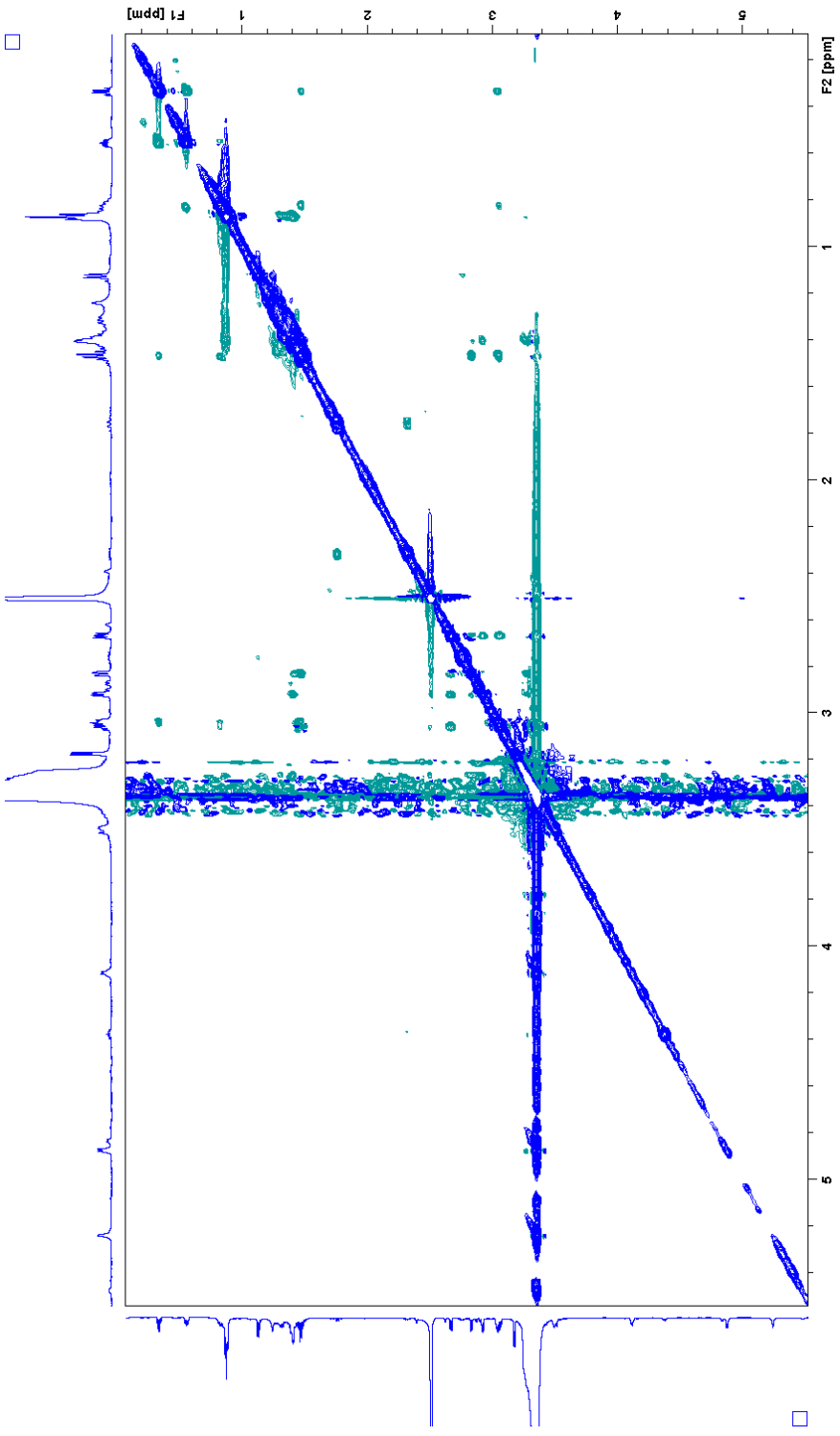

Figure S7. NOESY spectrum of toblerol A (1) in DMSO-d_6.

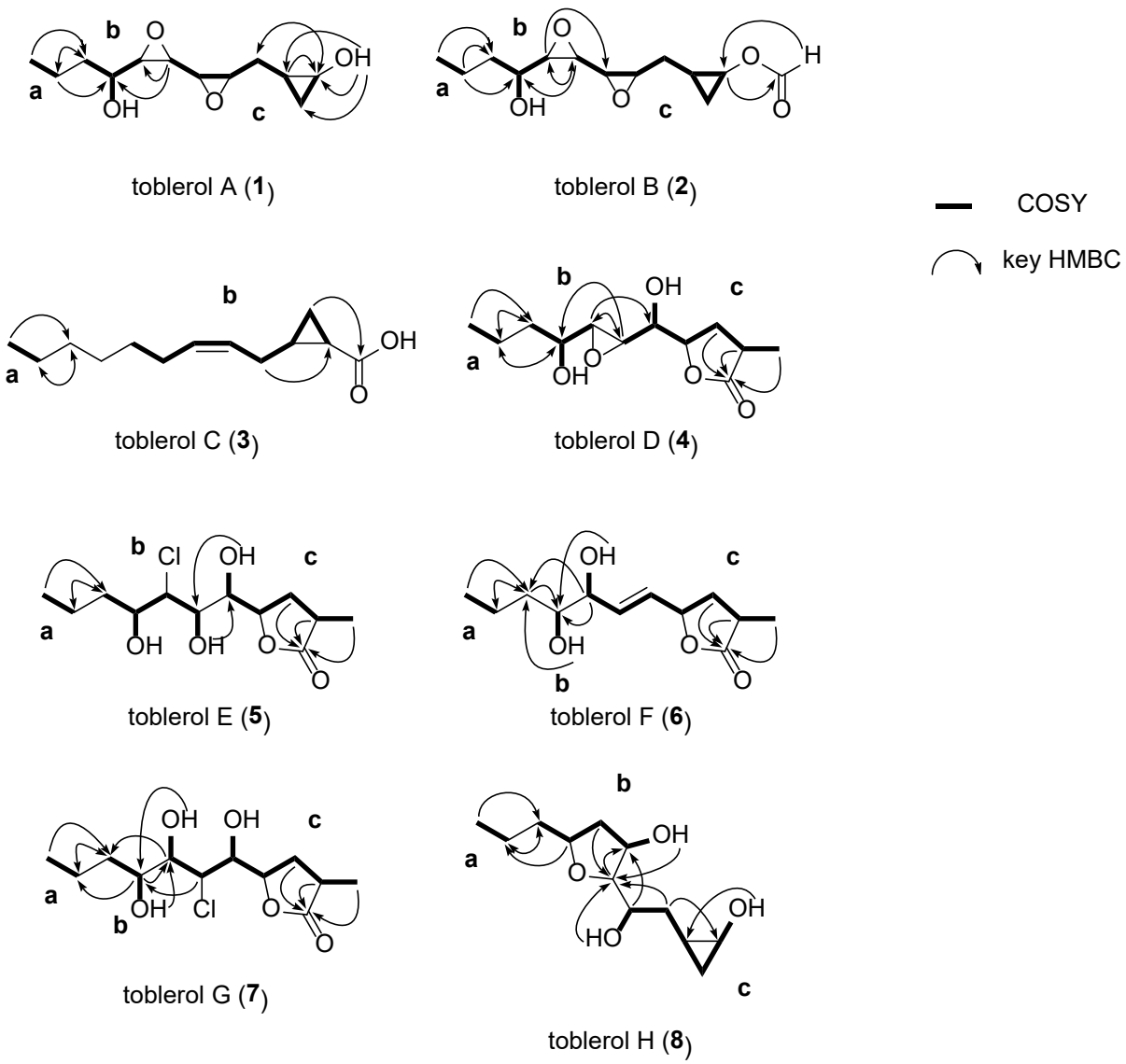

Figure S8. Structure elucidation of toblerols A-H (1-8).

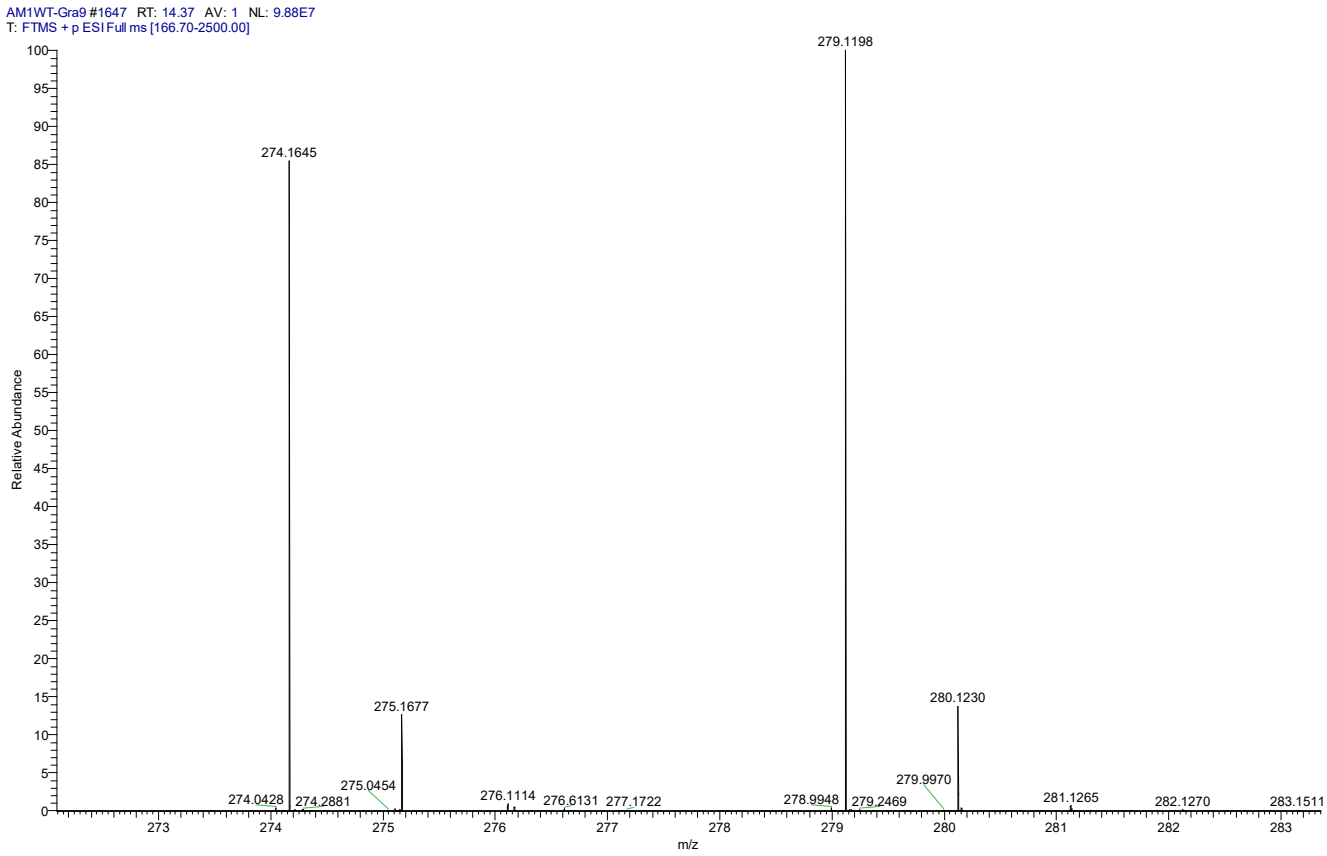

Figure S9: HR-LC-ESIMS data of toblerol B (**2**). Mass spectrum of the peak at 14.37 min (*m/z* 274.1645 $[M+NH_4]^+$ and *m/z* 279.1198 $[M+Na]^+$).

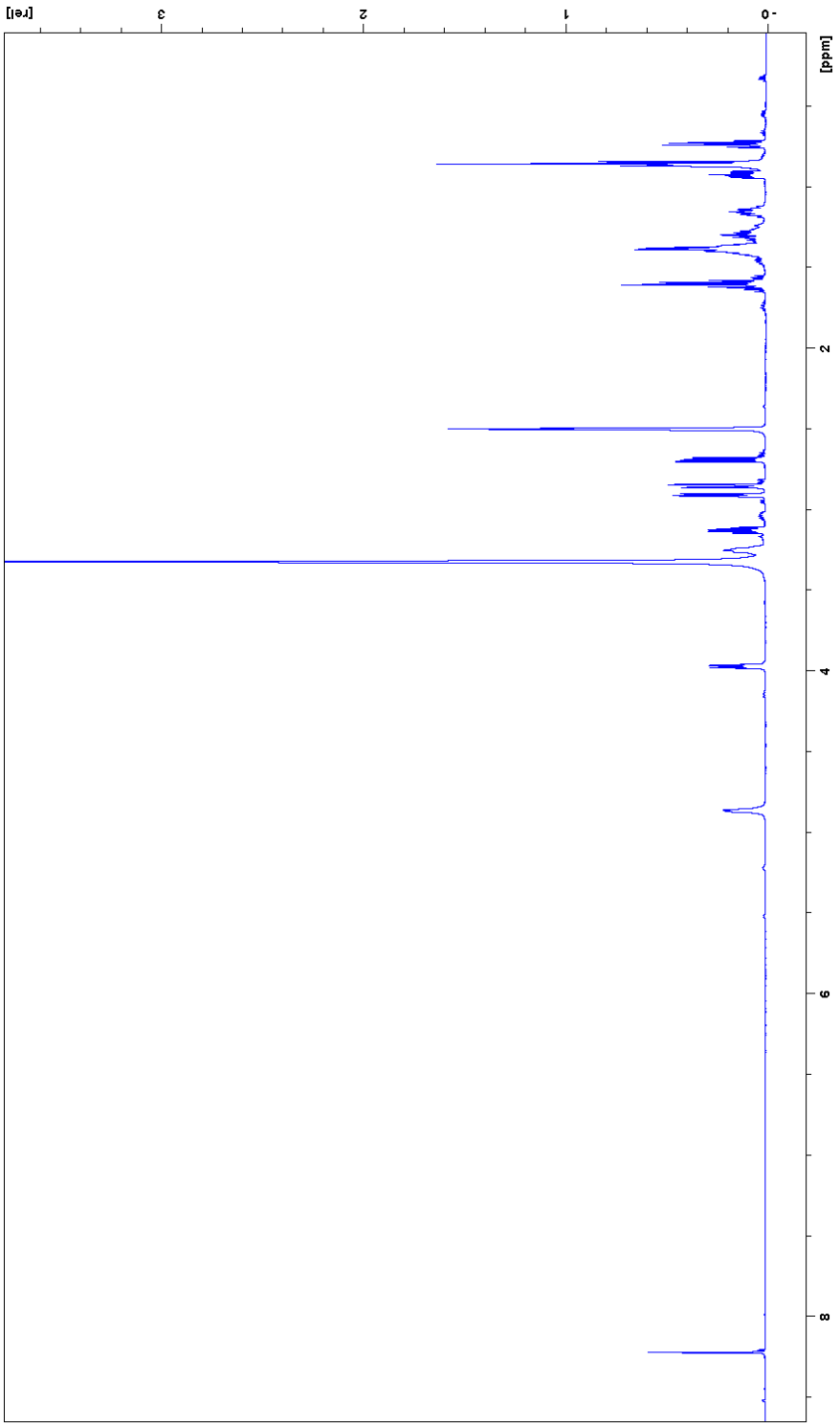

Figure S10. ^{1}H NMR spectrum of toblerol B (**2**) in DMSO-d_6.

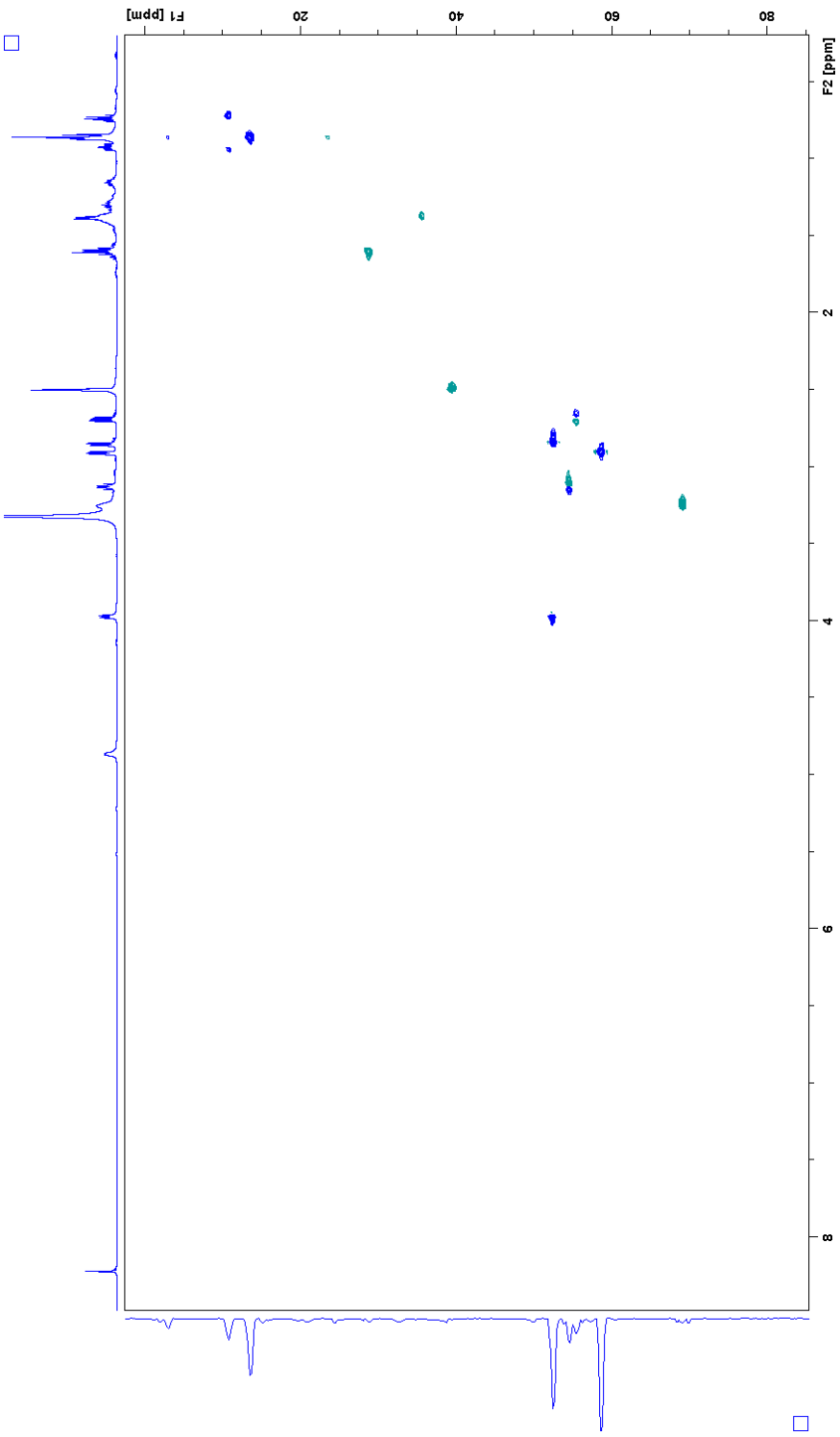

Figure S11. HSQC spectrum of toblerol B (**2**) in DMSO-d_6.

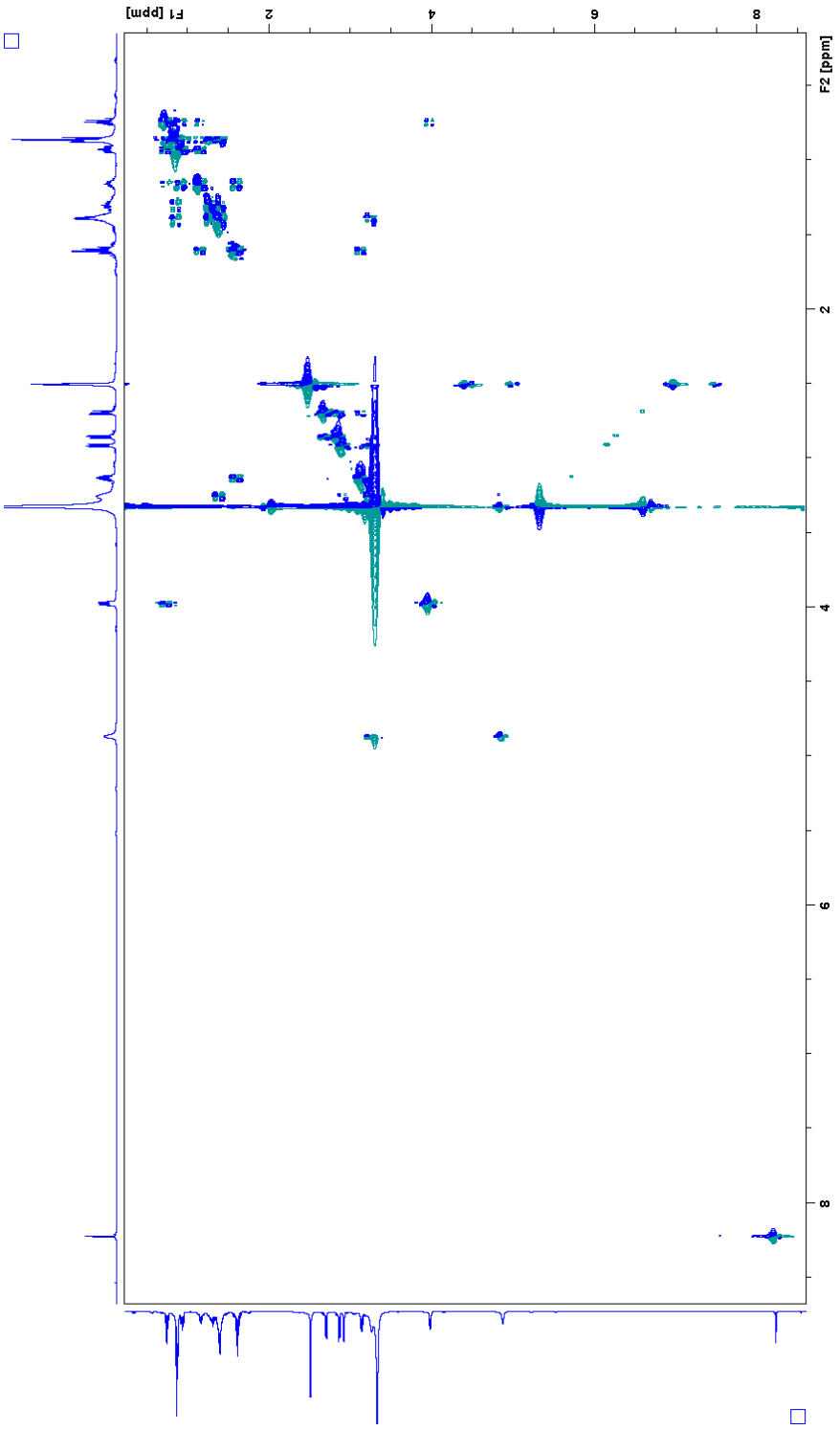

Figure S12. COSY spectrum of toblerol B (**2**) in DMSO-d_6.

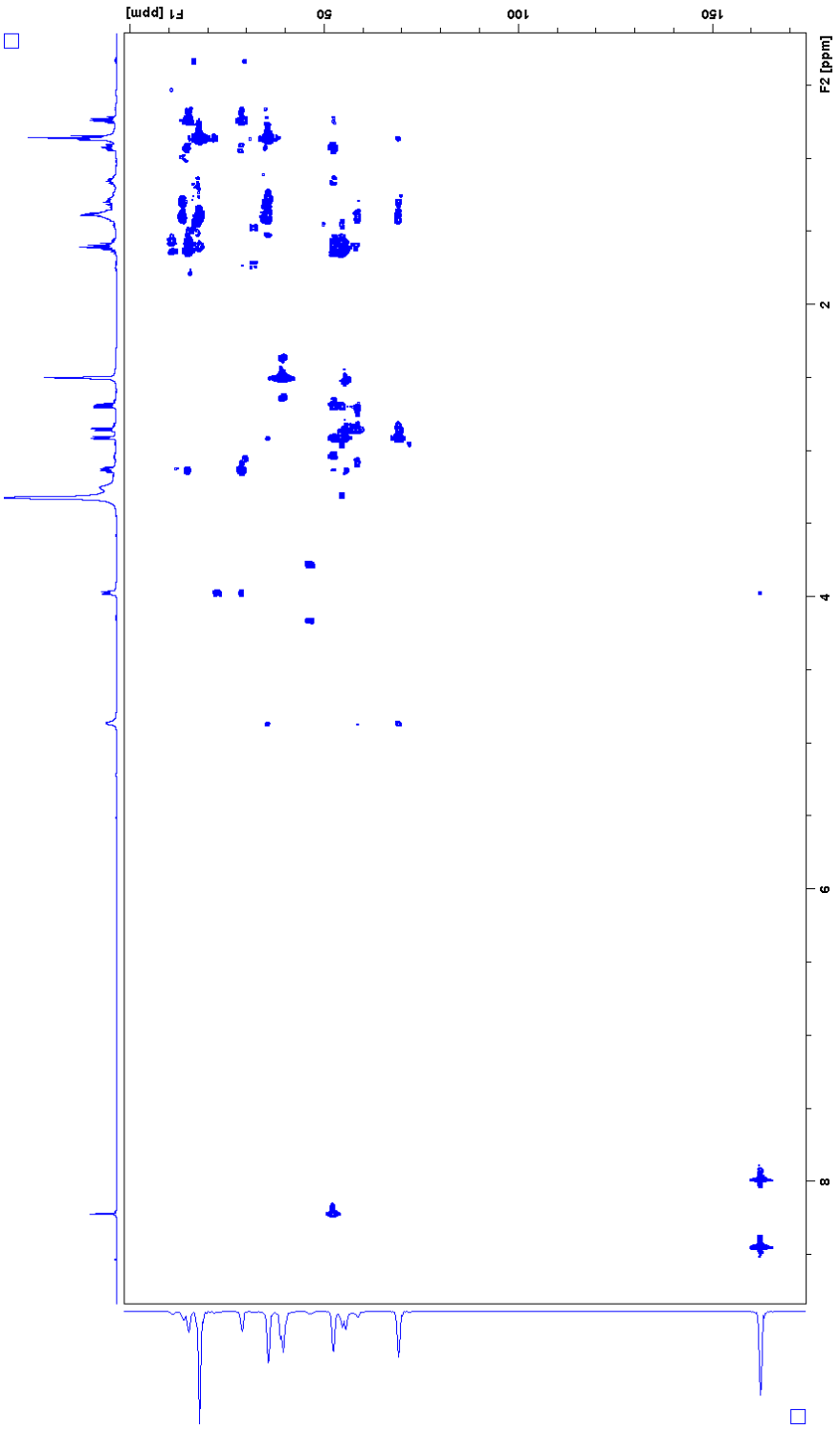

Figure S13. HMBC spectrum of toblerol B (**2**) in DMSO-d_6.

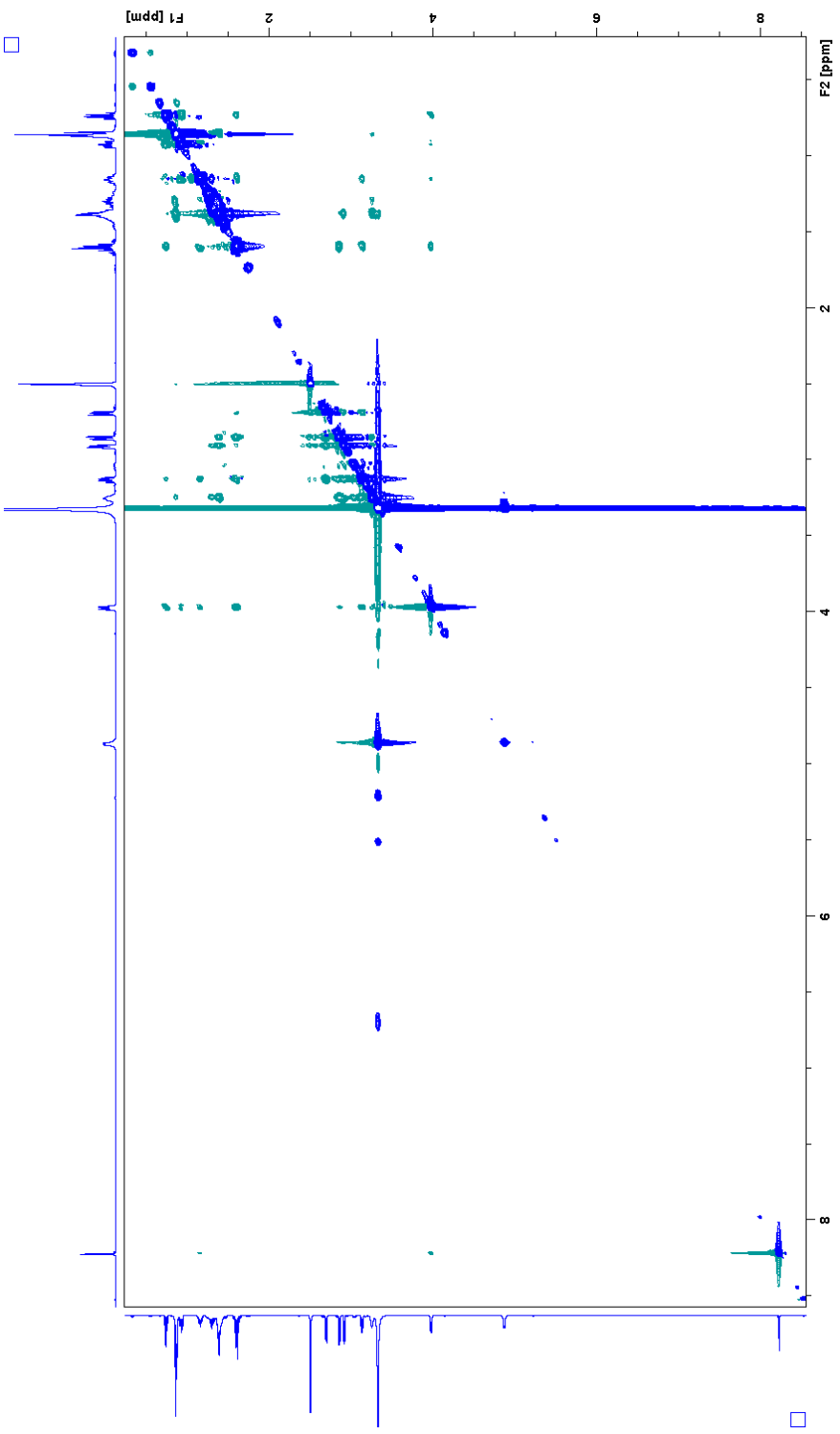

Figure S14. NOESY spectrum of toblerol B (**2**) in DMSO-d_6.

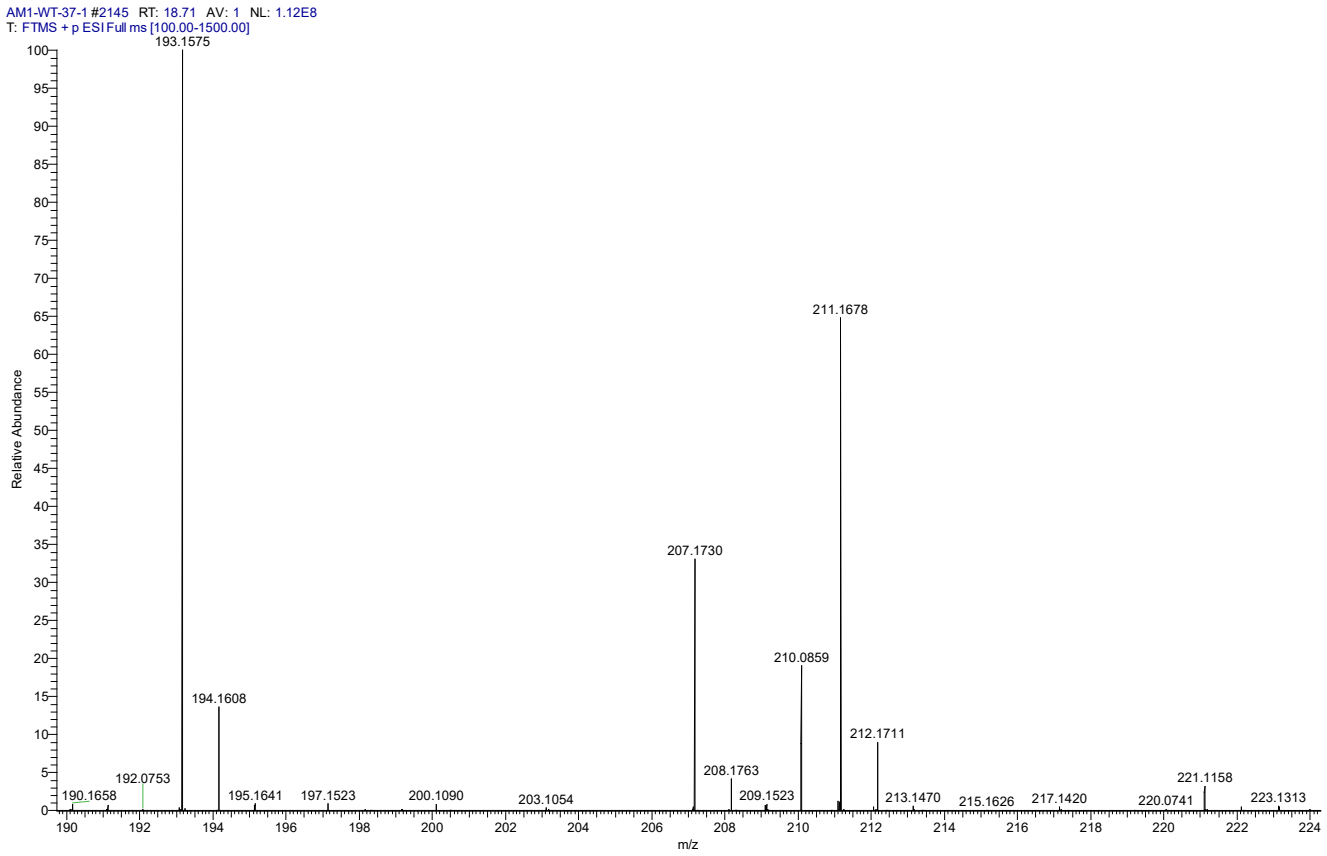

Figure S15: HR-LC-ESIMS data of toblerol C (**3**). Mass spectrum of the peak at 18.71 min (*m/z* 193.1575 $[M+H-H_2O]^+$ and *m/z* 211.1678 $[M+H]^+$).

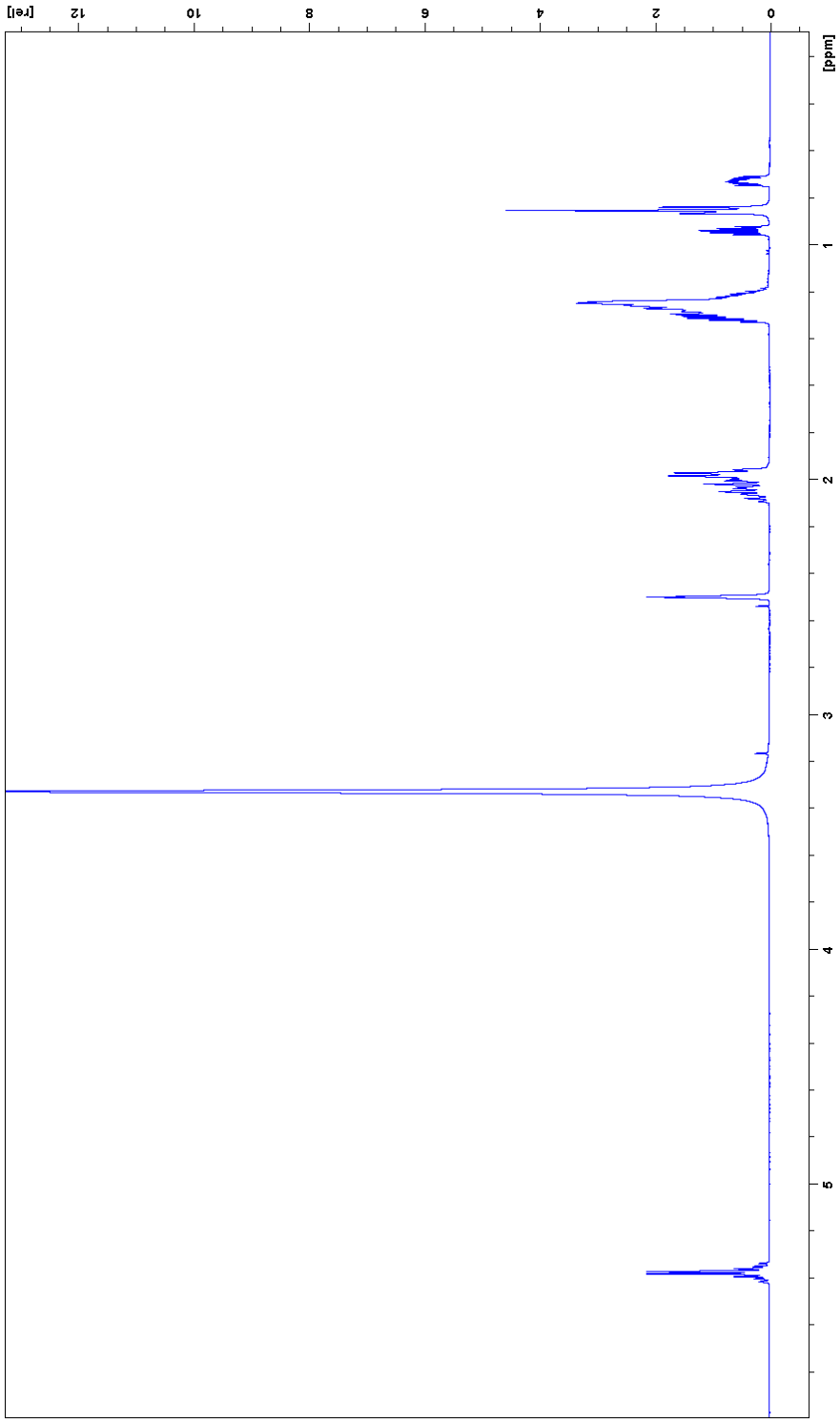

Figure S16. ^{1}H NMR spectrum of toblerol C (**3**) in DMSO-d_6.

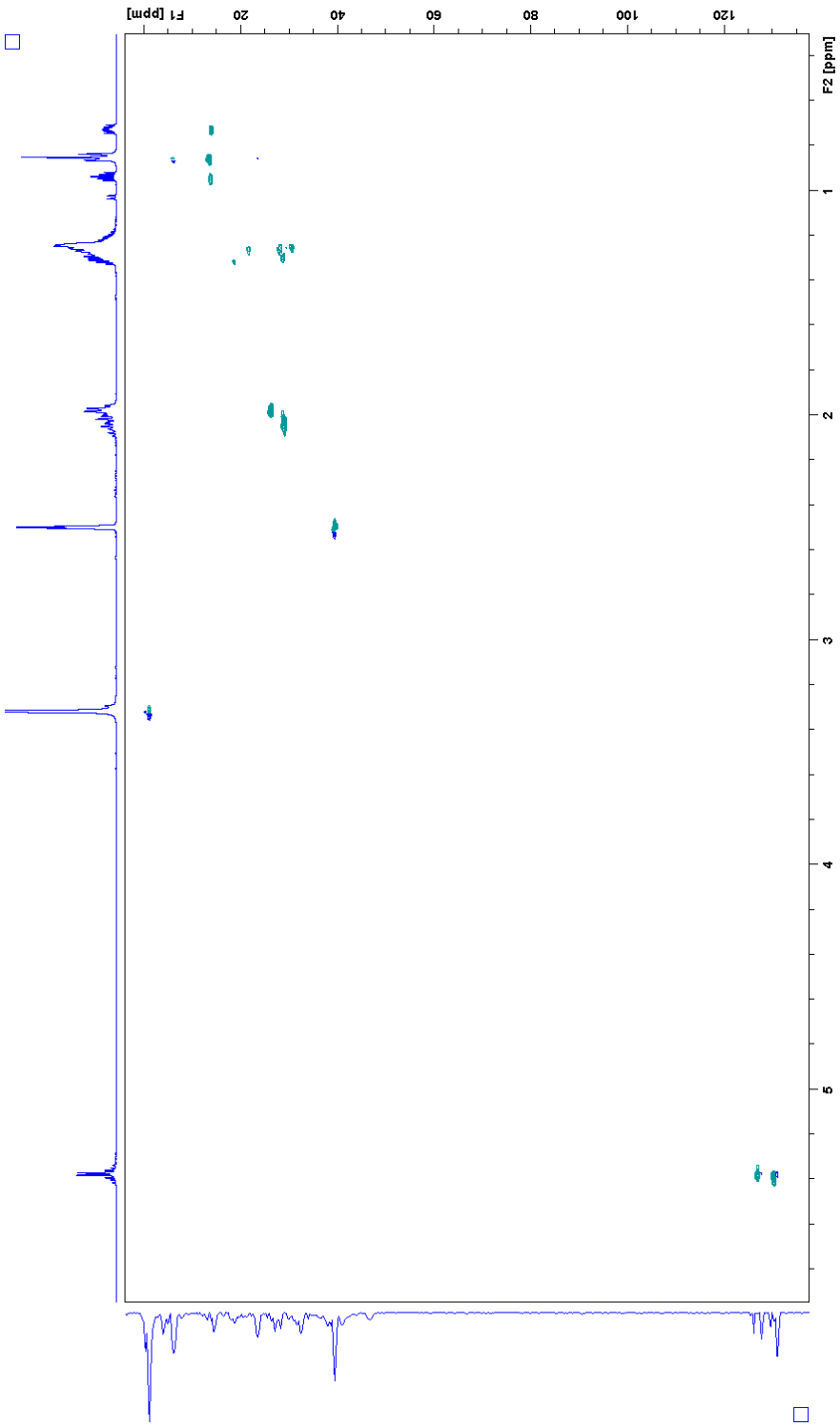

Figure S17. HSQC spectrum of toblerol C (**3**) in DMSO-d_6.

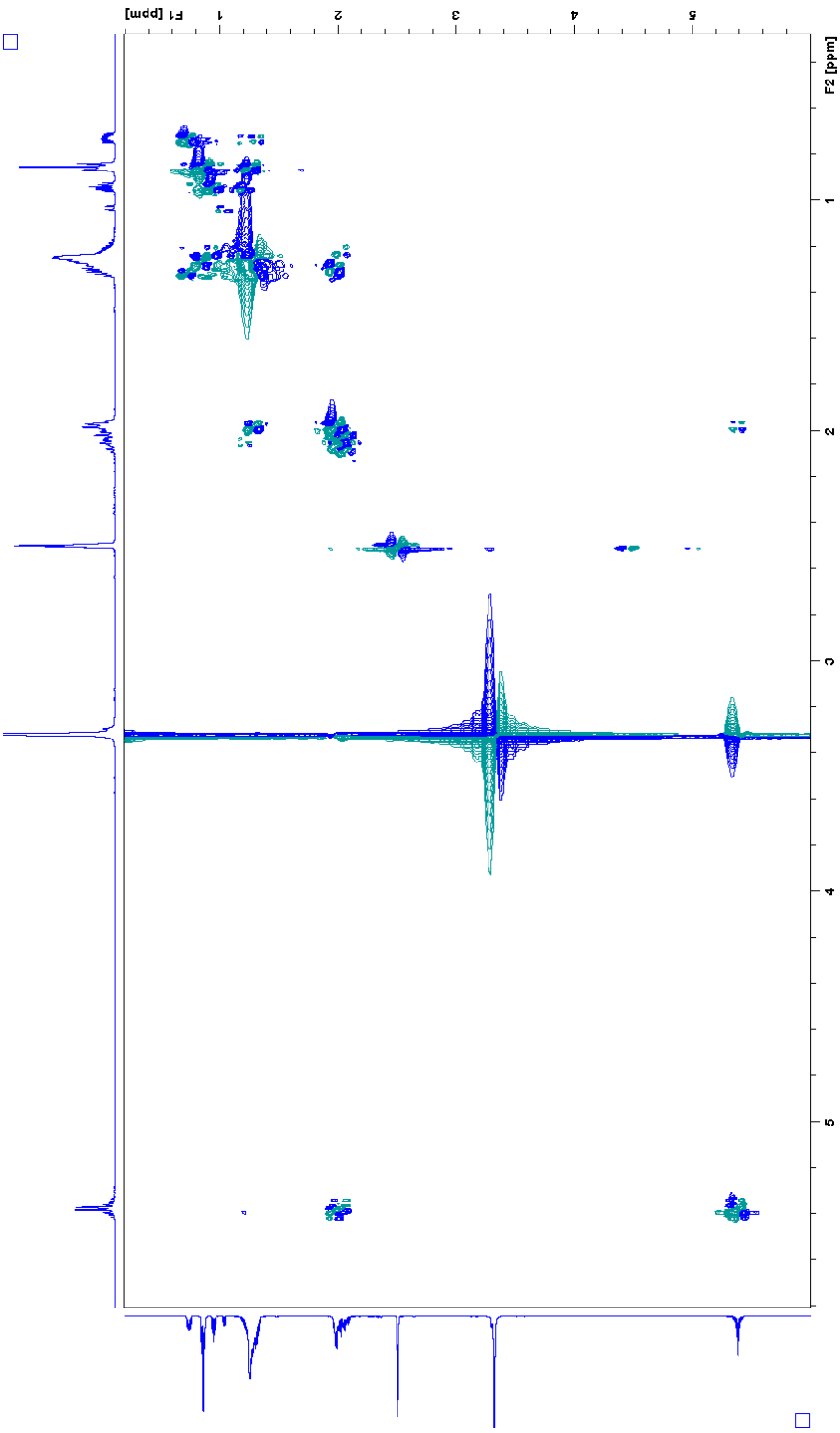

Figure S18. COSY spectrum of toblerol C (**3**) in DMSO-d_6.

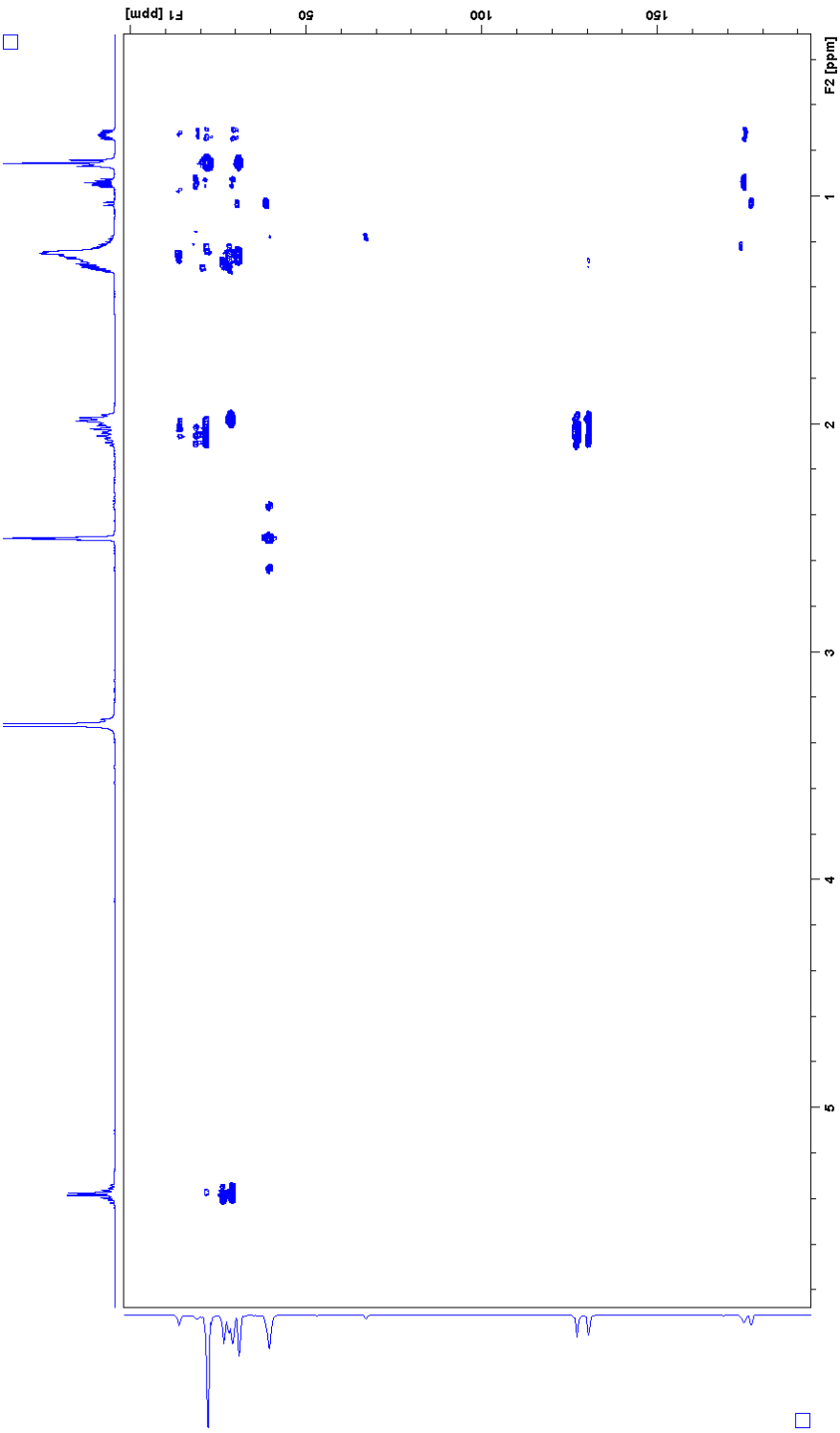

Figure S19. HMBC spectrum of toblerol C (**3**) in DMSO-d_6.

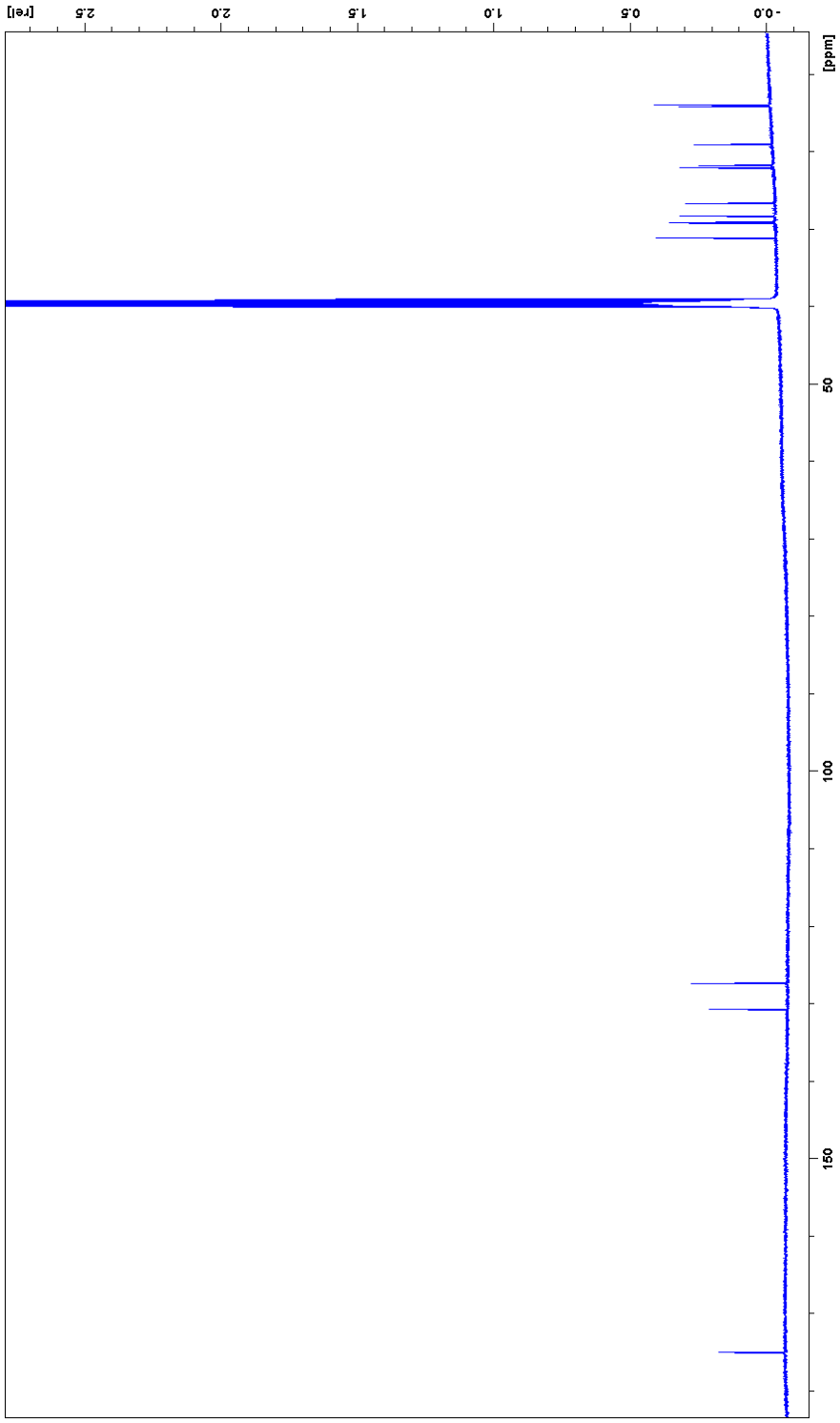

Figure S20. ^{13}C NMR spectrum of toblerol C (**3**) in DMSO-d_6.

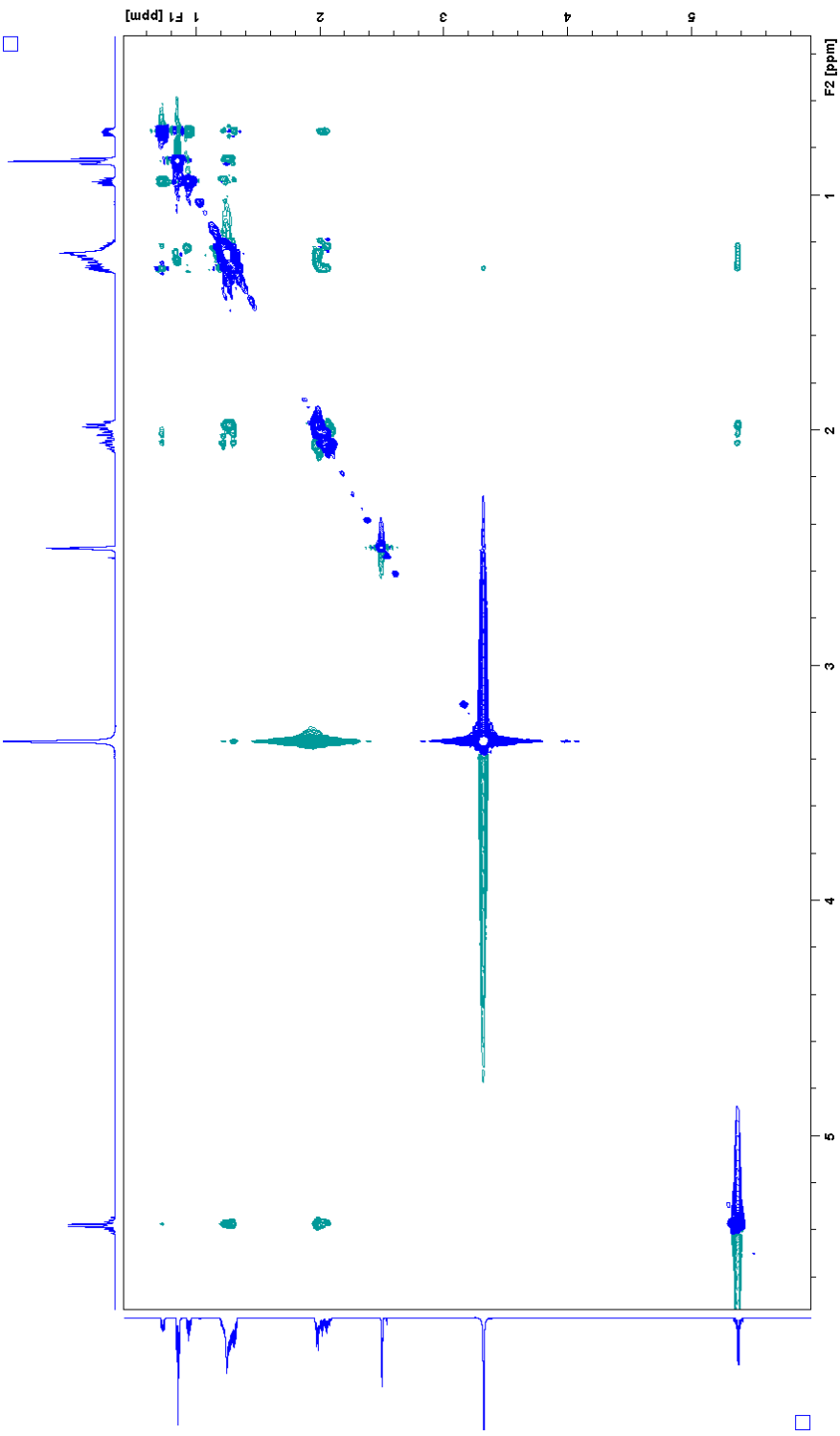

Figure S21. NOESY spectrum of toblerol C (**3**) in DMSO-d_6.

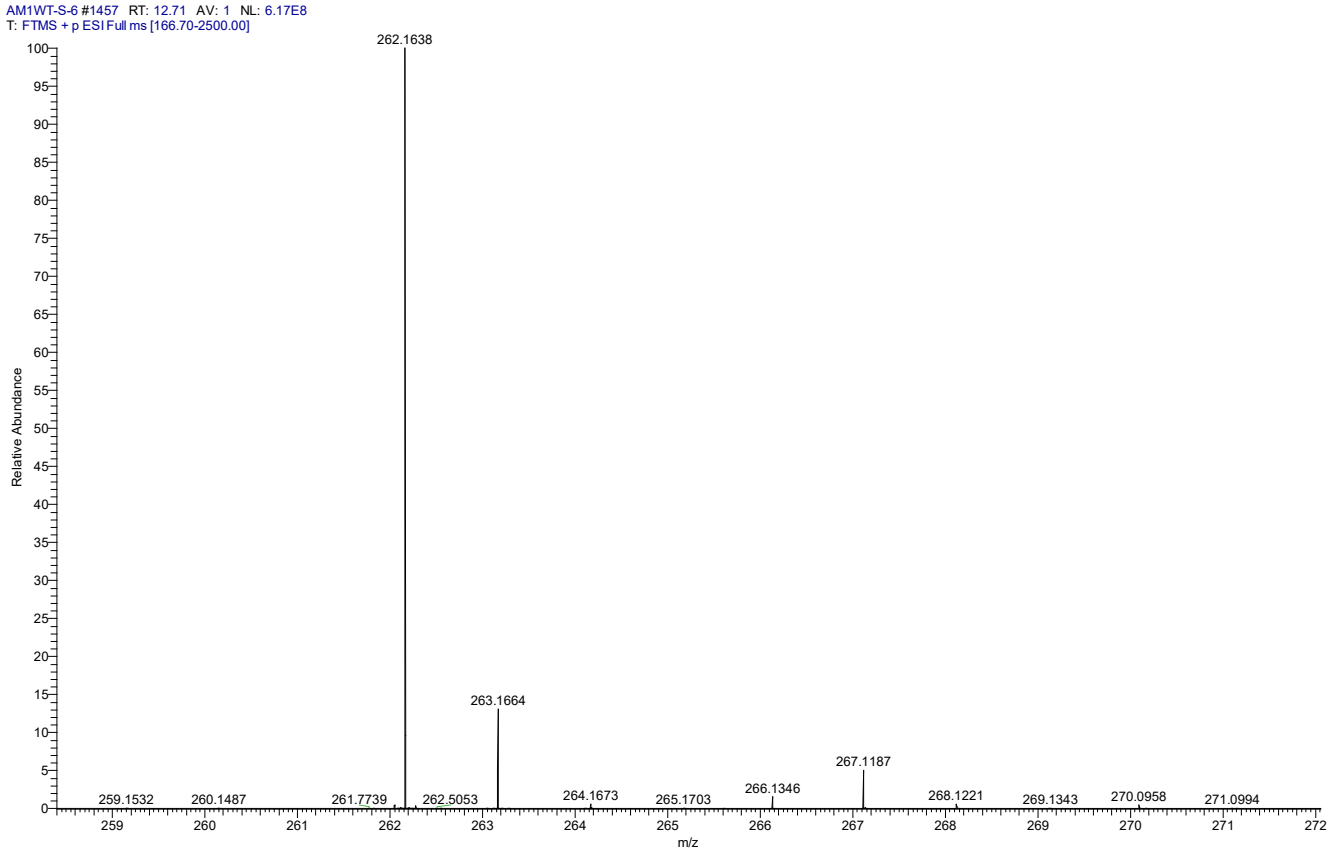

Figure S22: HR-LC-ESIMS data of toblerol D (**4**). Mass spectrum of the peak at 12.71 min (*m/z* 262.1638 $[M+NH_4]^+$ and *m/z* 267.1187 $[M+Na]^+$).

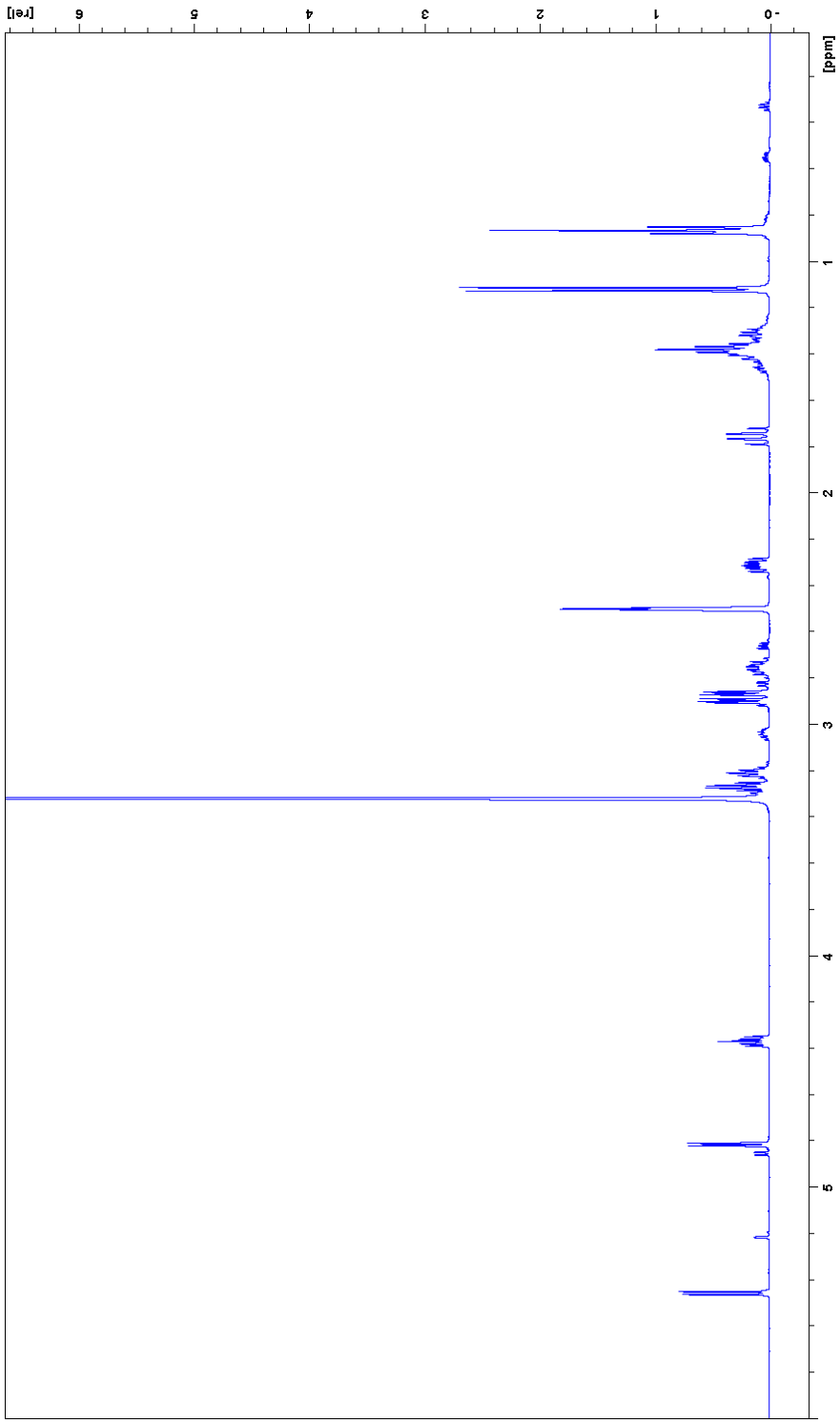

Figure S23. ^{1}H NMR spectrum of toblerol D (**4**) in DMSO-d_6.

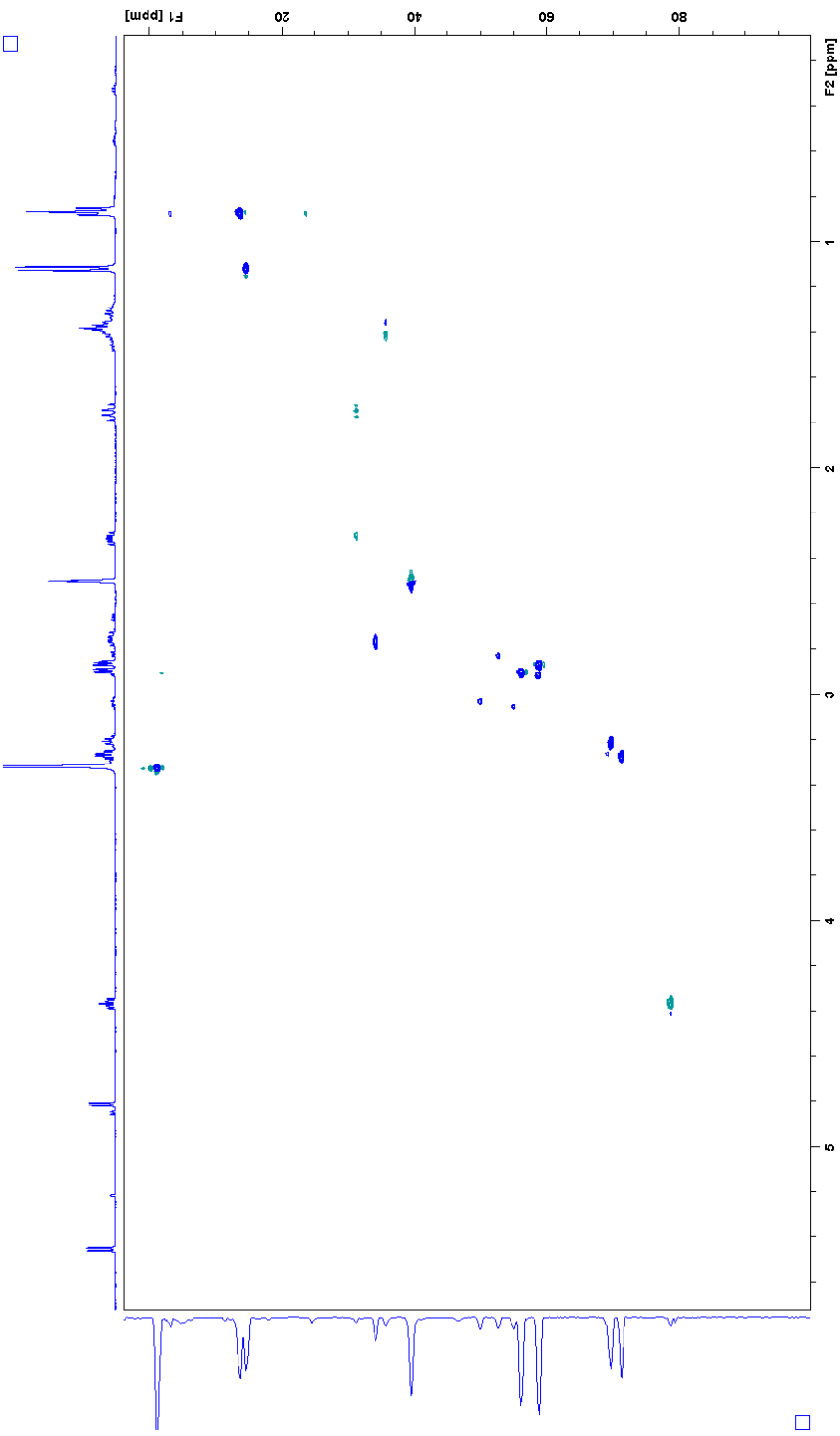

Figure S24. HSQC spectrum of toblerol D (**4**) in DMSO-d_6.

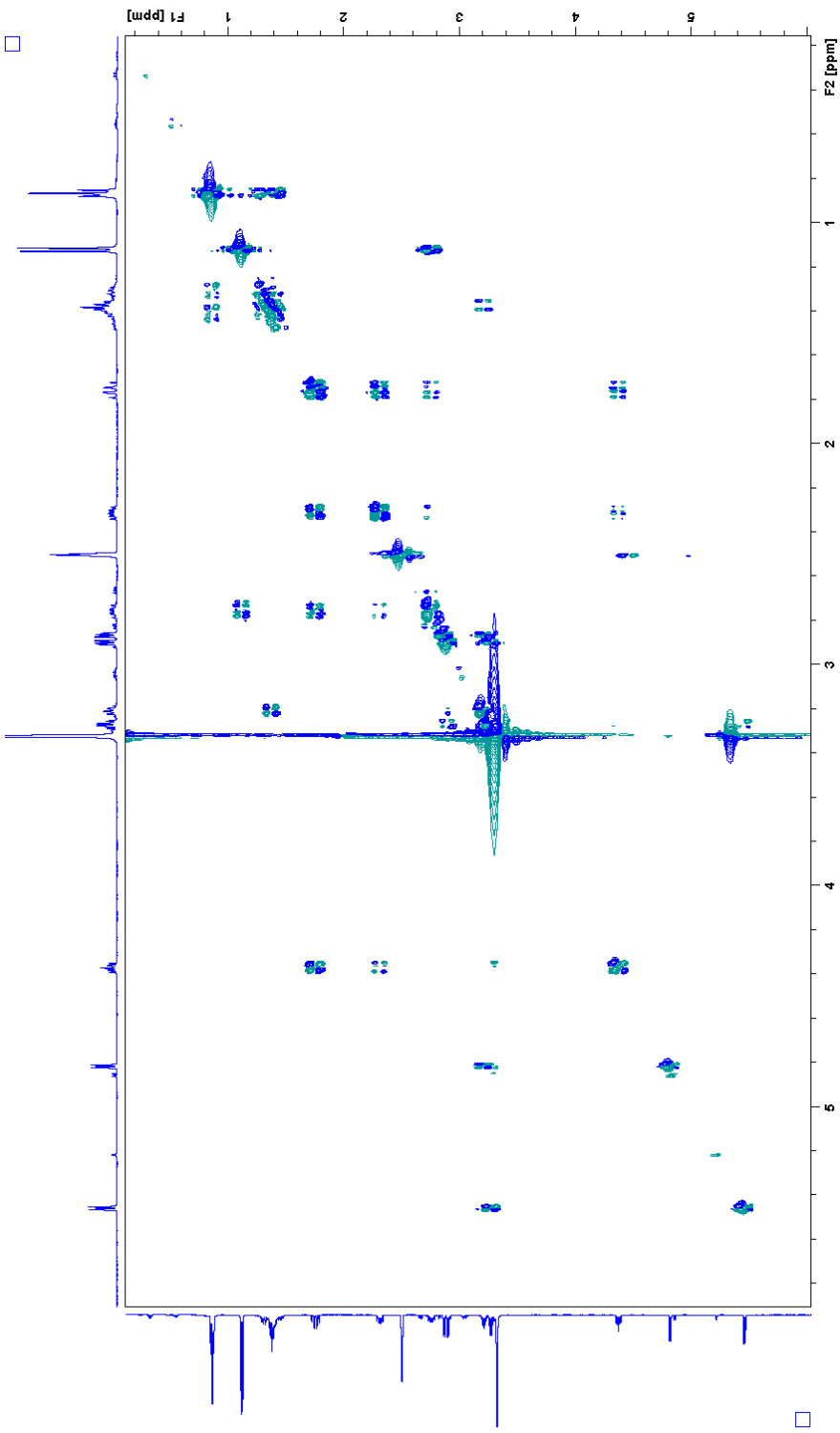

Figure S25. COSY spectrum of toblerol D (**4**) in DMSO-d_6.

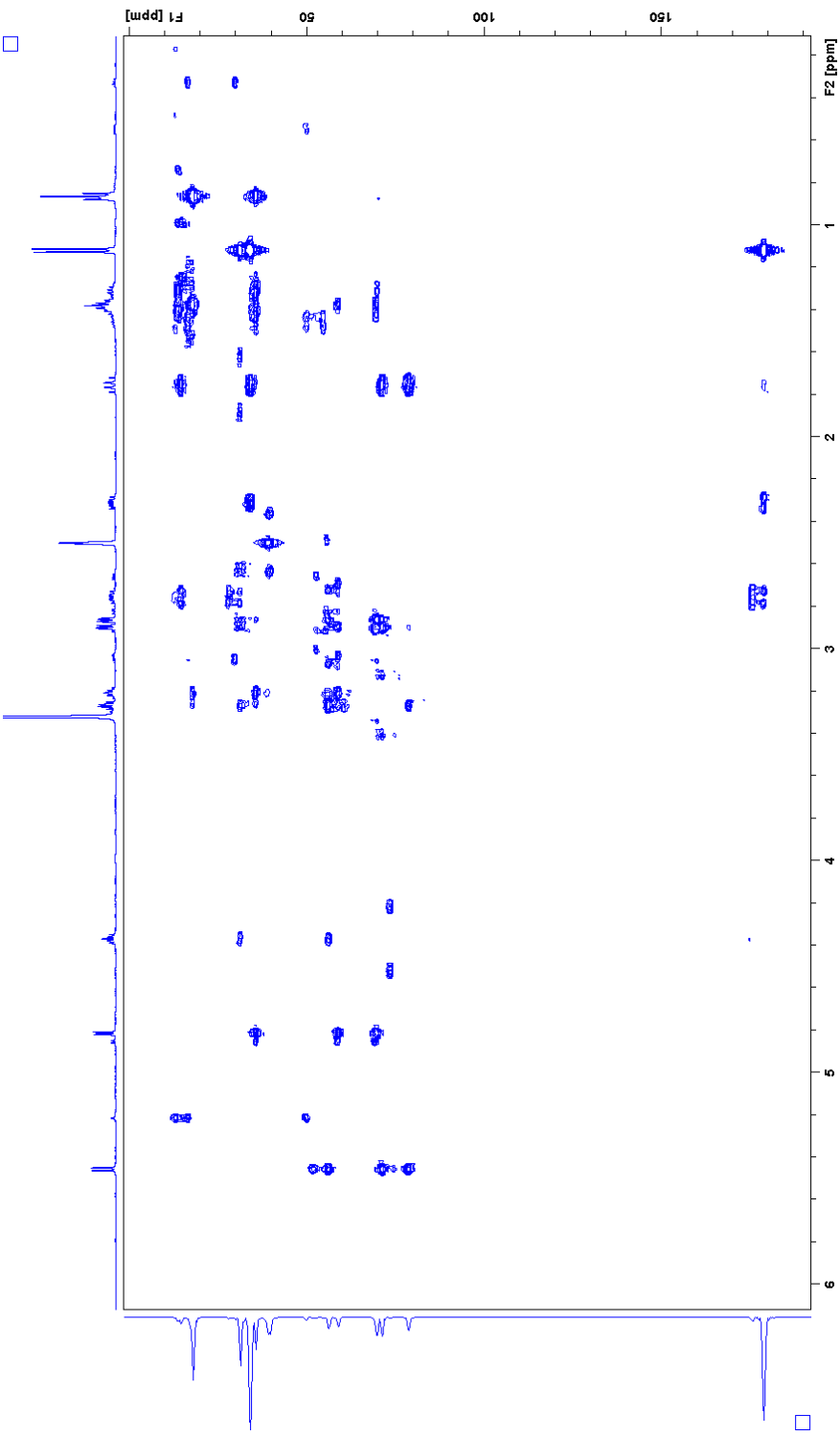

Figure S26. HMBC spectrum of toblerol D (**4**) in DMSO-d_6.

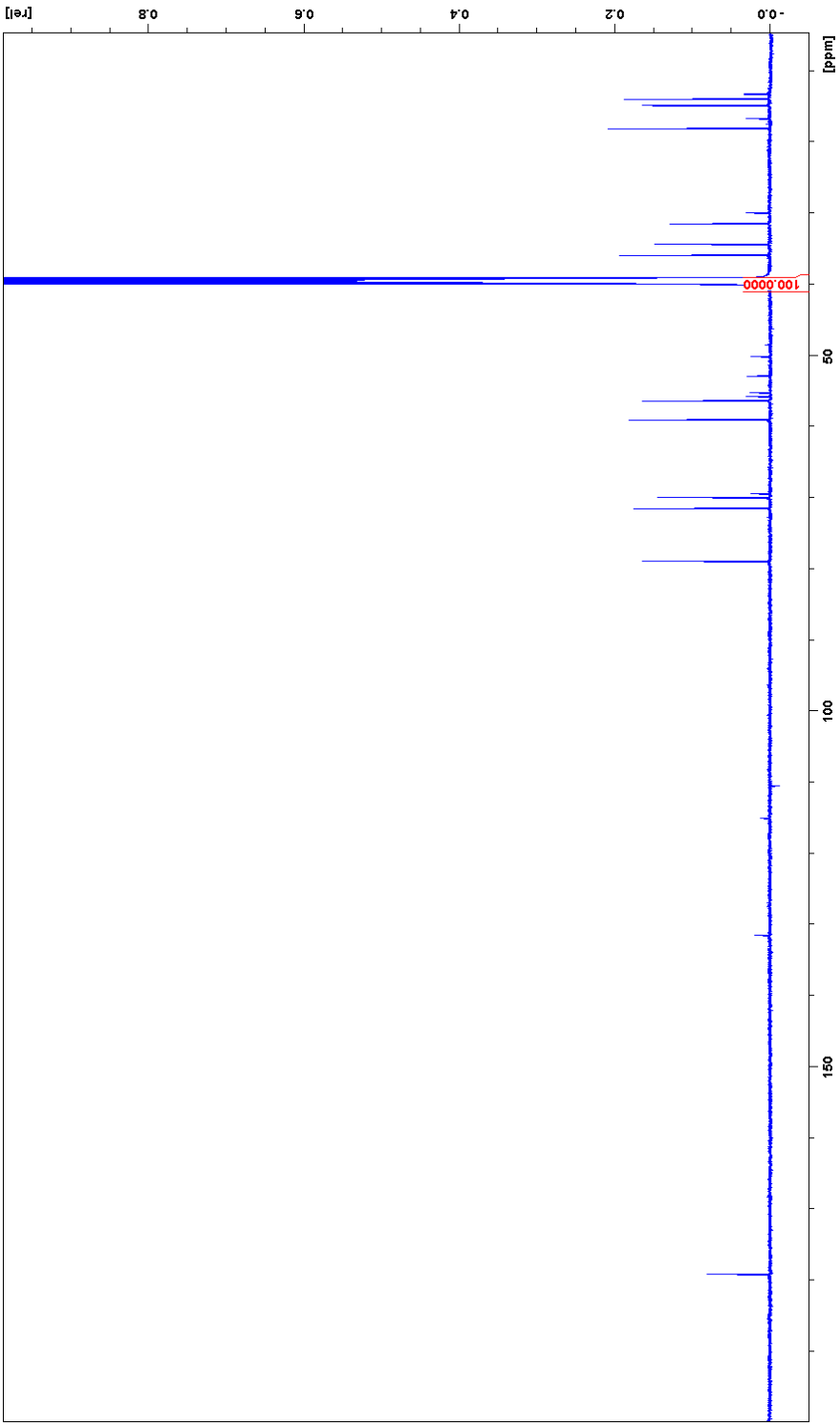

Figure S27. ^{13}C NMR spectrum of toblerol D (**4**) in DMSO-d_6.

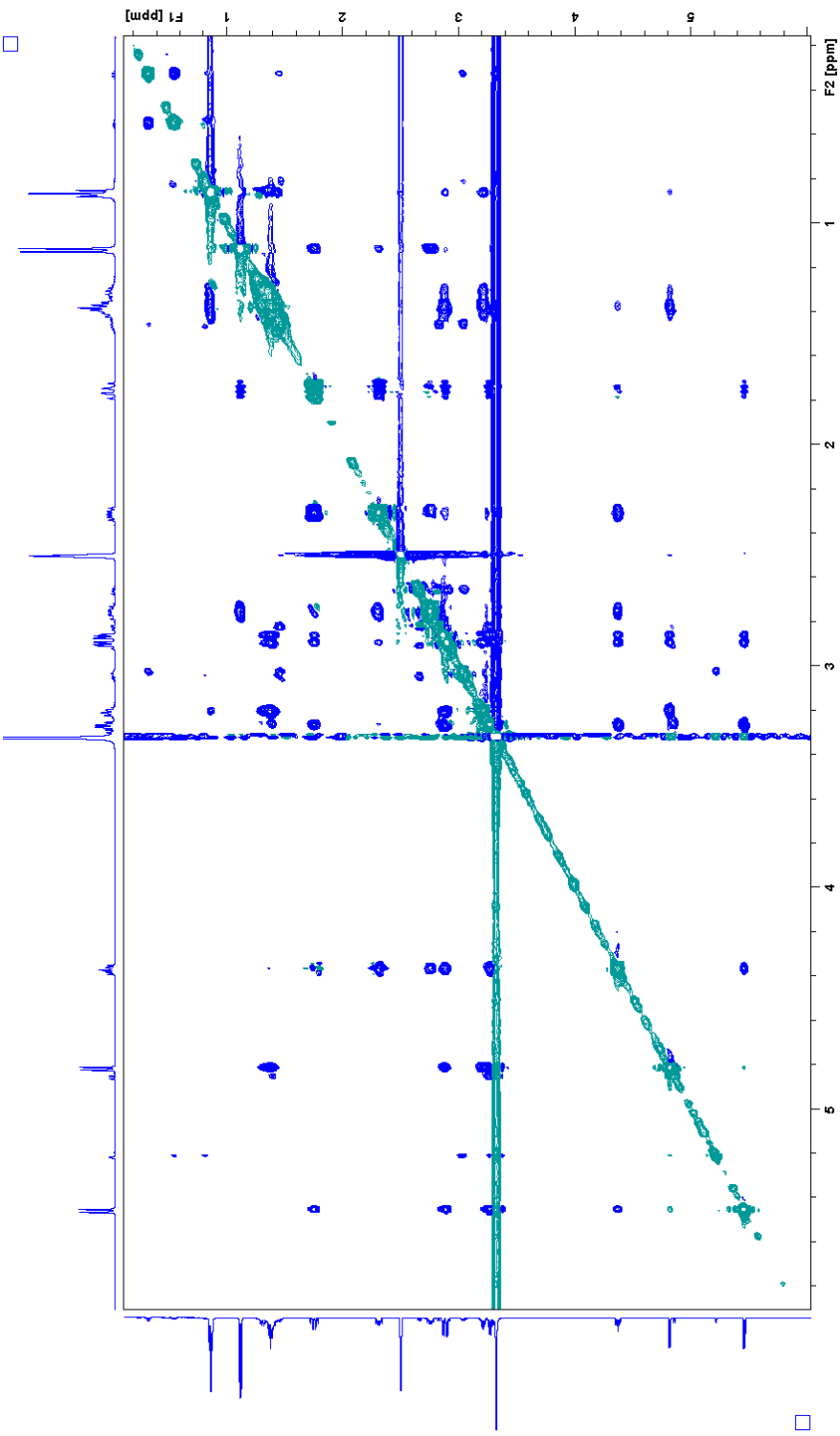

Figure S28. NOESY spectrum of toblerol D (**4**) in DMSO-d_6.

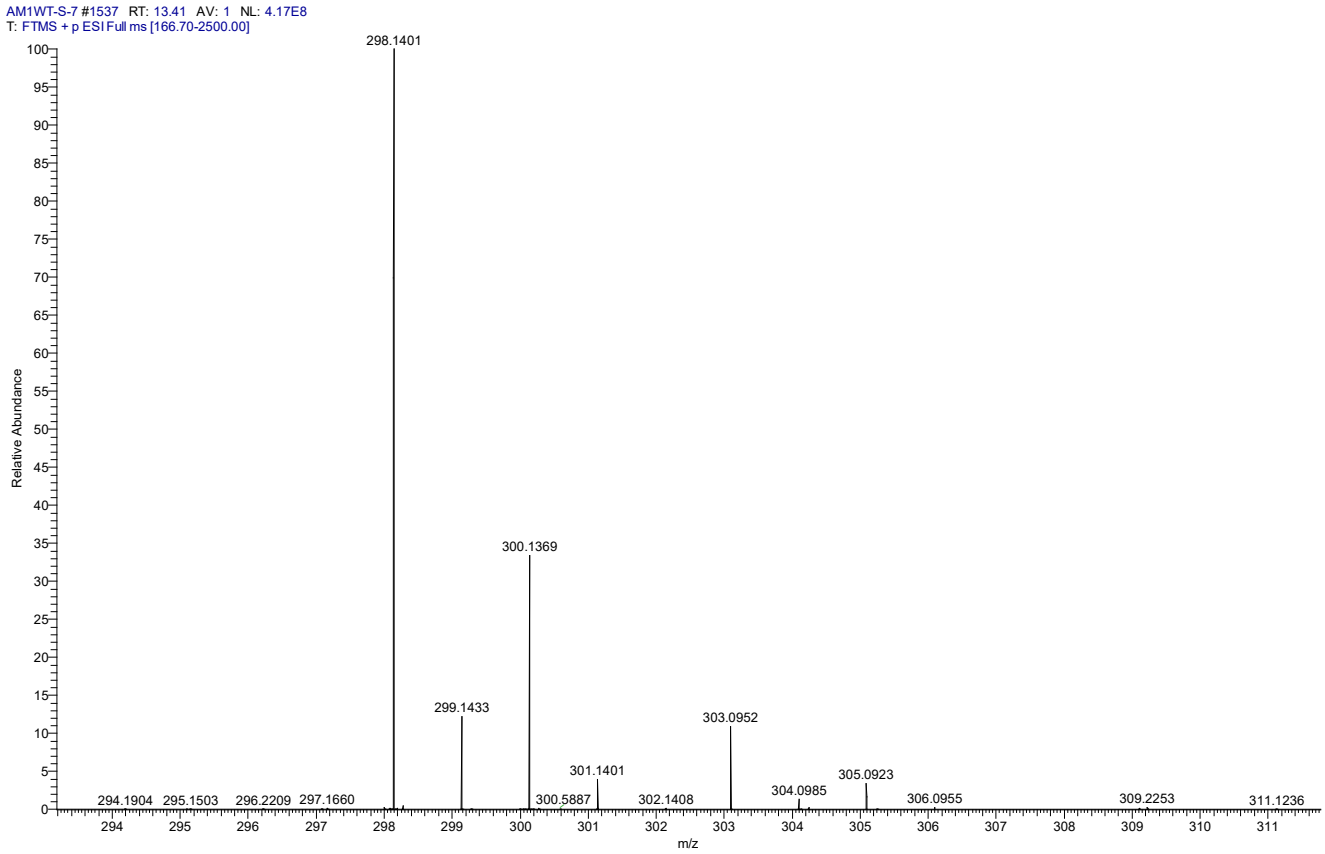

Figure S29: HR-LC-ESIMS data of toblerol E (**5**). Mass spectrum of the peak at 13.41 min (*m/z* 298.1401 $[M+NH_4]^+$ and *m/z* 303.0952 $[M+Na]^+$).

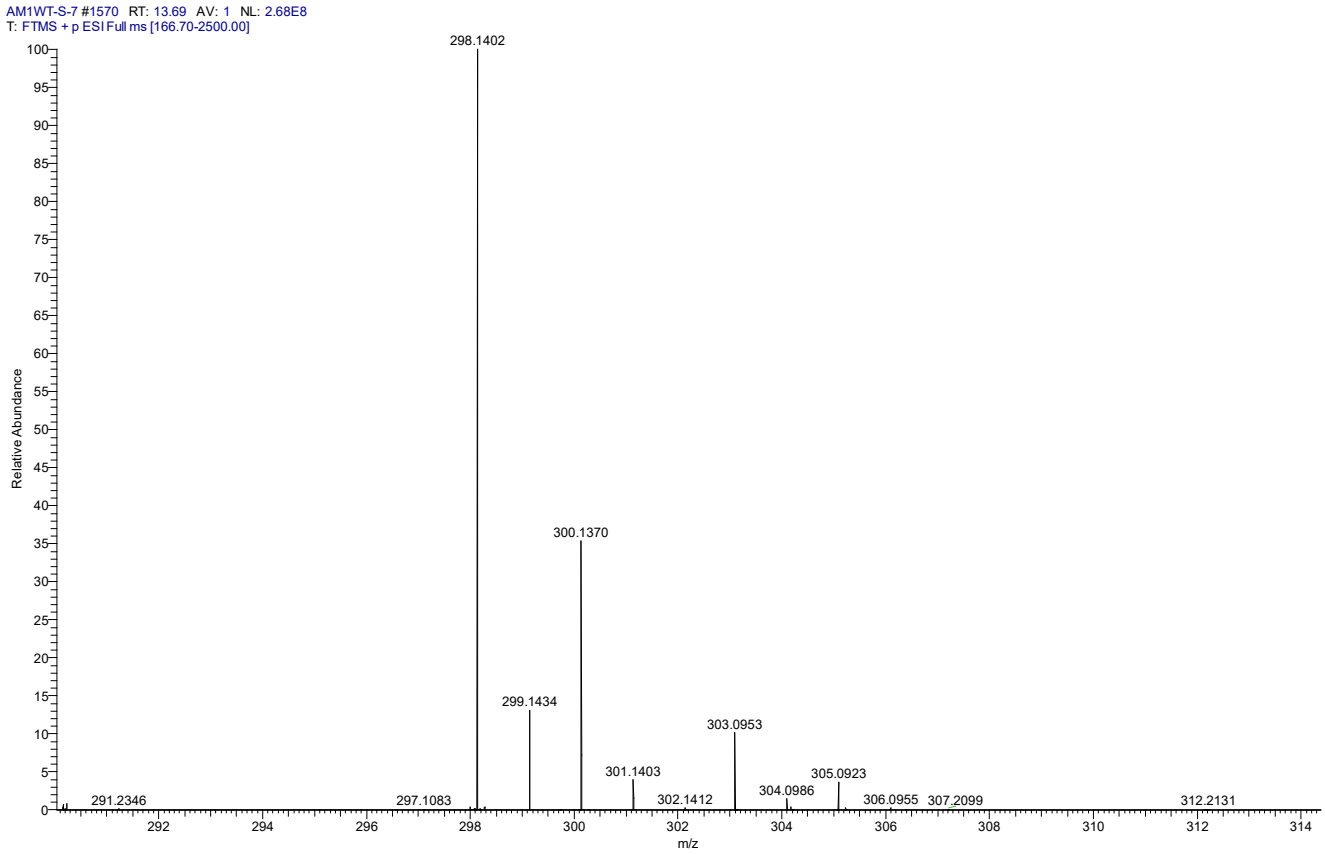

Figure S30: HR-LC-ESIMS data of toblerol G (**7**). Mass spectrum of the peak at 13.69 min (*m/z* 298.1402 $[M+NH_4]^+$ and *m/z* 303.0953 $[M+Na]^+$).

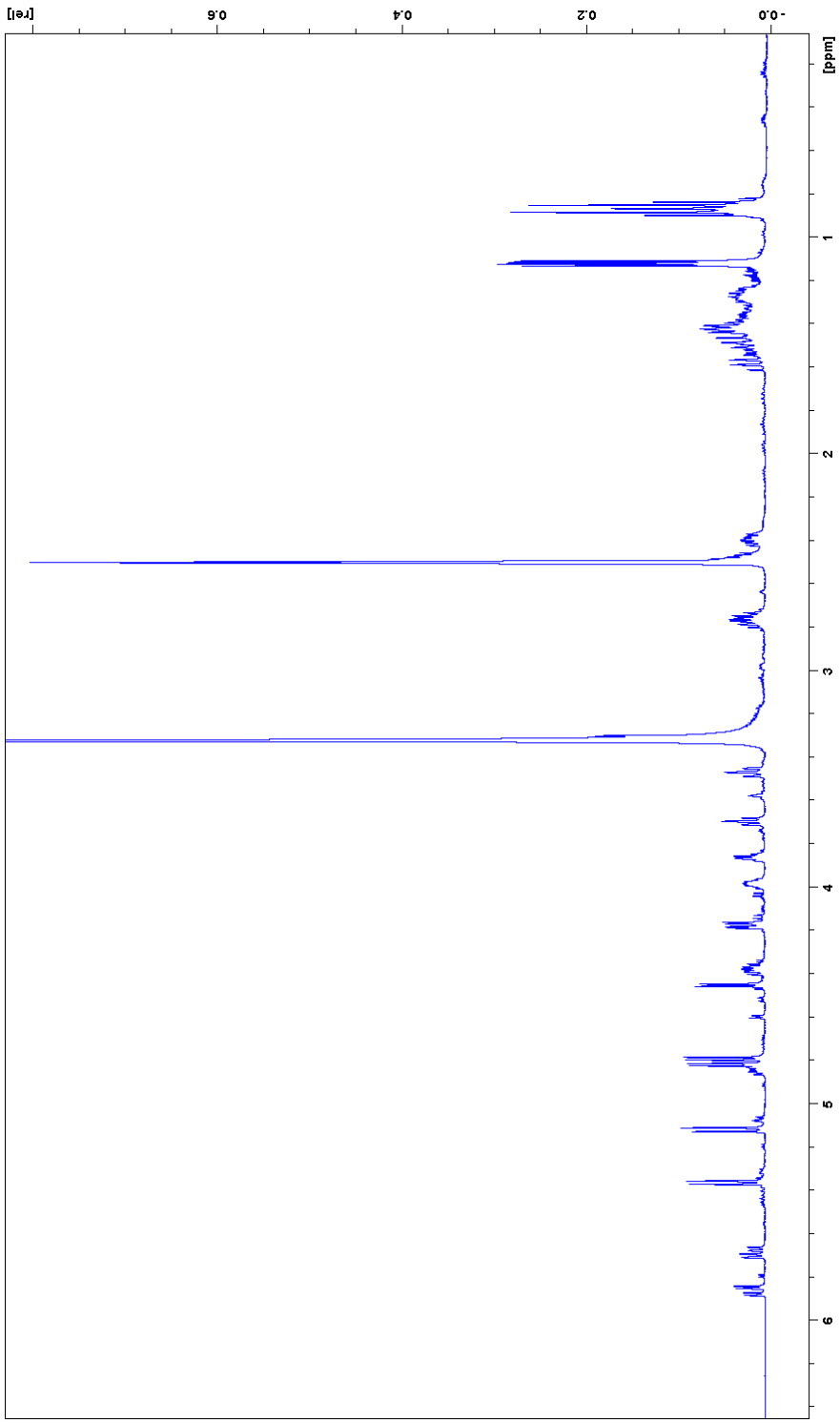

Figure S31. ^{1}H NMR spectrum of the mixture of toblerol E (**5**) and F (**6**) in DMSO-d_6.

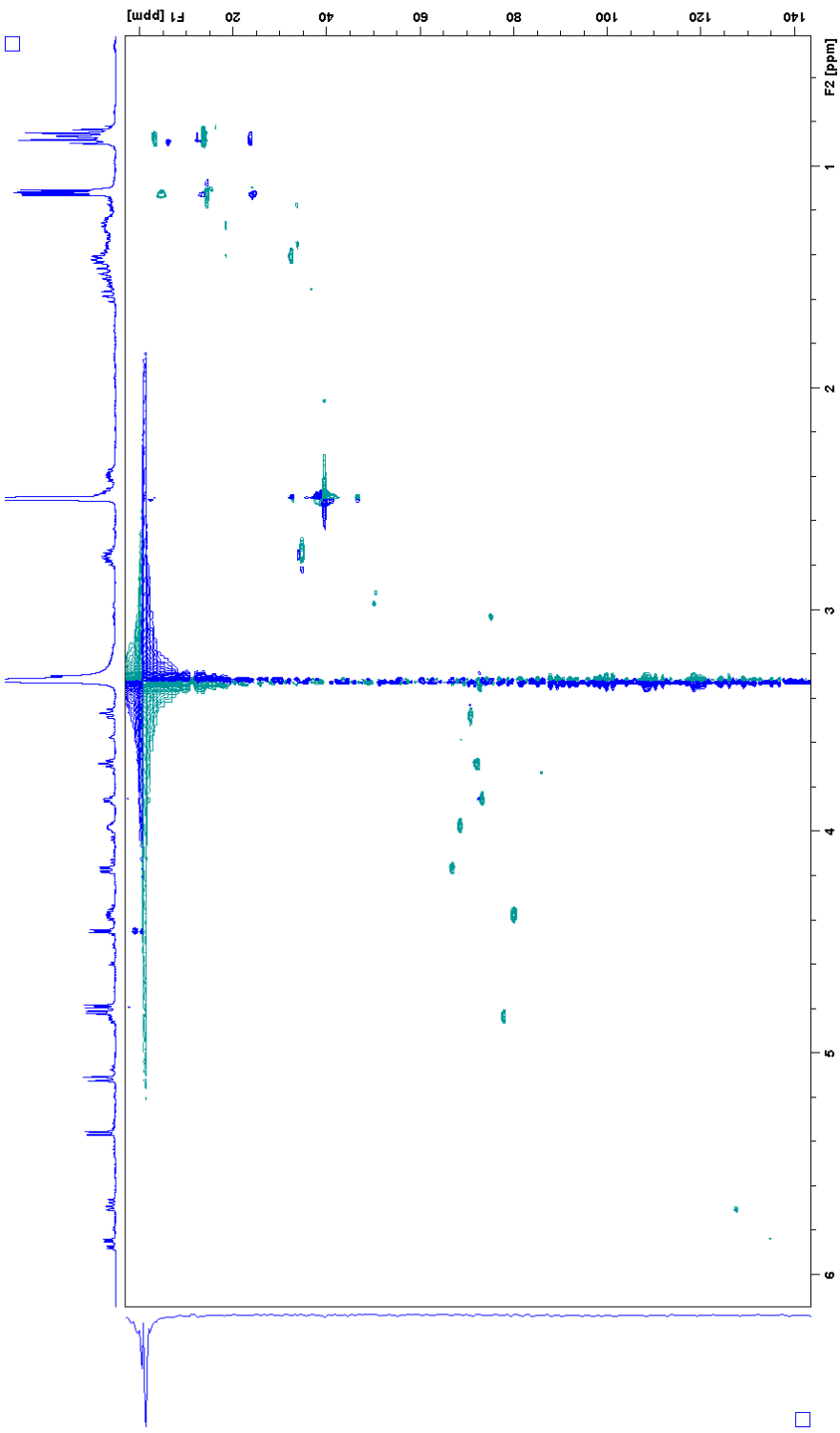

Figure S32. HSQC spectrum of toblerol E (**5**) and F (**6**) in DMSO-d_6.

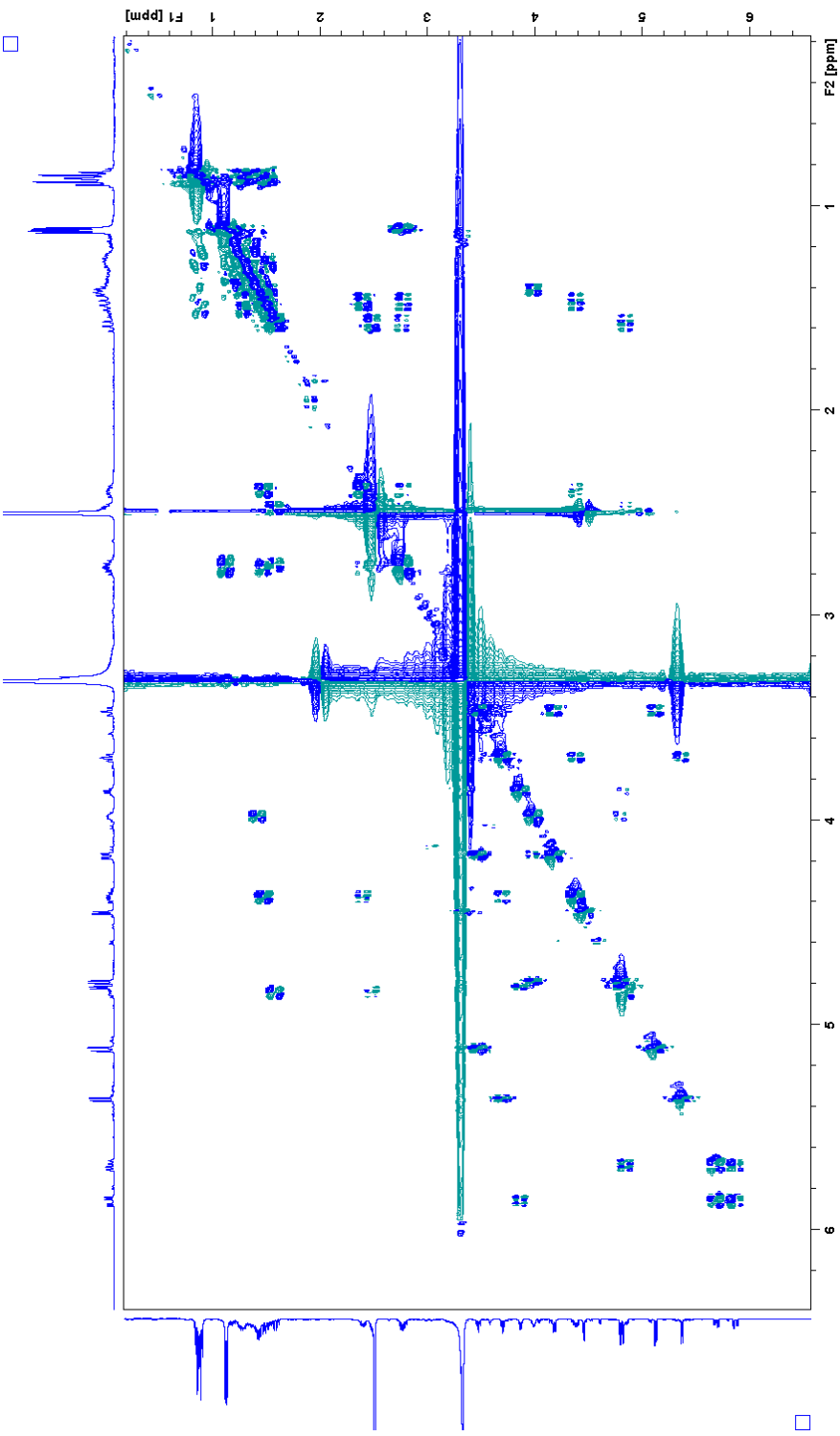

Figure S33. COSY spectrum of toblerol E (**5**) and F (**6**) in DMSO-d_6.

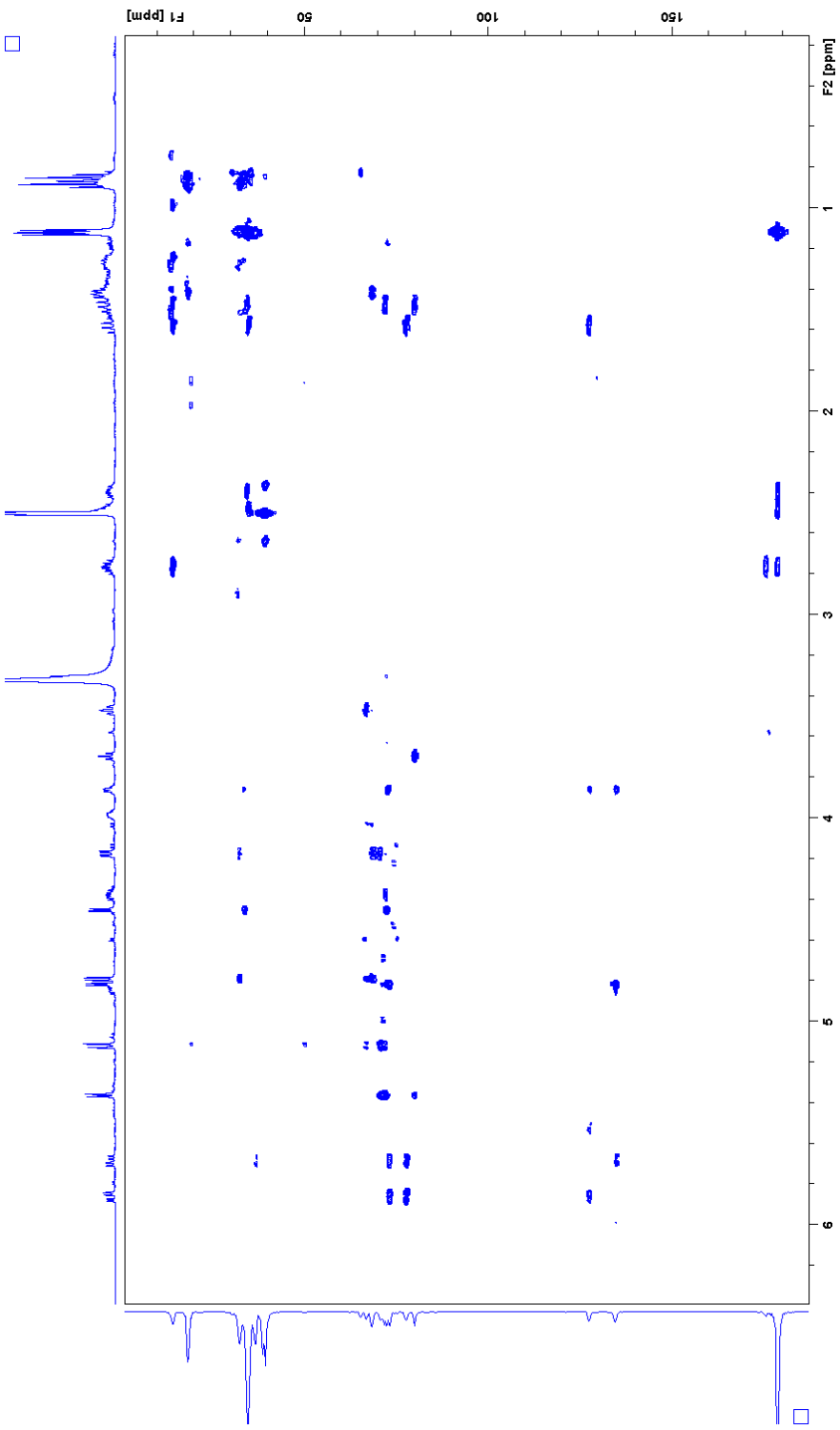

Figure S34. HMBC spectrum of toblerol E (**5**) and F (**6**) in DMSO-d_6.

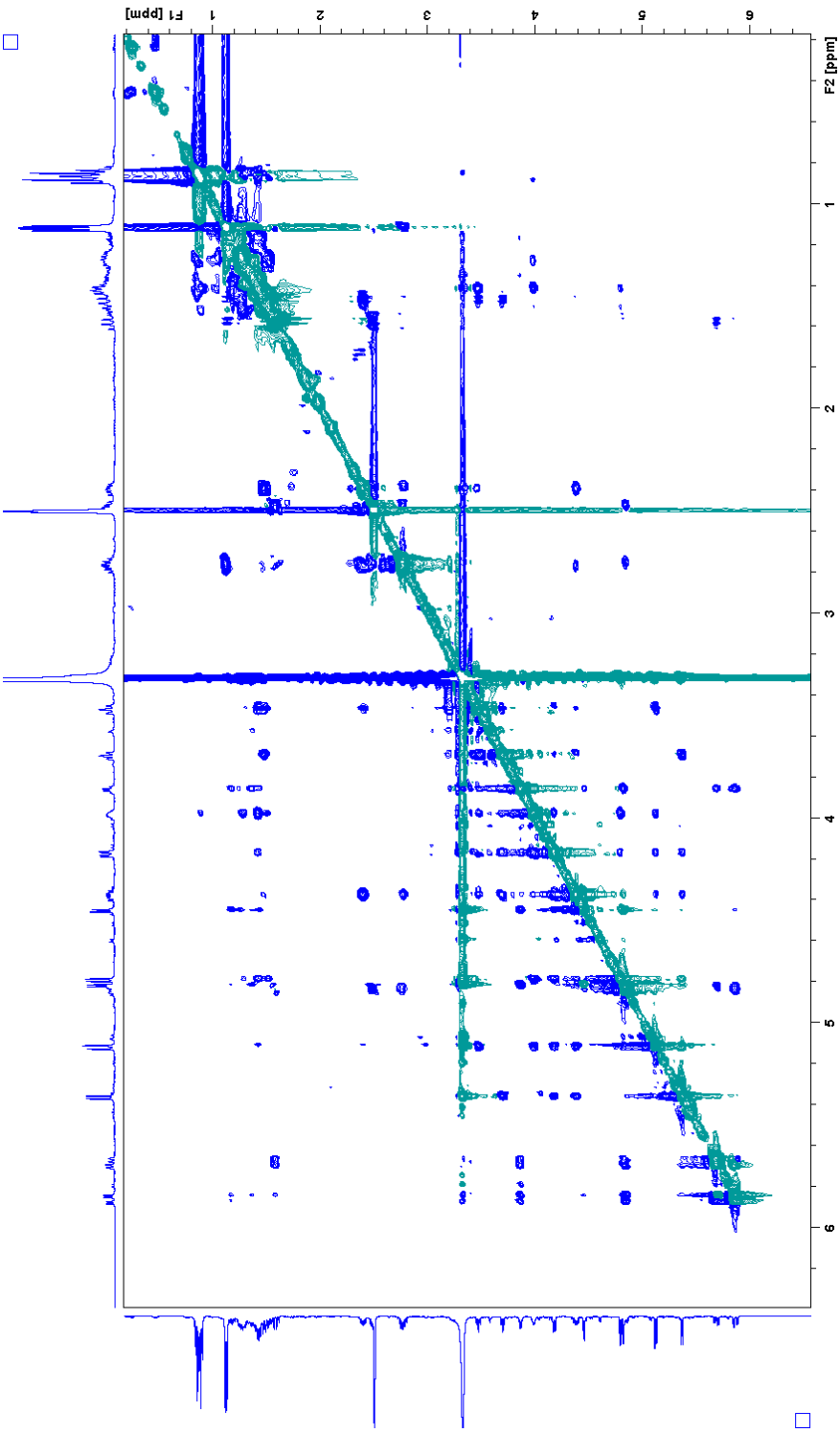

Figure S35. NOESY spectrum of toblerol E (**5**) and F (**6**) in DMSO-d_6.

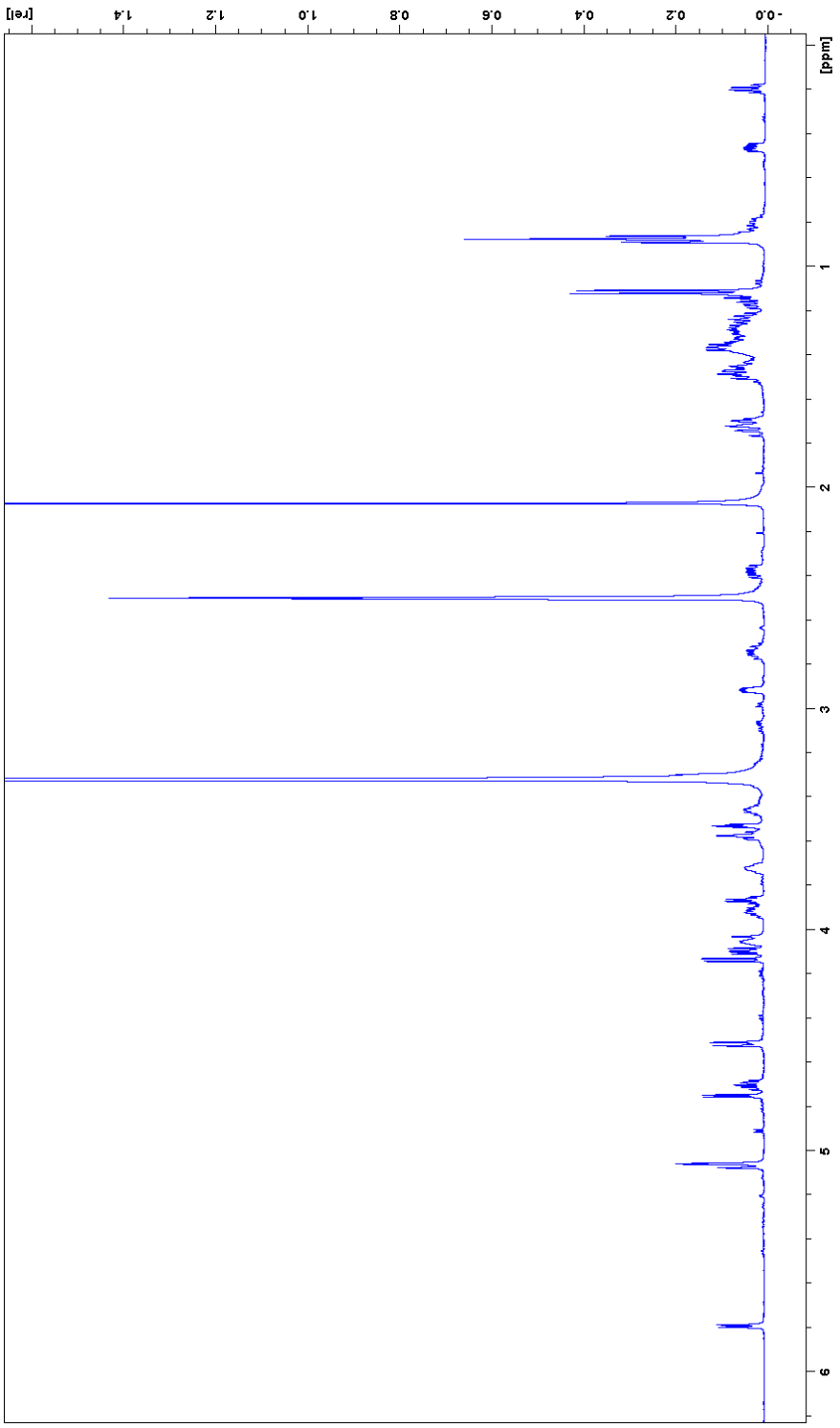

Figure S36. ^{1}H NMR spectrum of the mixture of toblerol G (**7**) and H (**8**) in DMSO-d_6.

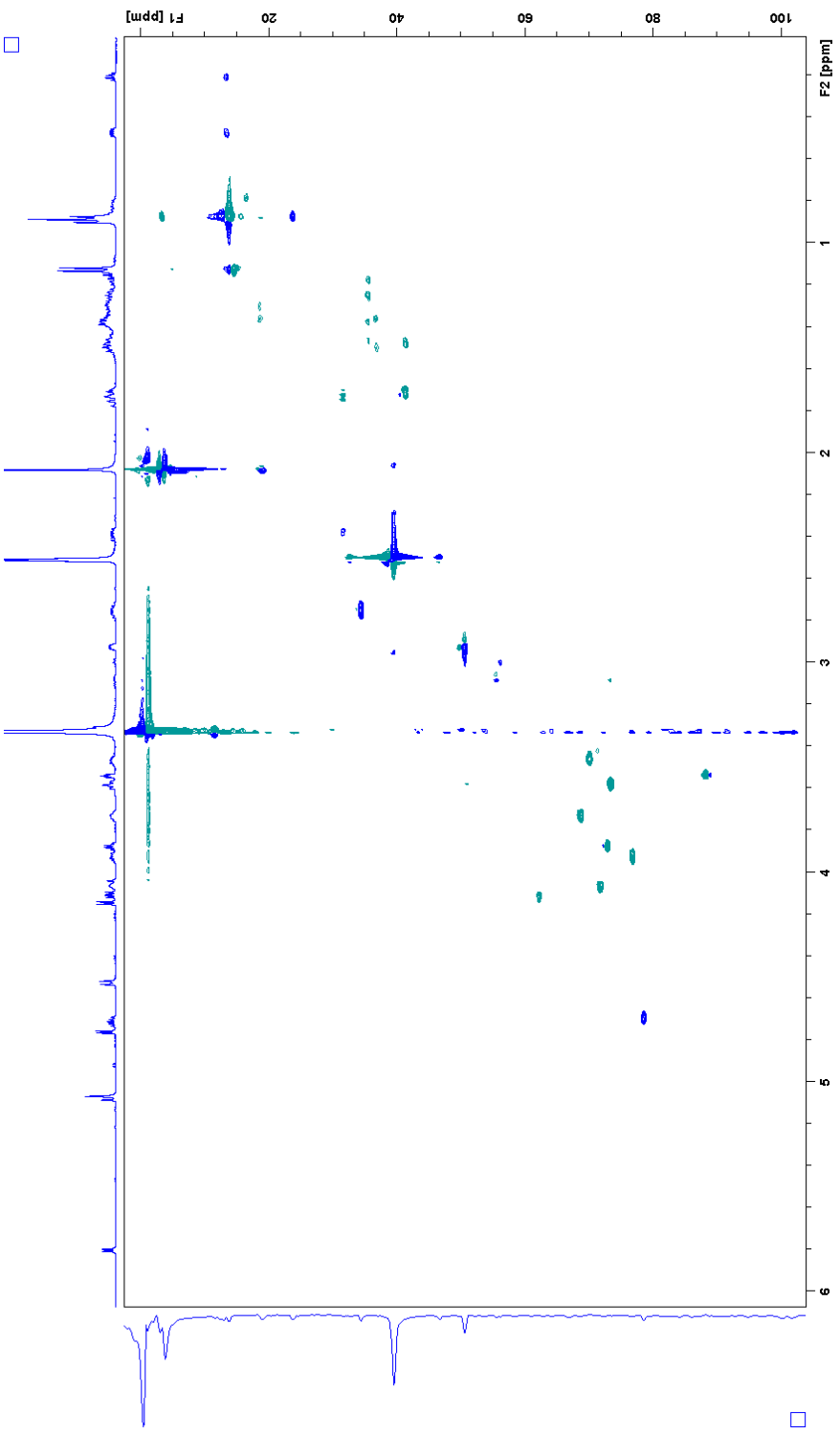

Figure S37. HSQC spectrum of toblerol G (**7**) and H (**8**) in DMSO-d_6.

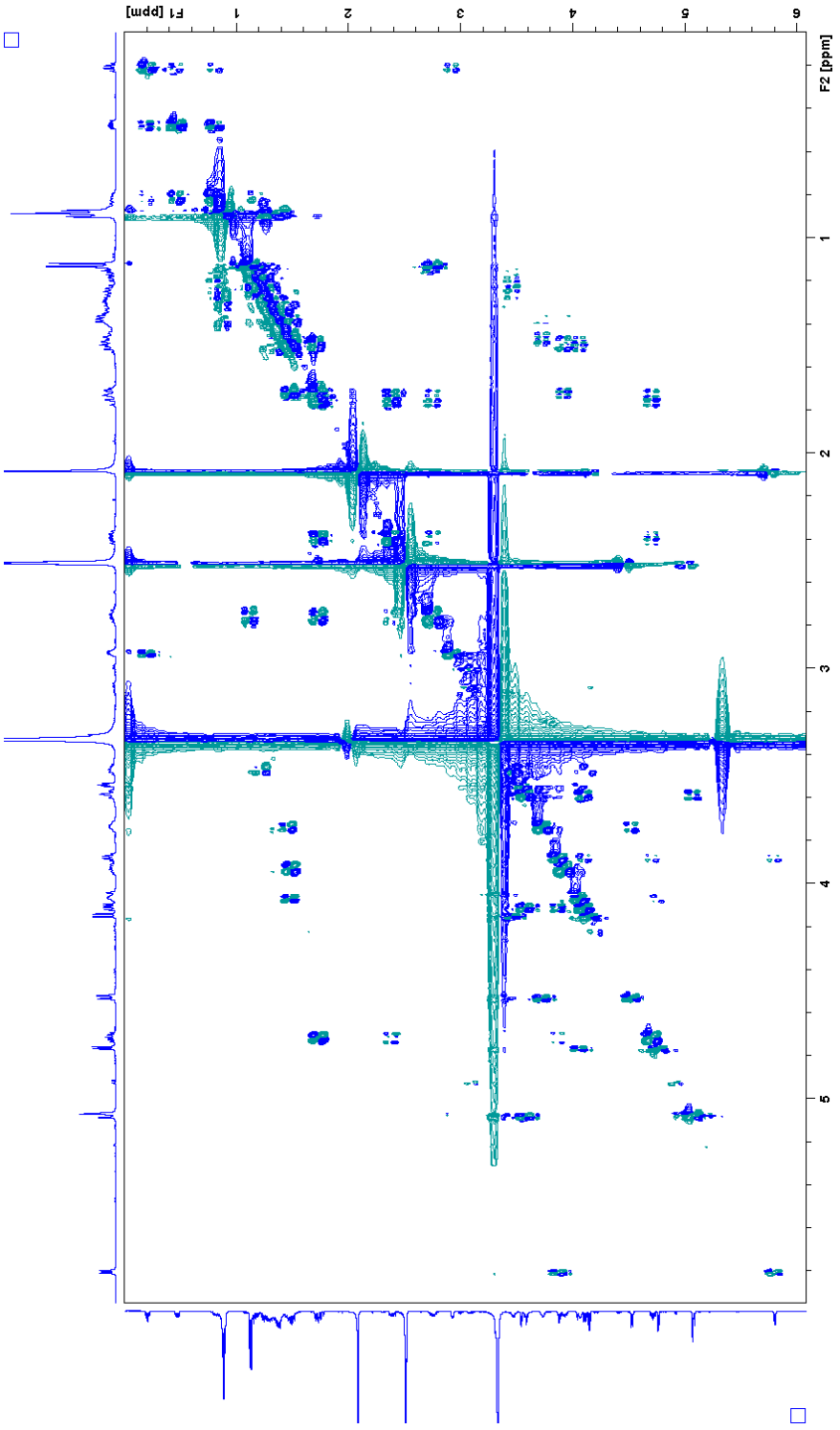

Figure S38. COSY spectrum of toblerol G (**7**) and H (**8**) in DMSO-d_6.

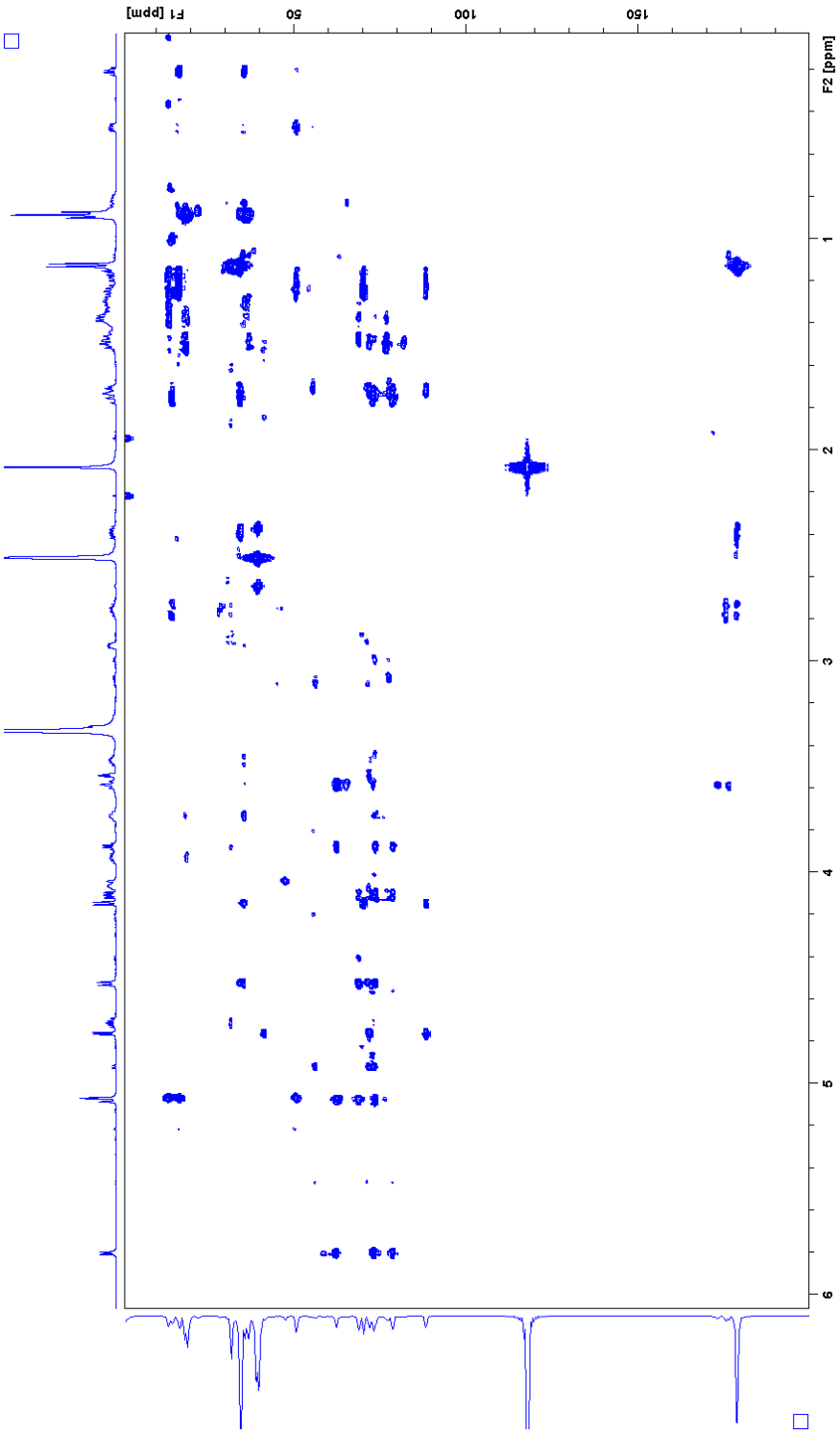

Figure S39. HMBC spectrum of toblerol G (**7**) and H (**8**) in DMSO-d_6.

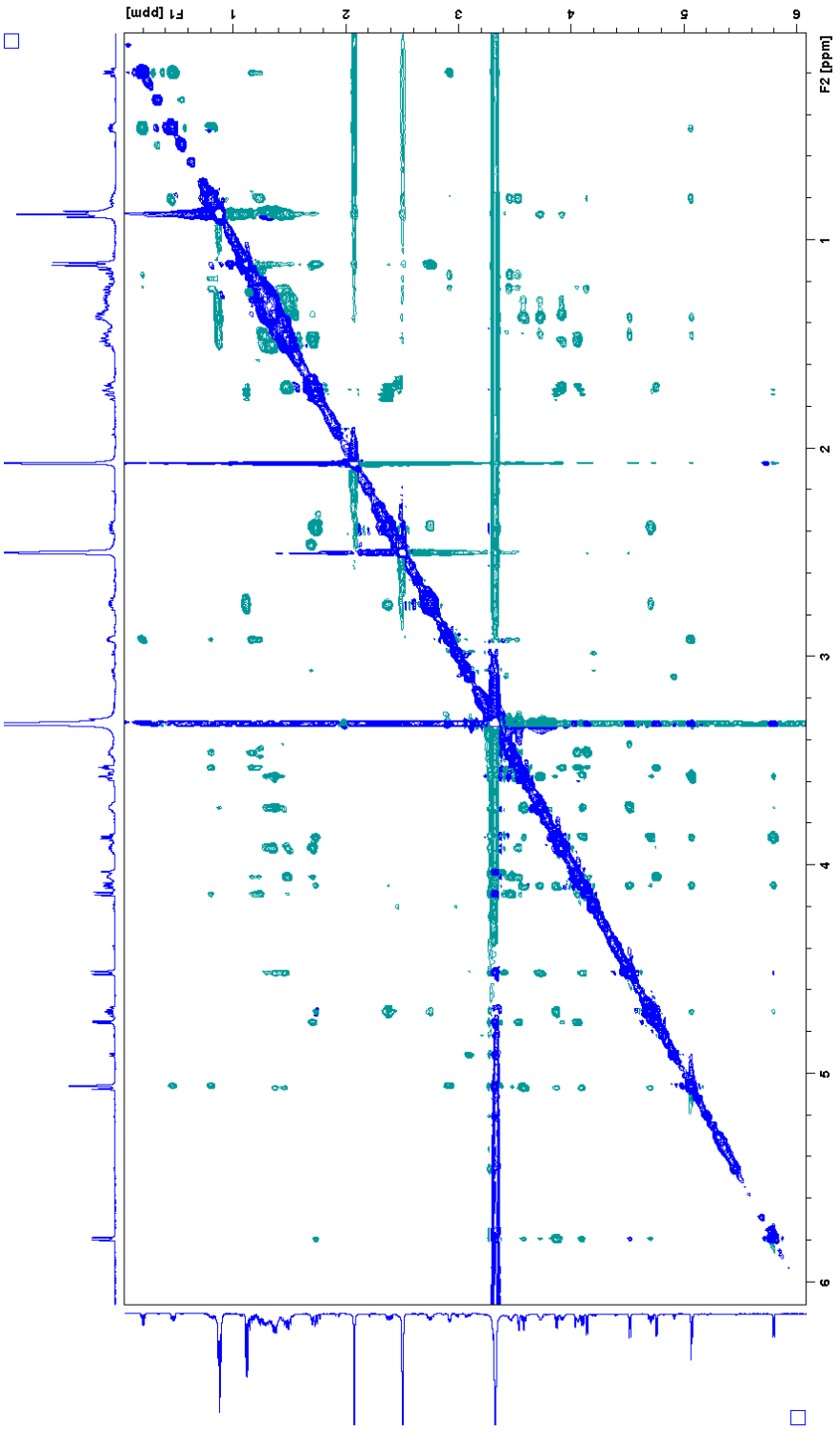

Figure S40. NOESY spectrum of toblerol G (**7**) and H (**8**) in DMSO-d_6.

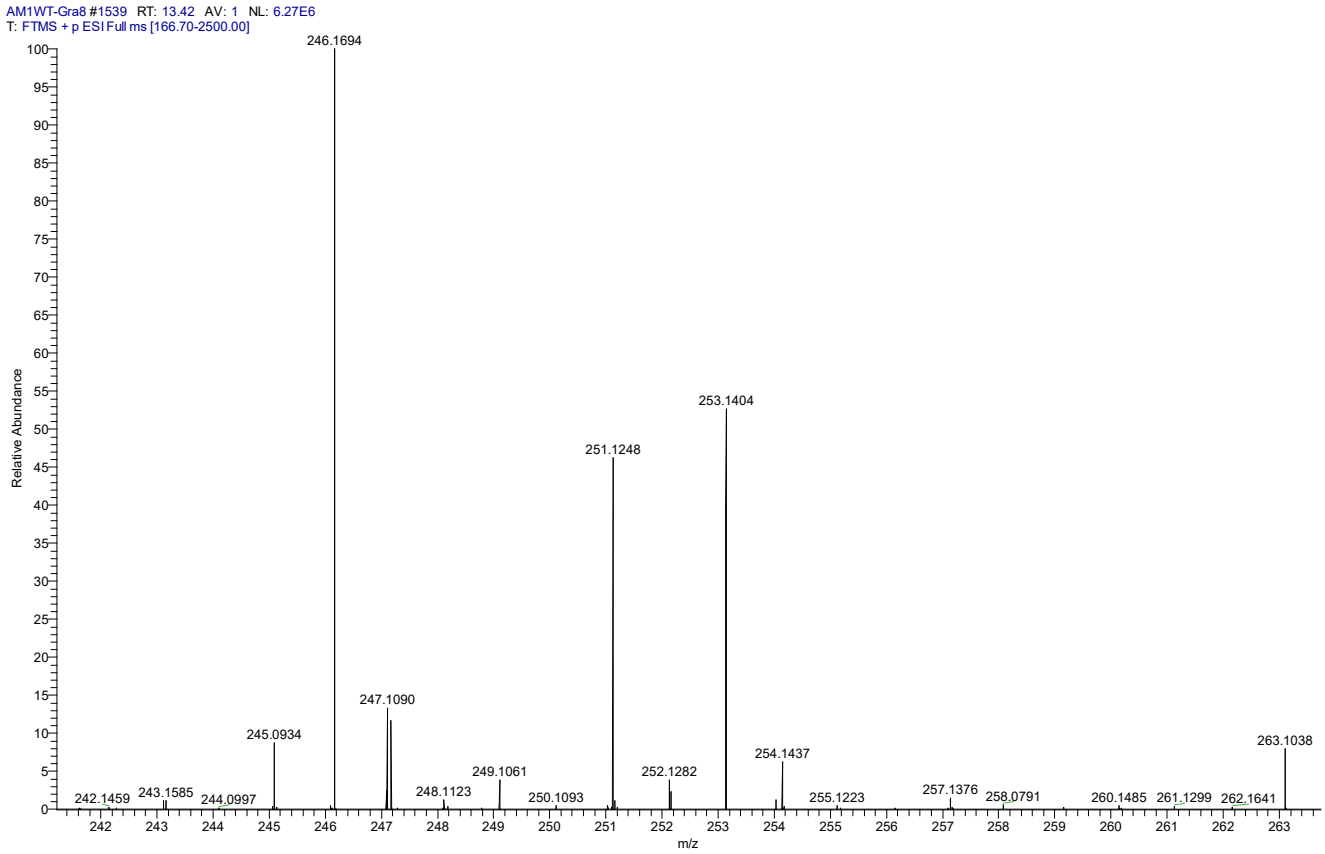

Figure S41: HR-LC-ESIMS data of toblerol F (**6**). Mass spectrum of the peak at 13.41 min (*m/z* 246.1696 $[M+NH_4]^+$ and *m/z* 251.1248 $[M+Na]^+$).

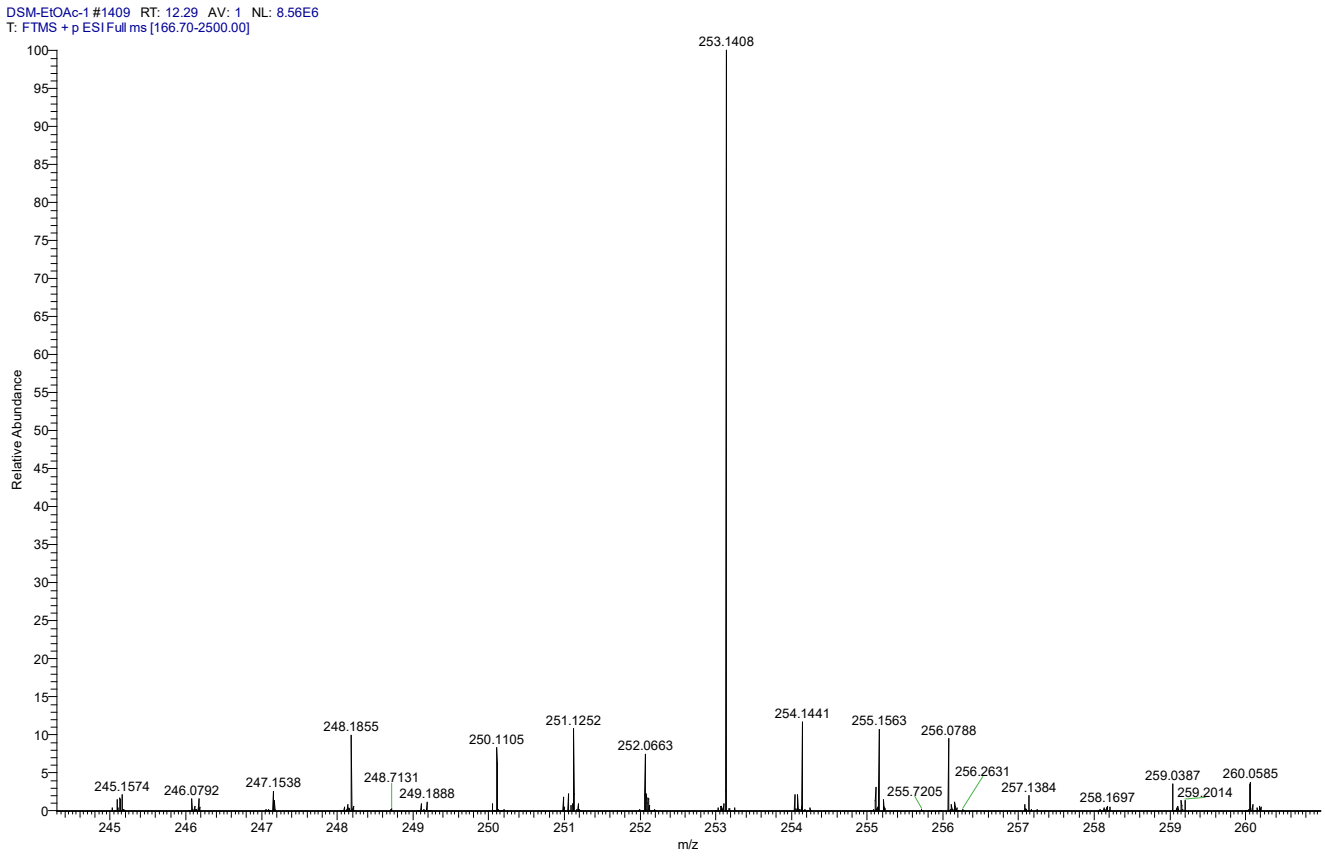

Figure S42: HR-LC-ESIMS data of toblerol H (**8**). Mass spectrum of the peak at 12.29 min (*m/z* 248.1855 $[M+NH_4]^+$ and *m/z* 253.1408 $[M+Na]^+$).

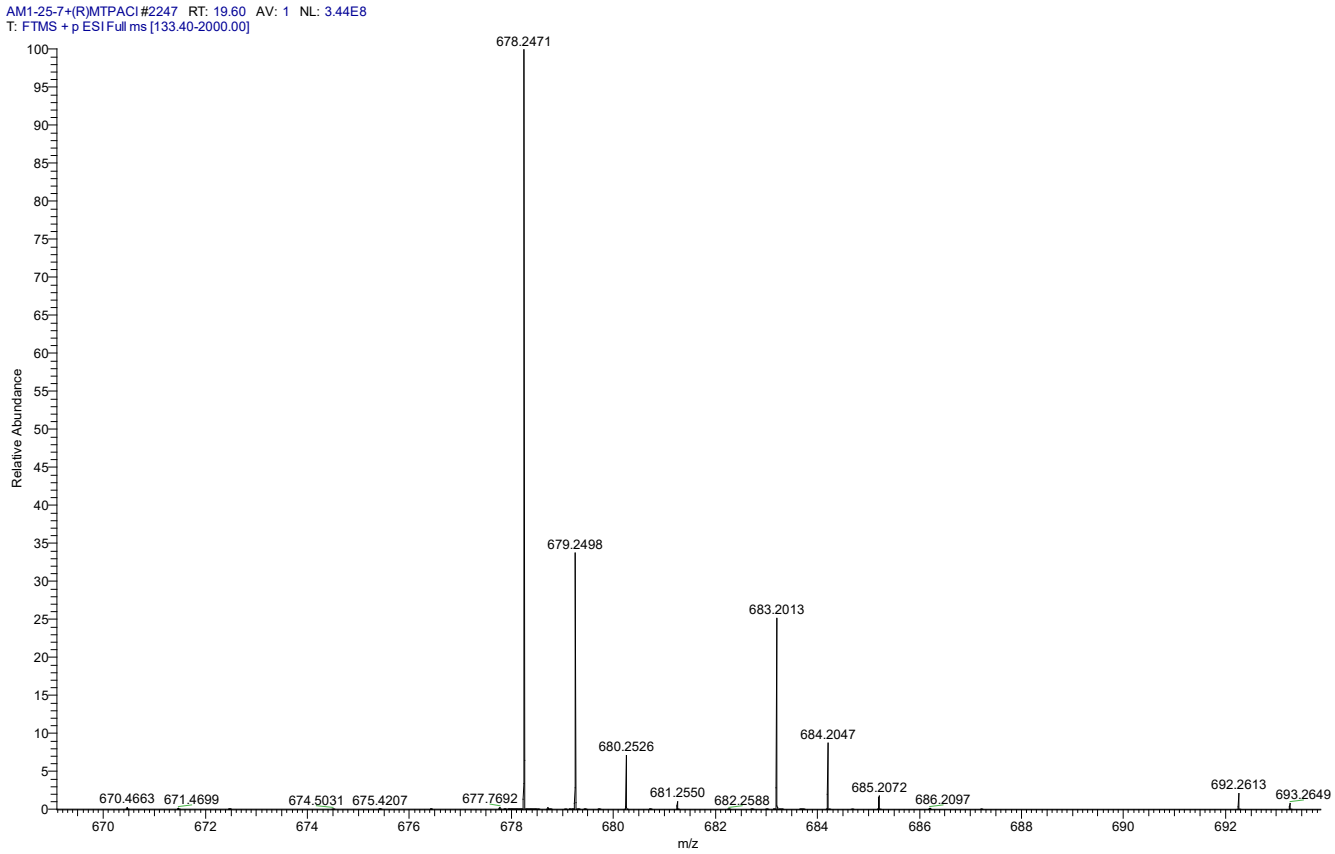

Figure S43: HR-LC-ESIMS data of toblerol B-(*S*)-MTPA ester (**2b**). Mass spectrum of the peak at 19.60 min (*m/z* 678.2471 $[M+NH_4]^+$ and *m/z* 683.2013 $[M+Na]^+$).

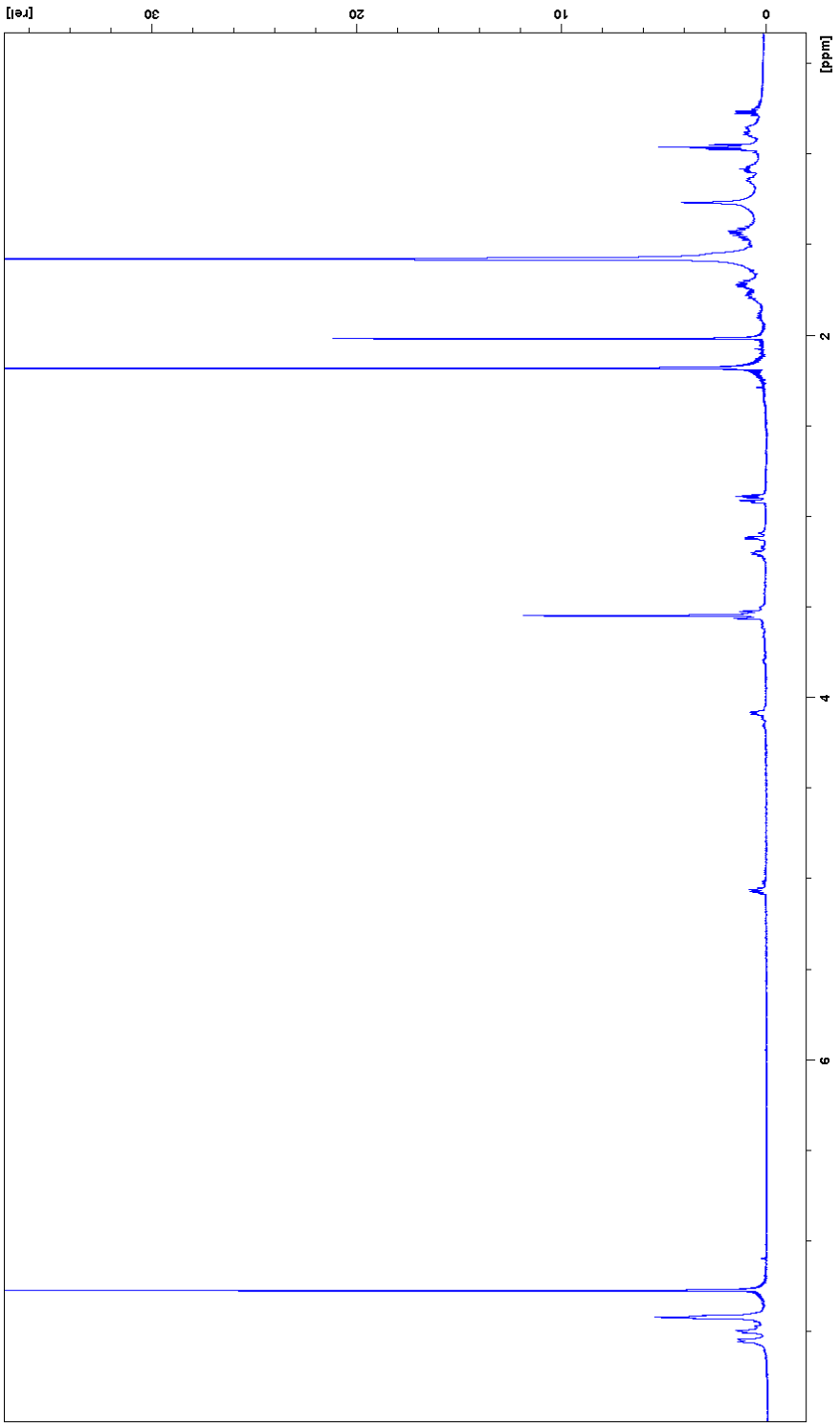

Figure S44. ^{1}H NMR spectrum of toblerol B-(*S*)-MTPA ester (**2b**) in chloroform-*d*.

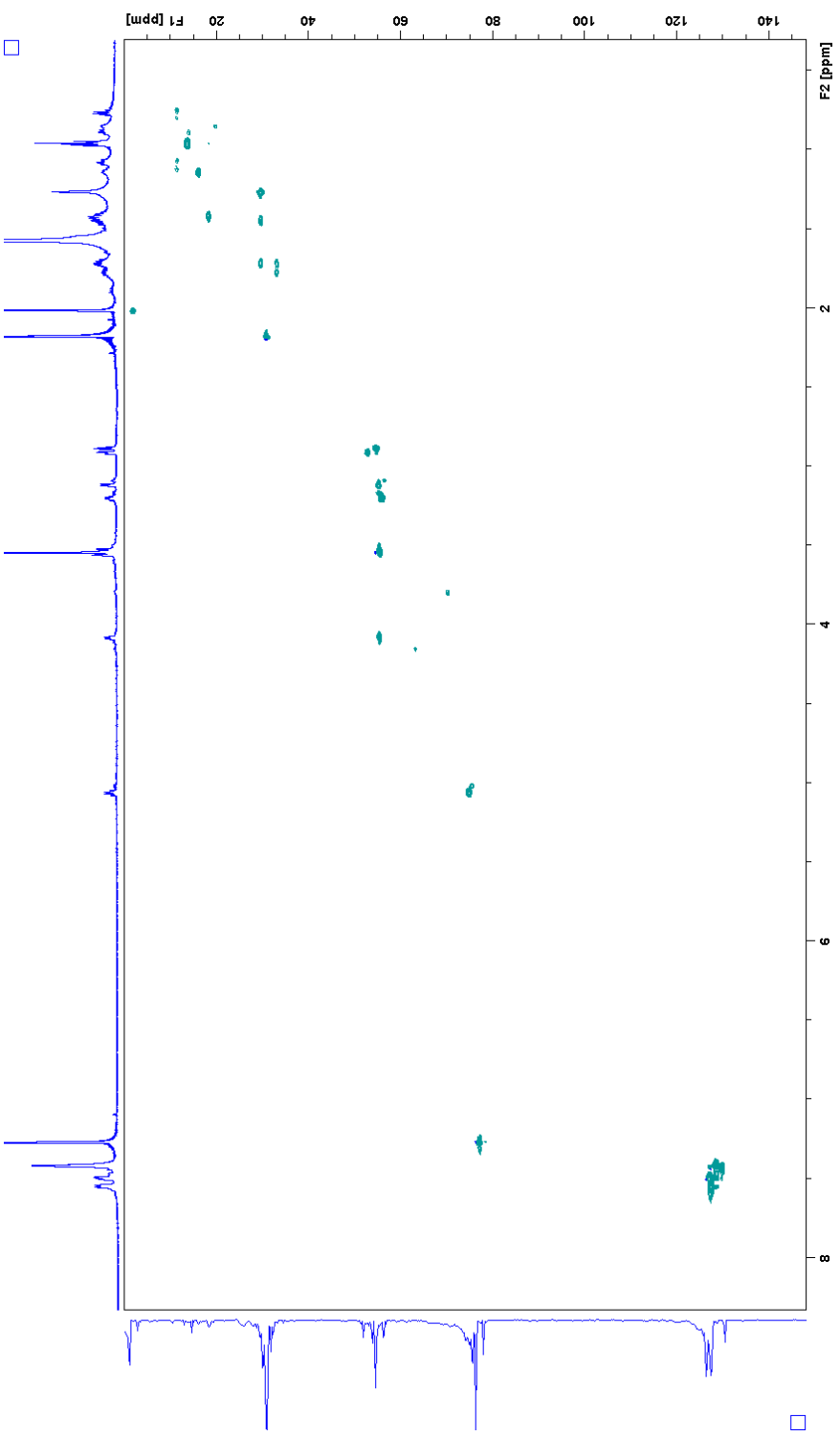

Figure S45. HSQC spectrum of toblerol B-(*S*)-MTPA ester (**2b**) in chloroform-*d*.

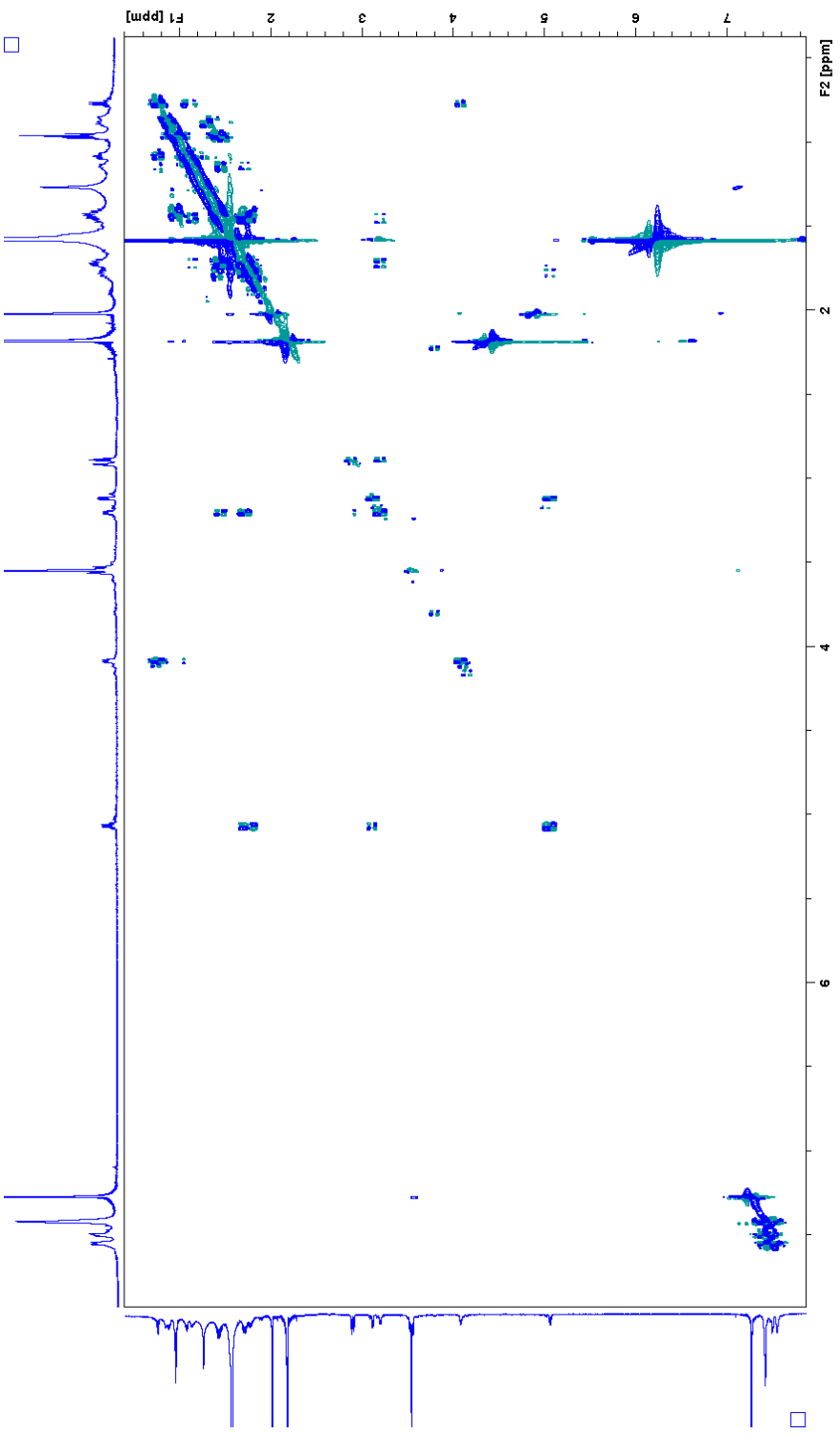

Figure S46. COSY spectrum of toblerol B-(*S*)-MTPA ester (**2b**) in chloroform-*d*.

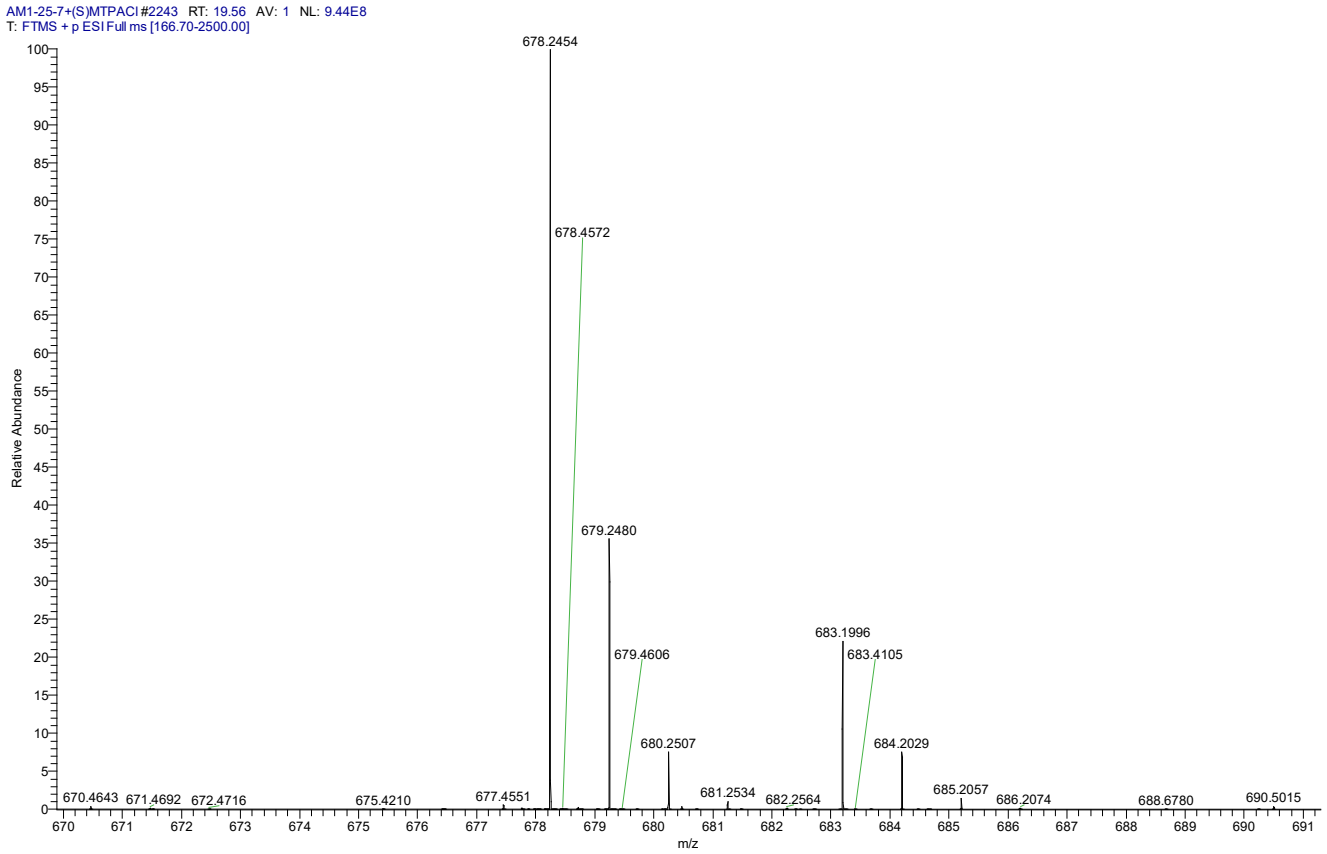

Figure S47: HR-LC-ESIMS data of toblerol B-(*R*)-MTPA ester (**2c**). Mass spectrum of the peak at 19.56 min (*m/z* 678.2454 $[M+NH_4]^+$ and *m/z* 683.1996 $[M+Na]^+$).

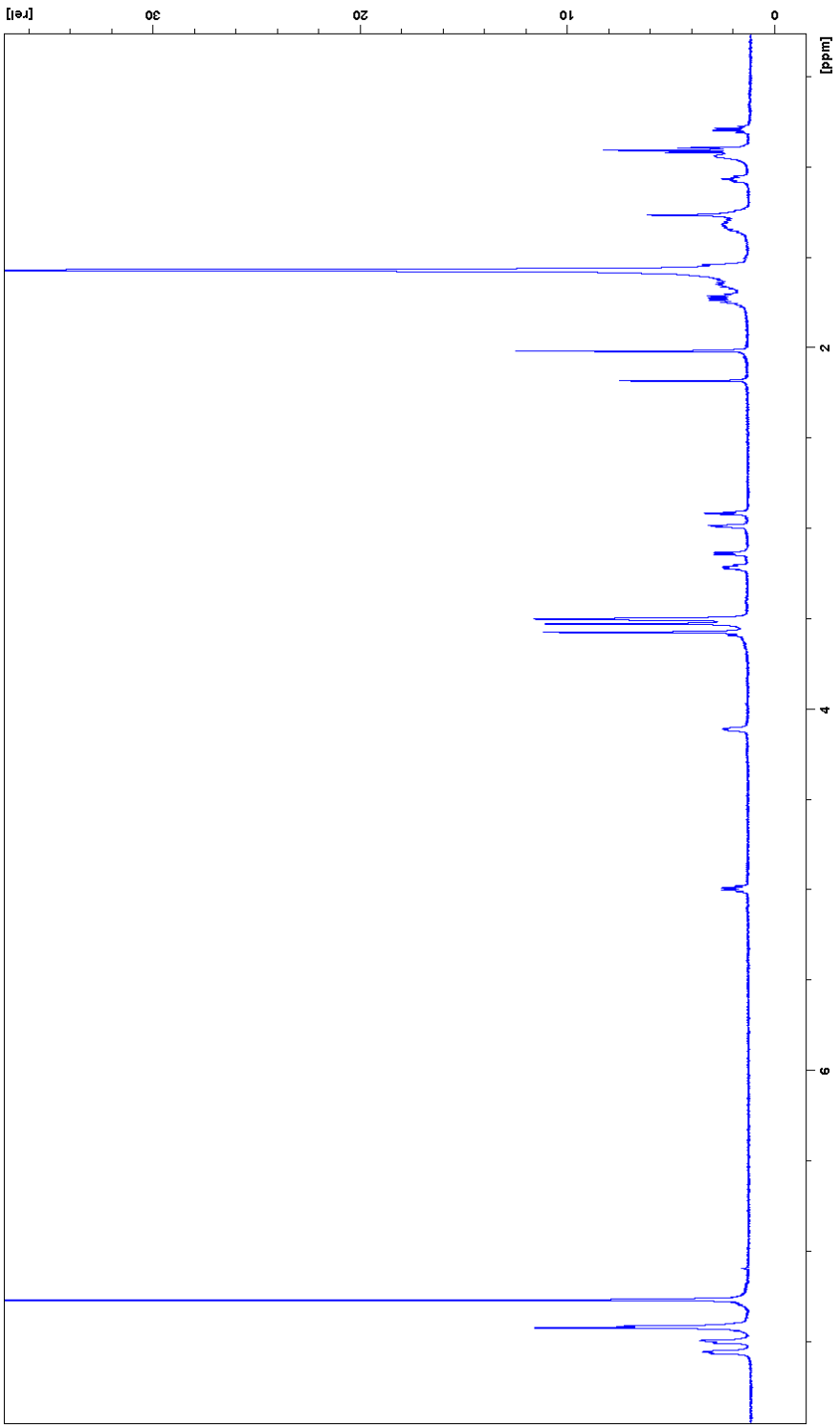

Figure S48. ^{1}H NMR spectrum of toblerol B-(*R*)-MTPA ester (**2c**) in chloroform-*d*.

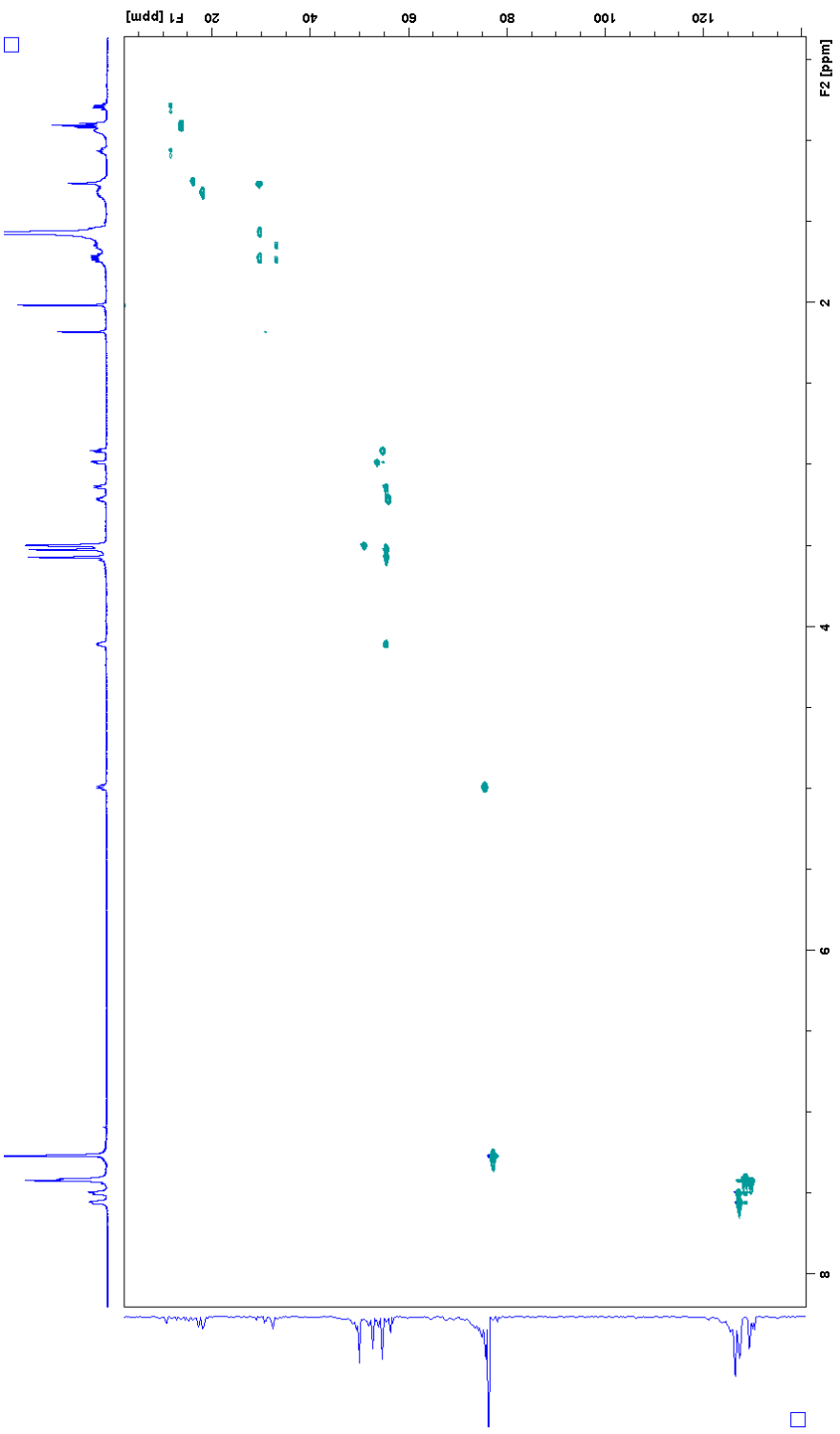

Figure S49. HSQC spectrum of toblerol B-(*R*)-MTPA ester (**2c**) in chloroform-*d*.

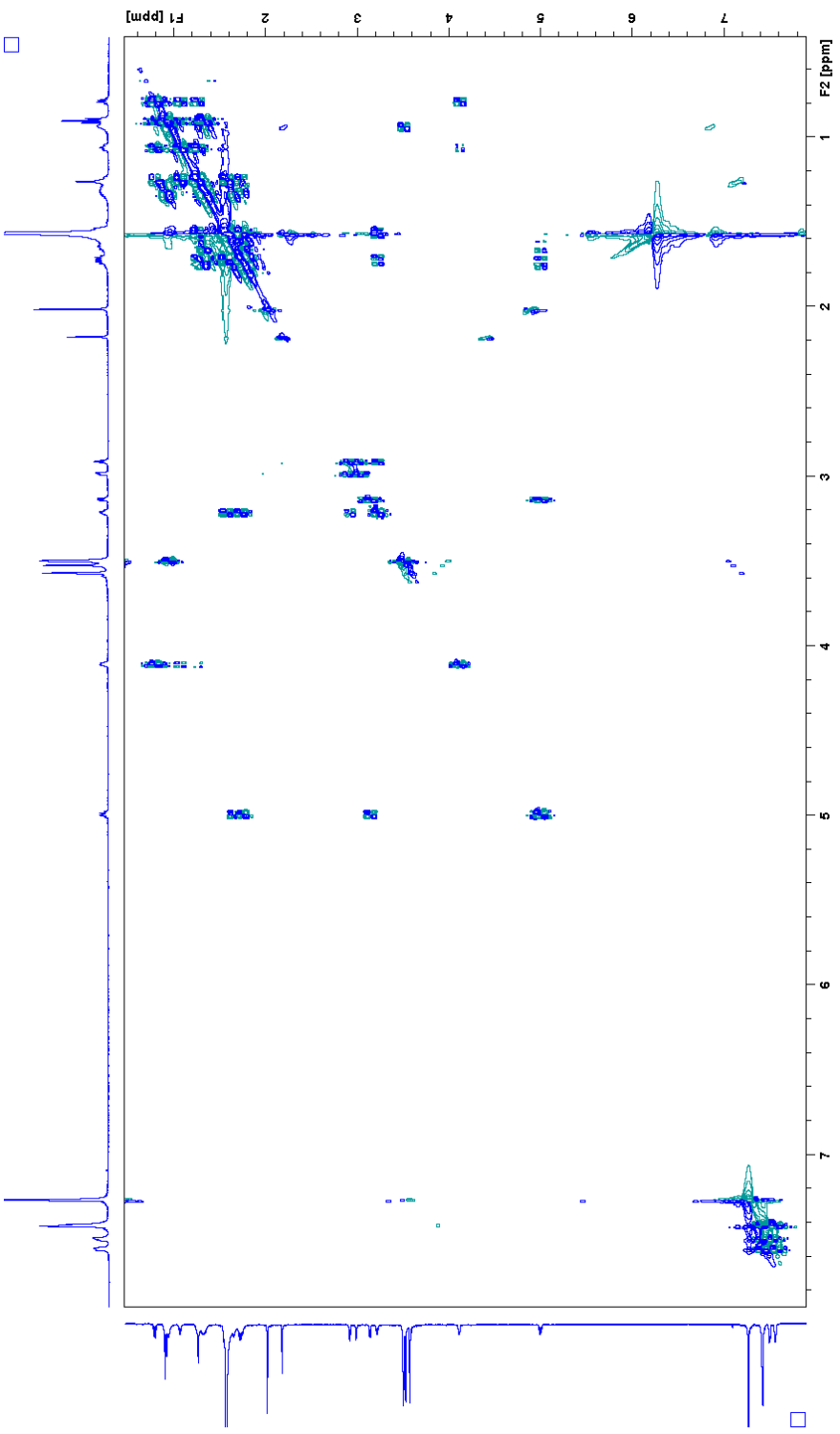

Figure S50. COSY spectrum of toblerol B-(*R*)-MTPA ester (**2c**) in chloroform-*d*.

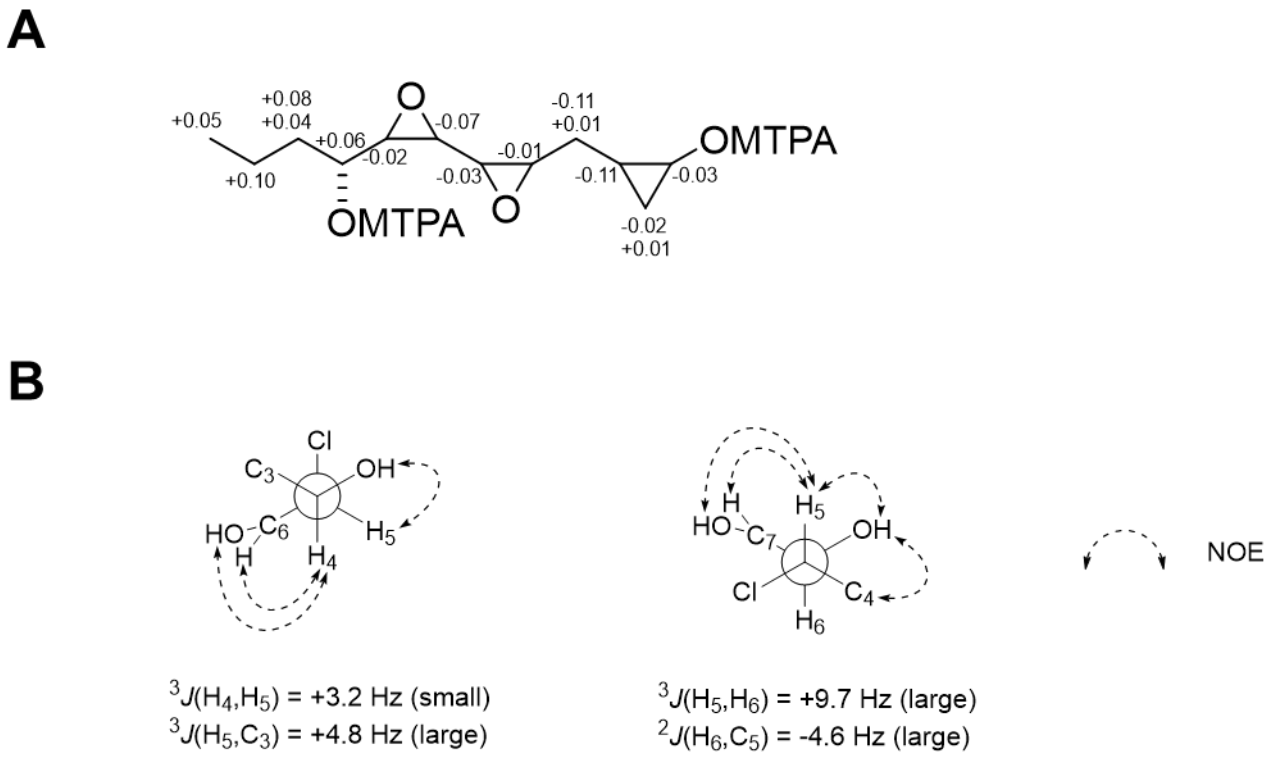

Figure S51. (A) Modified Mosher analysis of toblerol B (**2**). $\Delta\delta_H$ = toblerol B-(*S*)-MTPA ester (**2b**) - toblerol B-(*R*)-MTPA ester (**2c**). (B) *J*-based analysis of toblerol E (**5**).

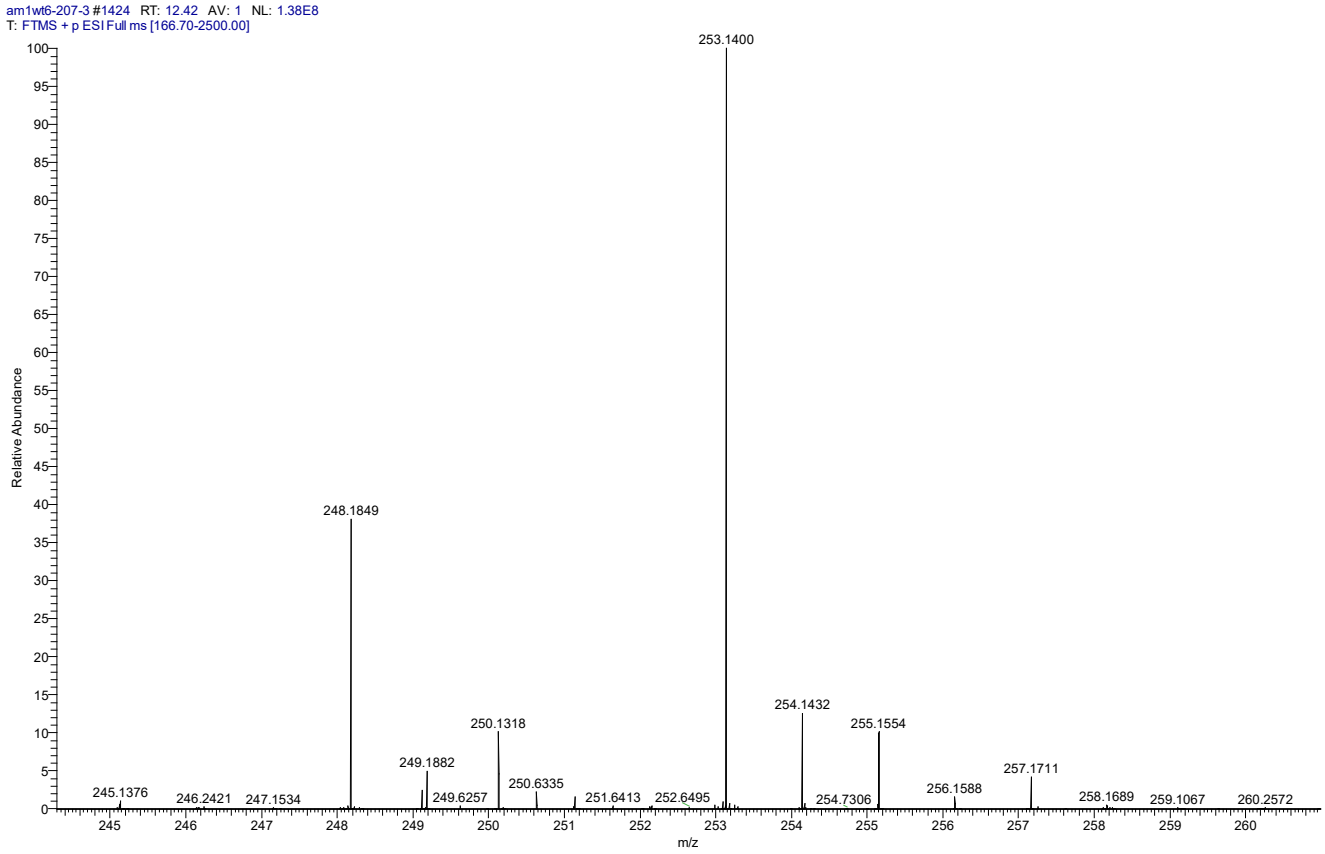

Figure S52: HR-LC-ESIMS data of the product from toblerol A (**1**) by Red-Al. Mass spectrum of the peak at 12.42 min (*m/z* 248.1849 $[M+NH_4]^+$ and *m/z* 253.1400 $[M+Na]^+$).

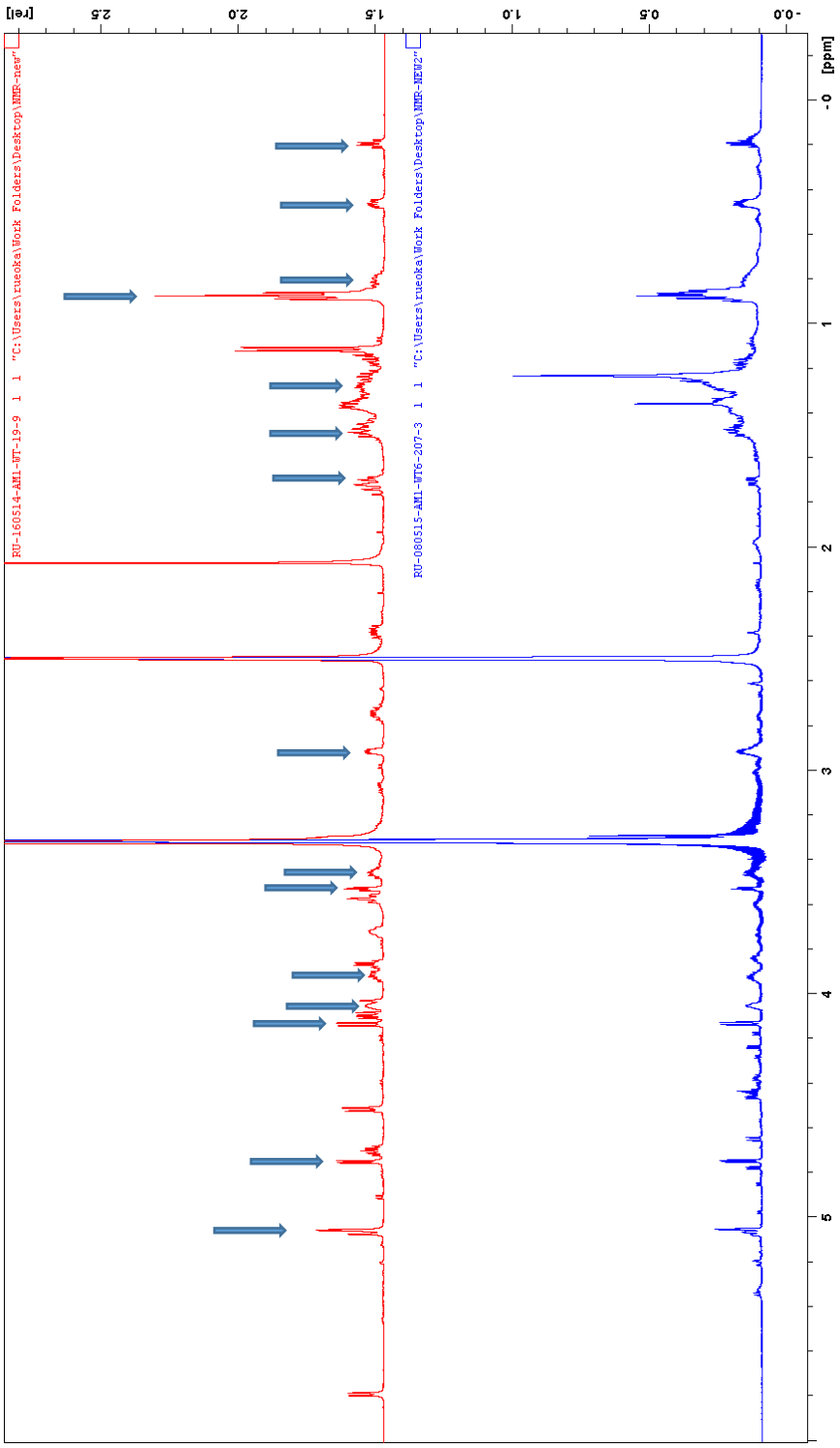

Figure S53. ^{1}H NMR spectrum of the mixture of toblerol G (**7**) and H (**8**) (upper: arrows showed signals for **8**) and the product from toblerol A (**1**) by Red-Al (lower) in DMSO-d_6.

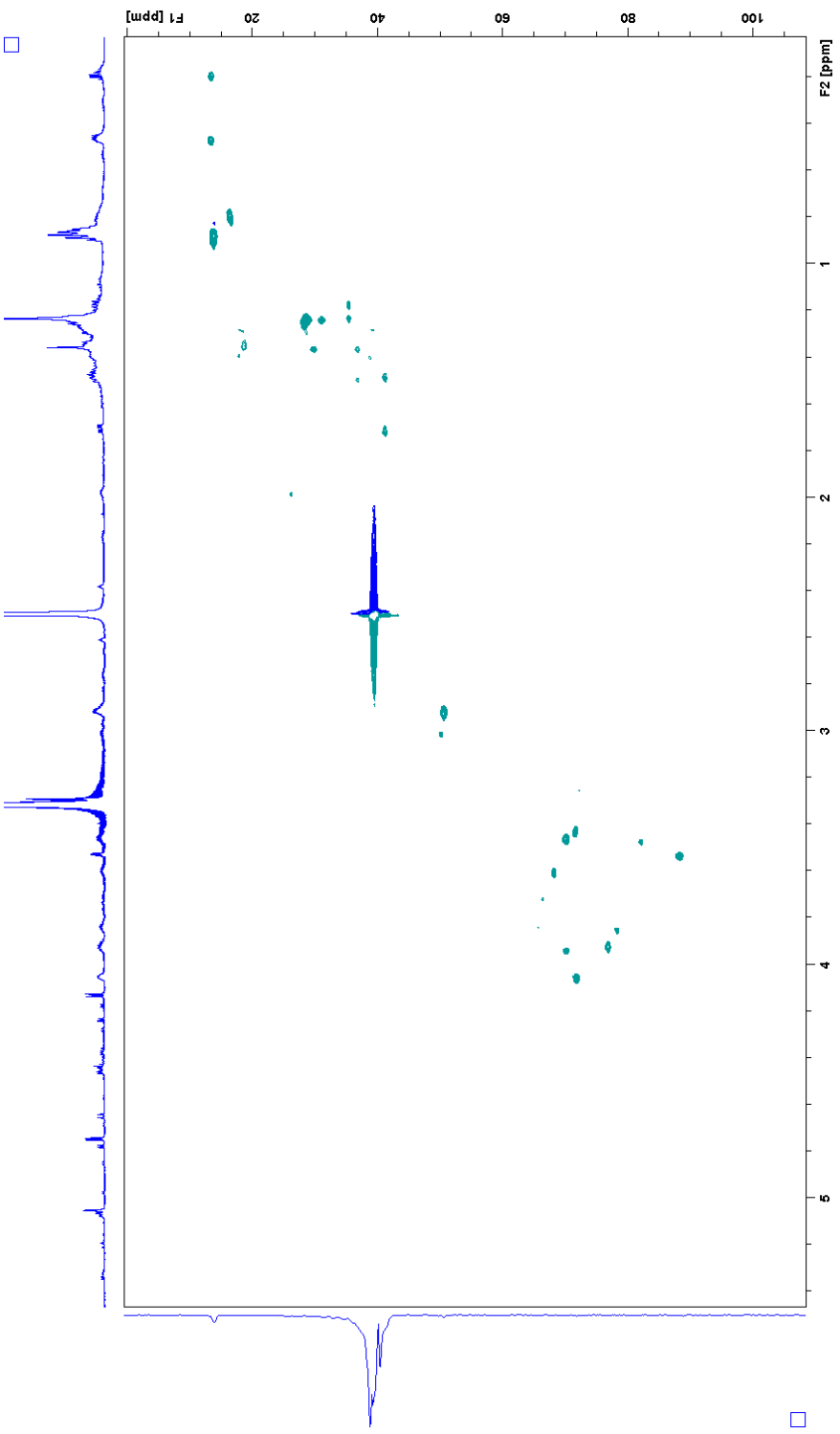

Figure S54. HSQC spectrum of the product from toblerol A (**1**) by Red-Al in DMSO-d_6.

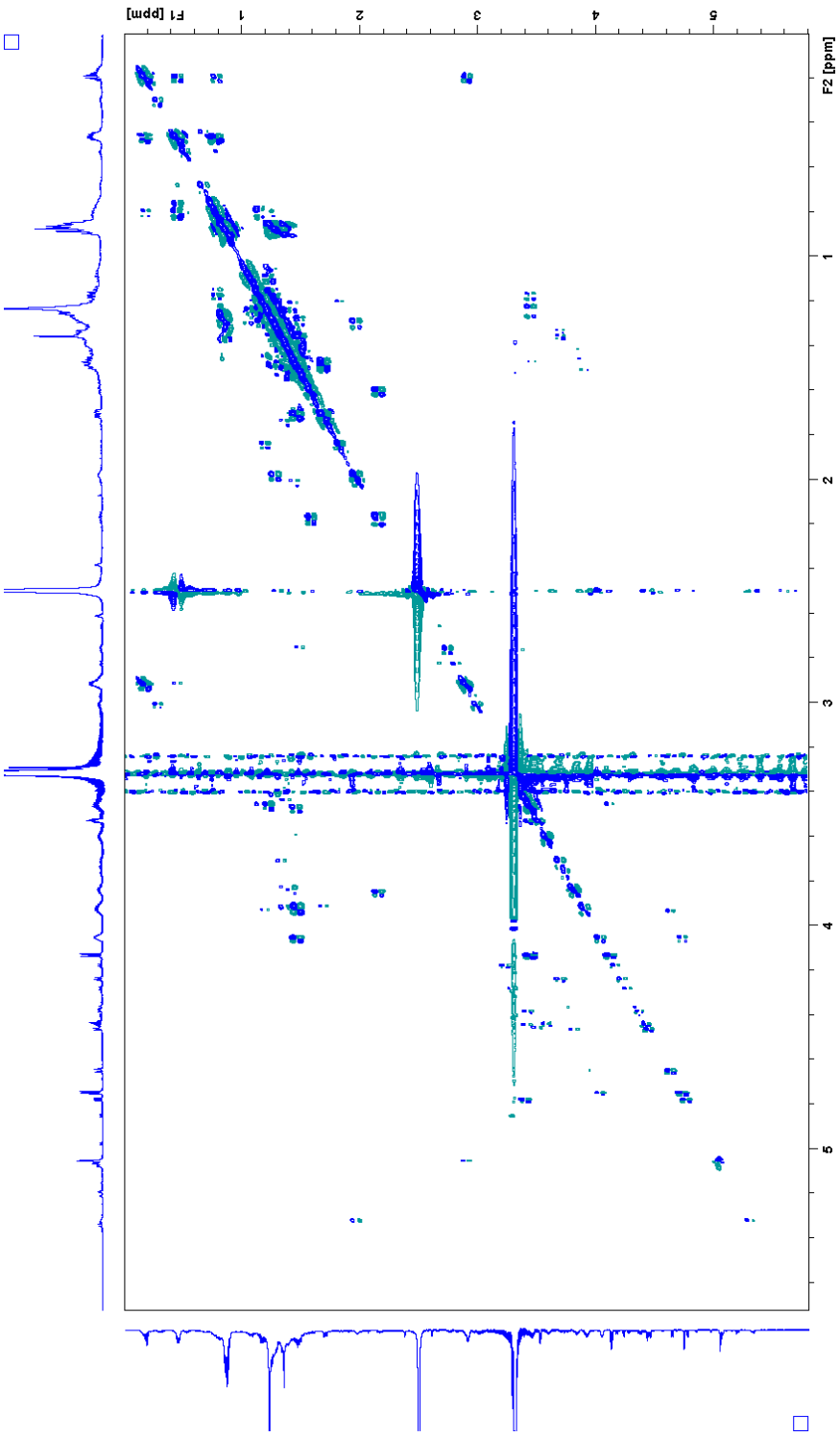

Figure S55. COSY spectrum of the product from toblerol A (**1**) by Red-Al in DMSO-d_6.

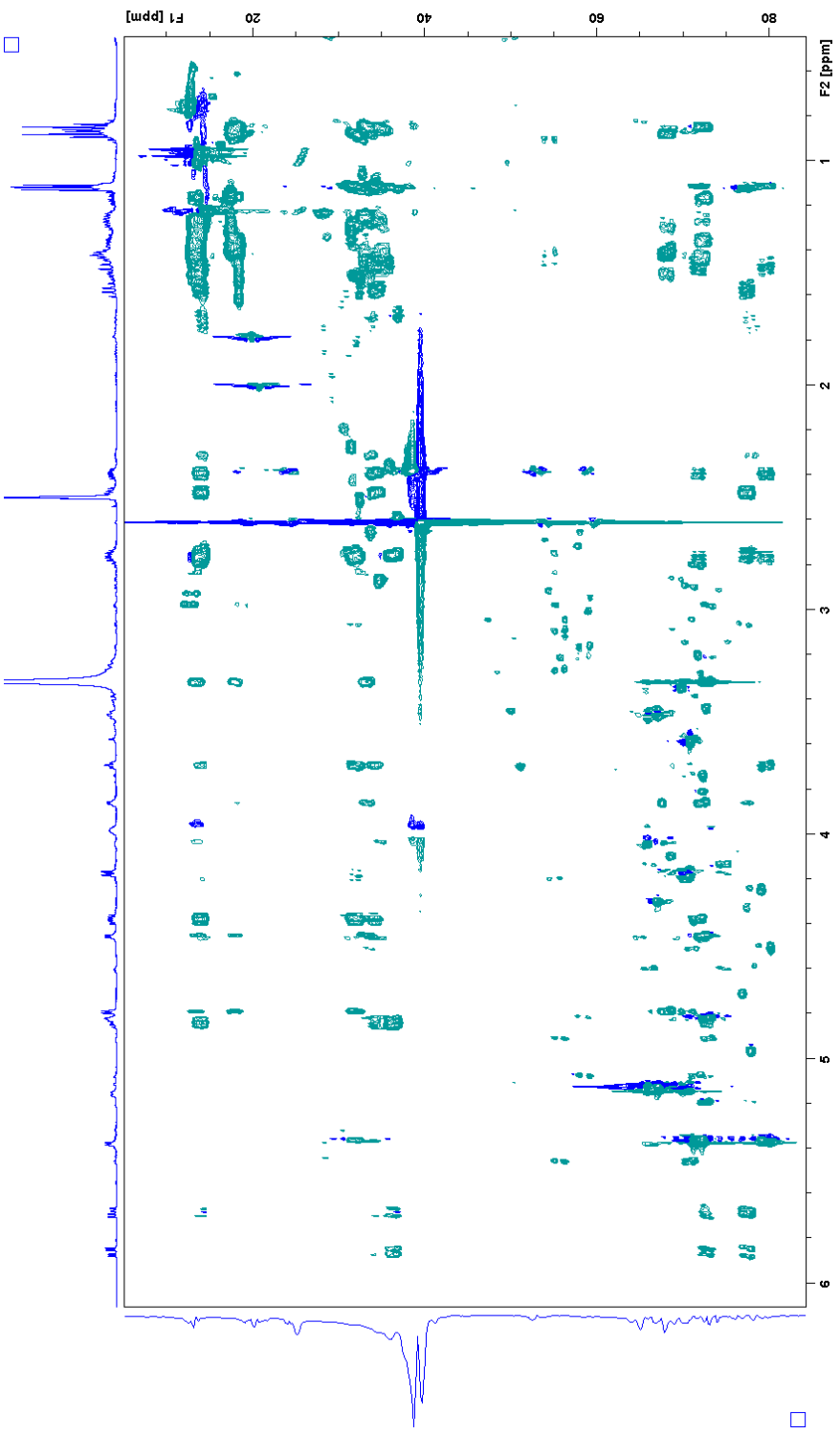

Figure S56. HECADE spectrum of toblerol E (**5**) and F (**6**) in DMSO-d_6.

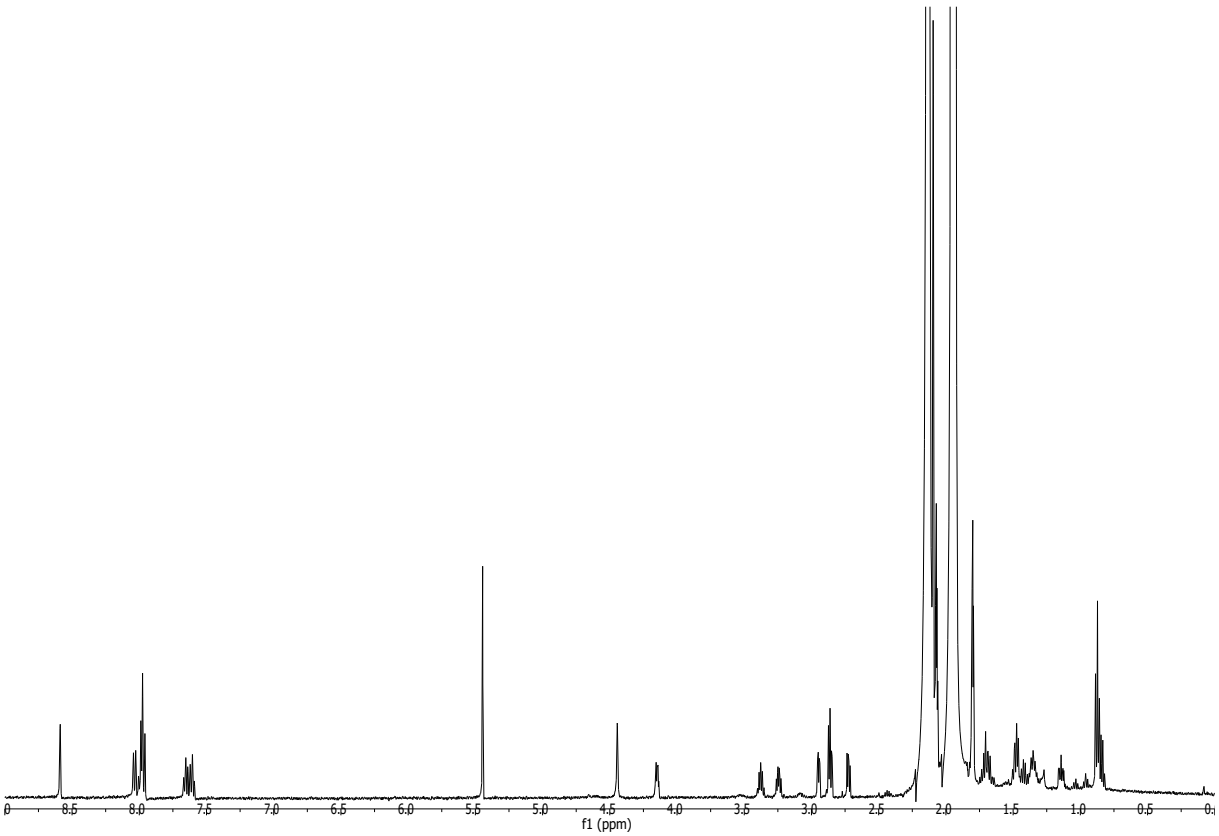

Figure S57. ^{1}H NMR spectrum (600 MHz, CD_3CN) for mono-napthoate ester **9**.

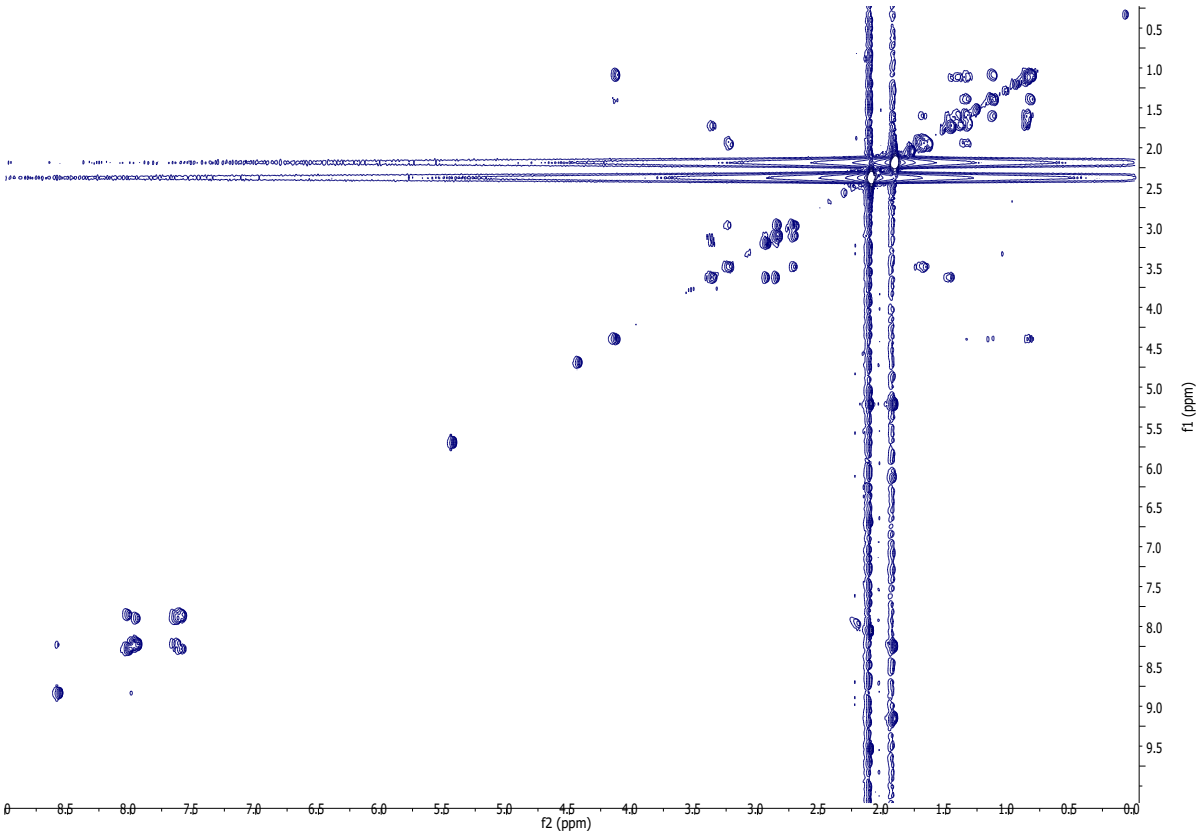

Figure S58. COSY spectrum (600 MHz, CD_3CN) for mono-napthoate ester **9**.

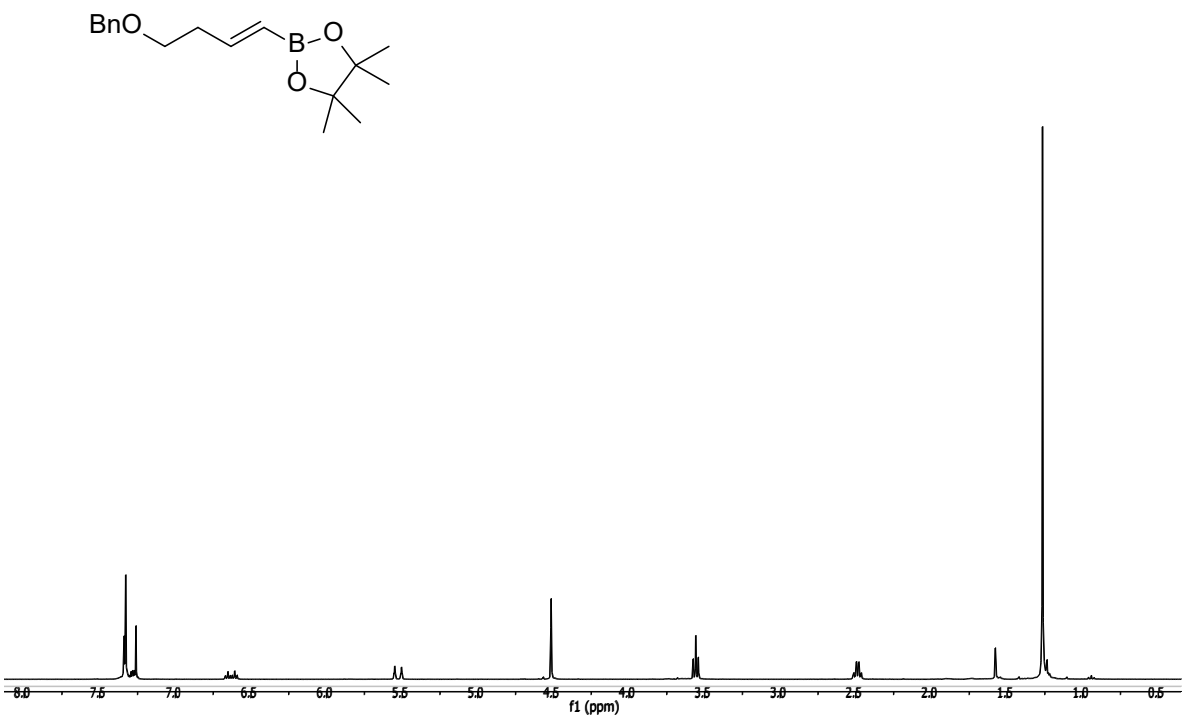

Figure S59. ^{1}H NMR spectrum (400 MHz, $CDCl_3$) for compound **S2**.

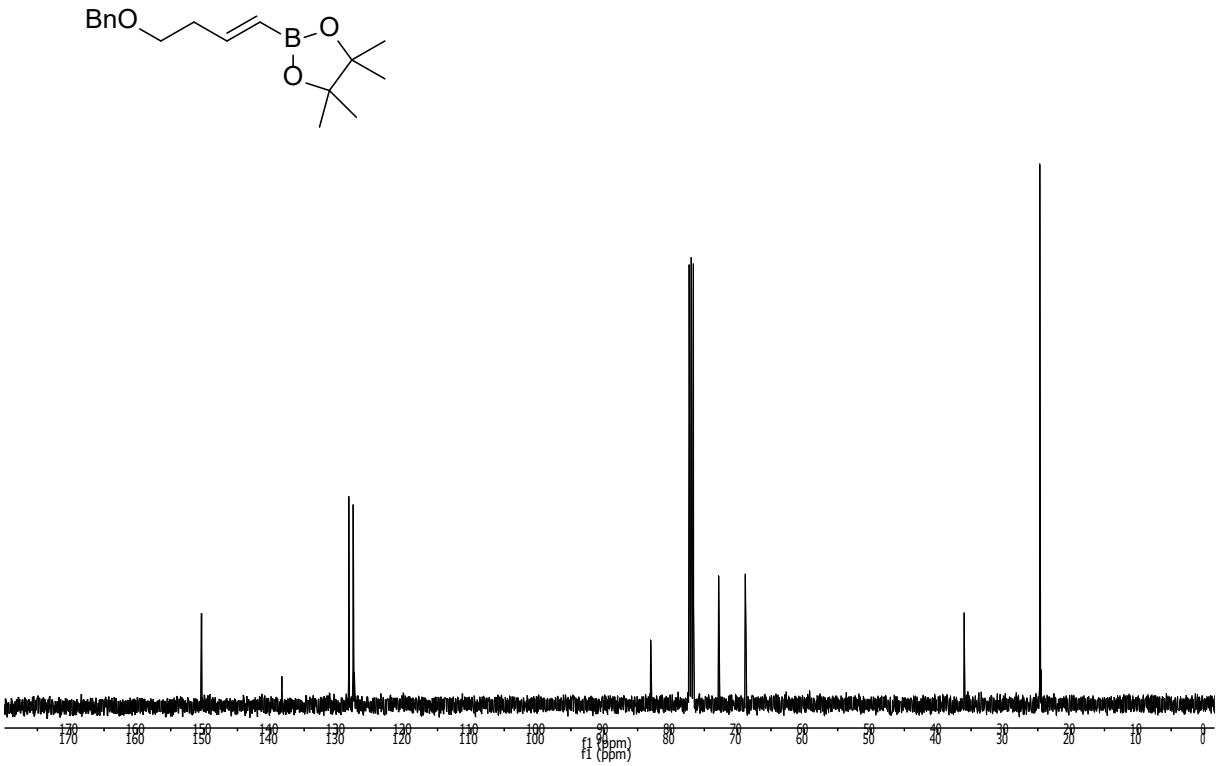

Figure S60. ^{13}C NMR spectrum (100 MHz, $CDCl_3$) for compound **S2**.

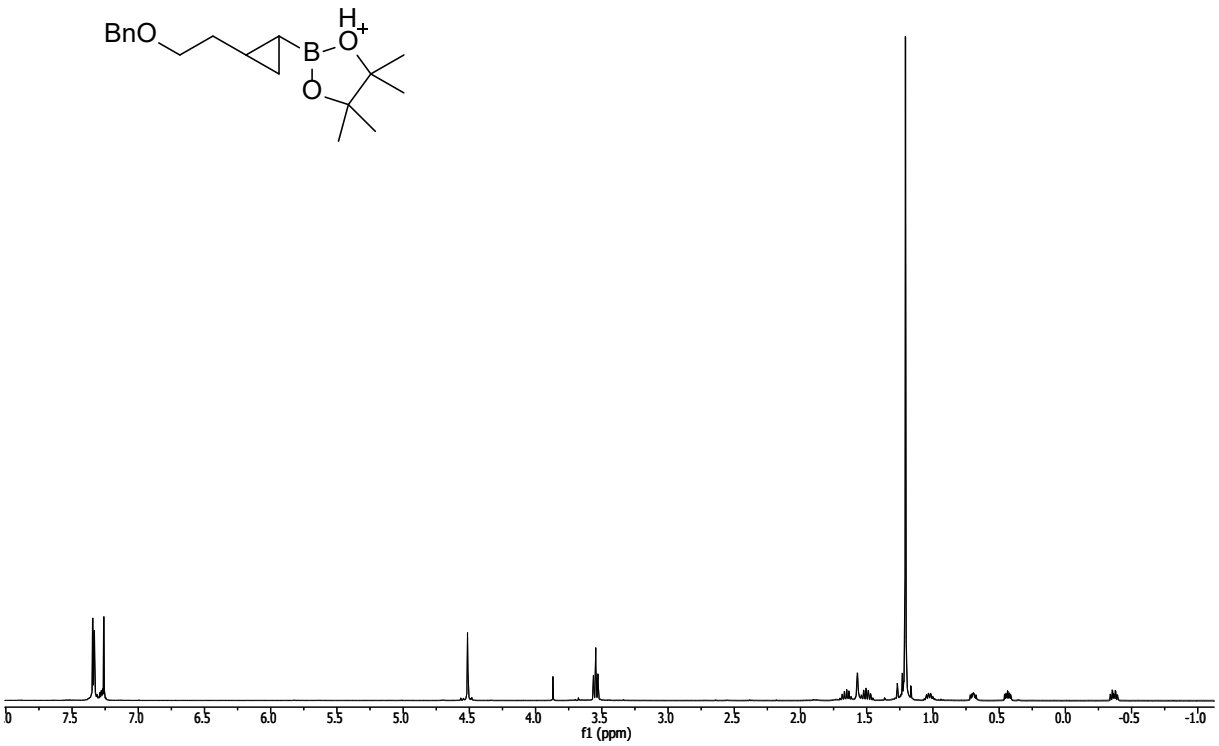

Figure S61. ^{1}H NMR spectrum (400 MHz, $CDCl_3$) for compound **S3**.

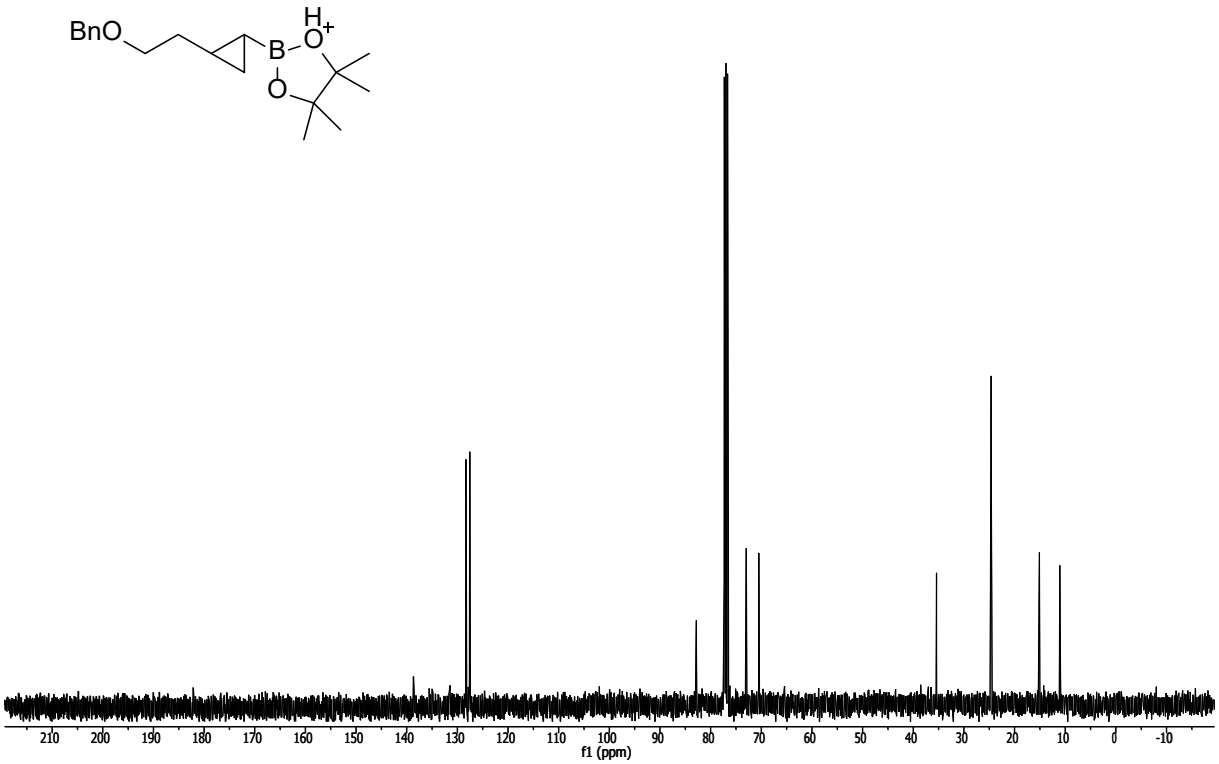

Figure S62. ^{13}C NMR spectrum (100 MHz, $CDCl_3$) for compound **S3**.

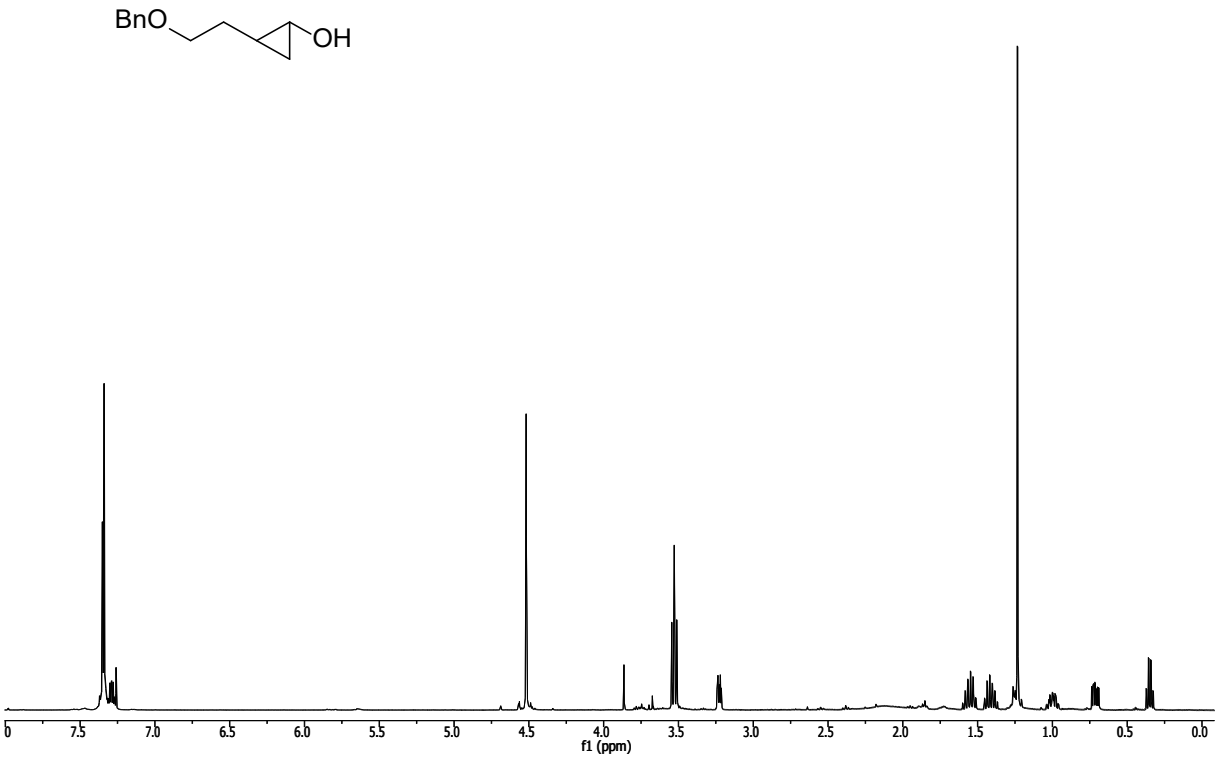

Figure S63. ^{1}H NMR spectrum (400 MHz, $CDCl_3$) for compound **S4**.

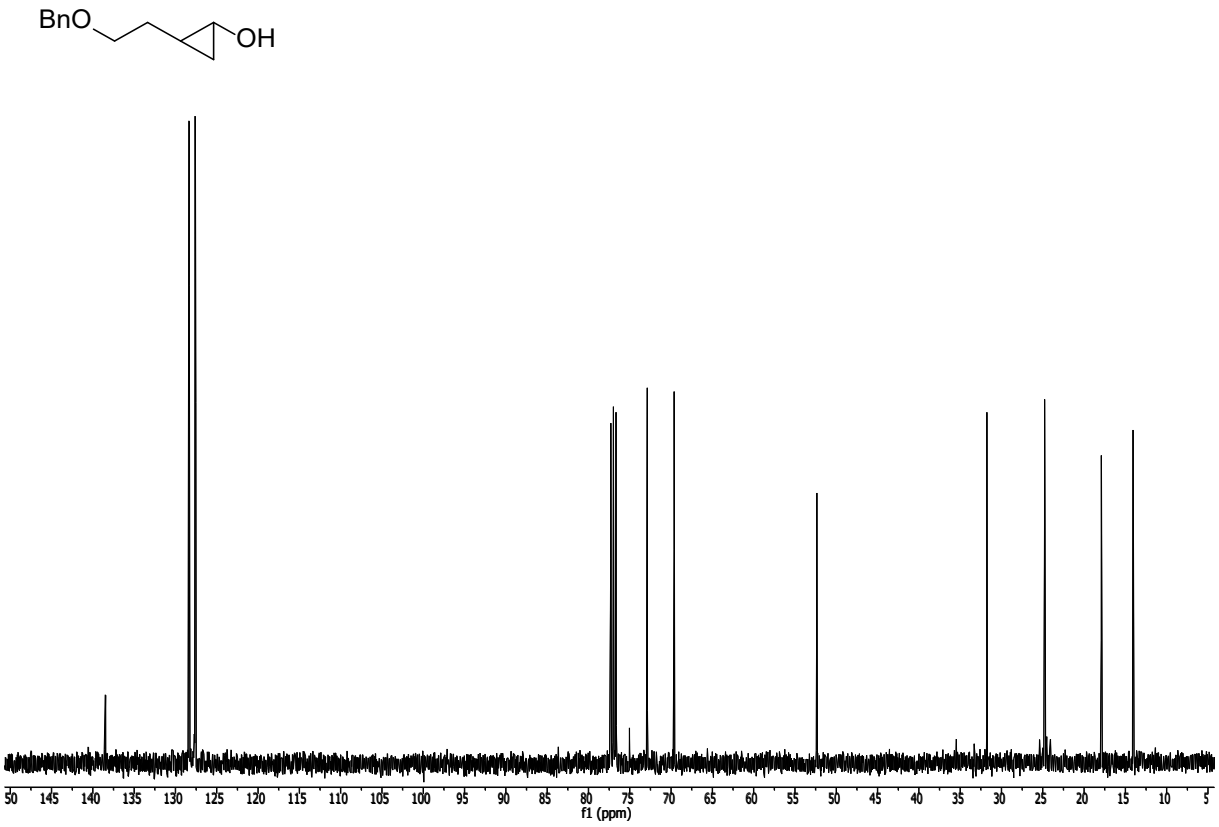

Figure S64. ^{13}C NMR spectrum (100 MHz, $CDCl_3$) for compound **S4**.

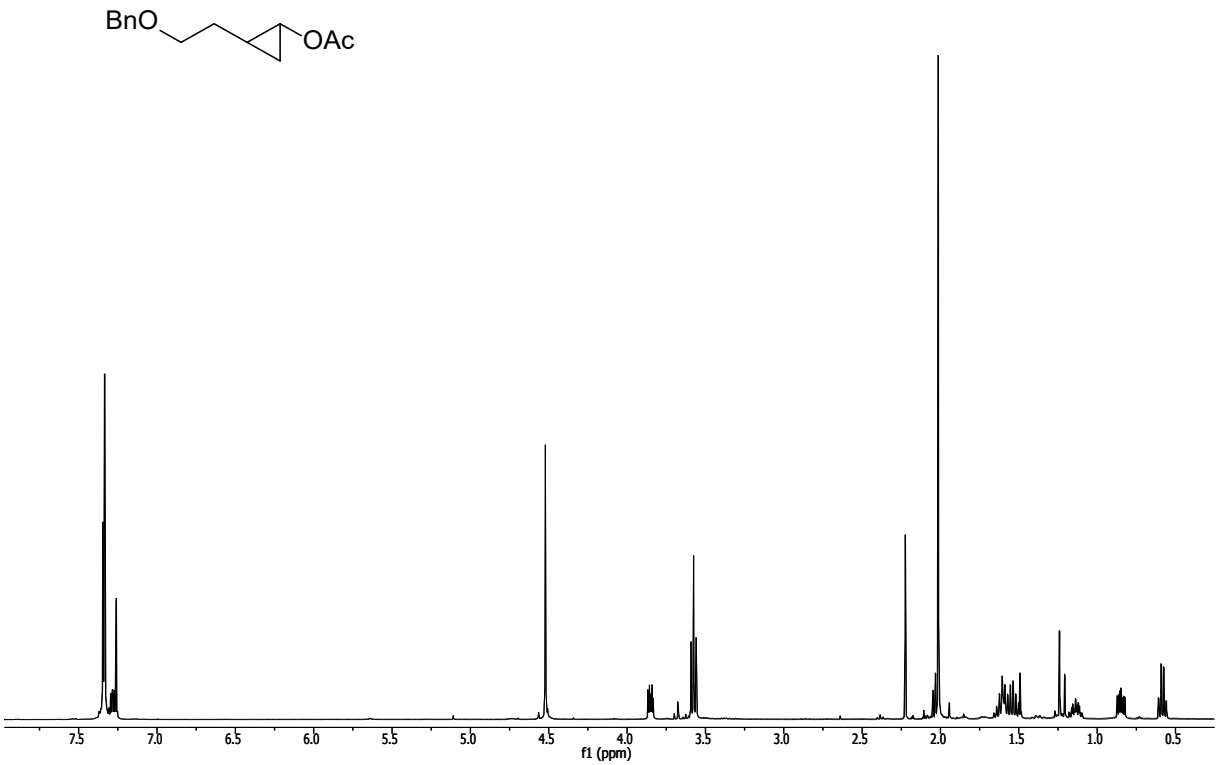

Figure S65. ^{1}H NMR spectrum (400 MHz, $CDCl_3$) for compound **S5**.

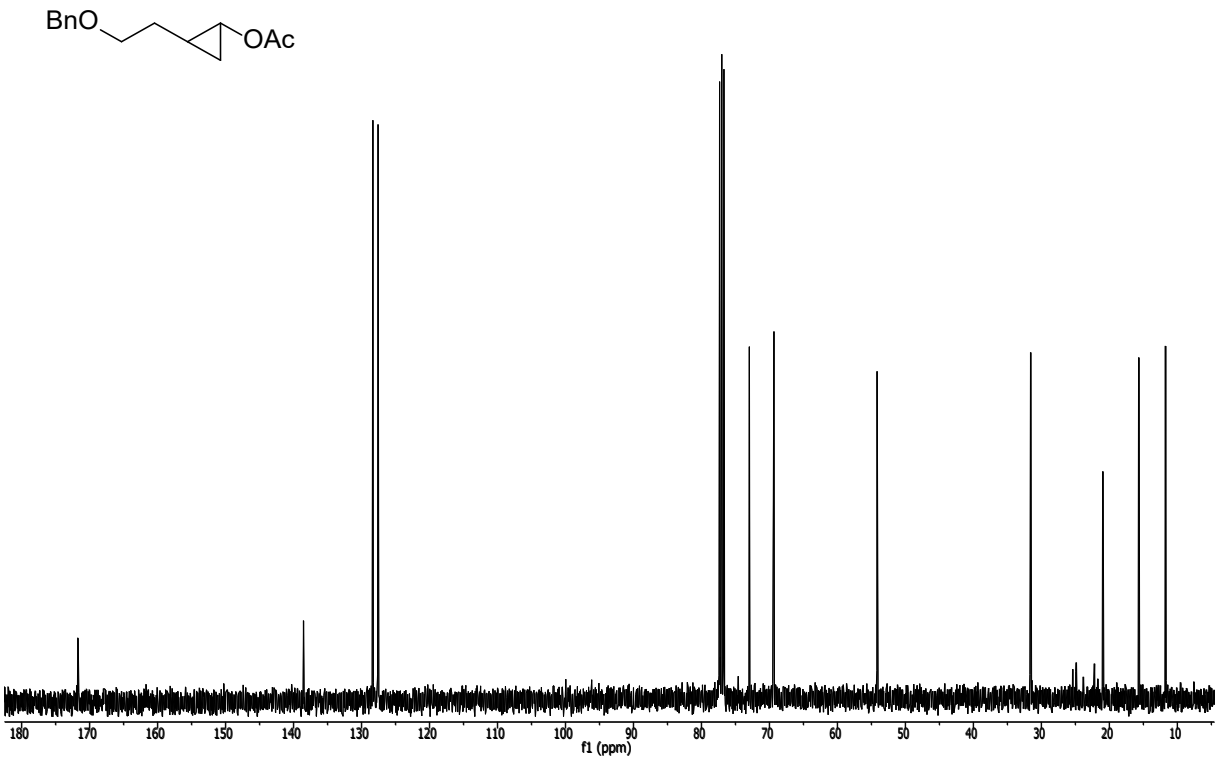

Figure S66. ^{13}C NMR spectrum (100 MHz, $CDCl_3$) for compound **S5**.

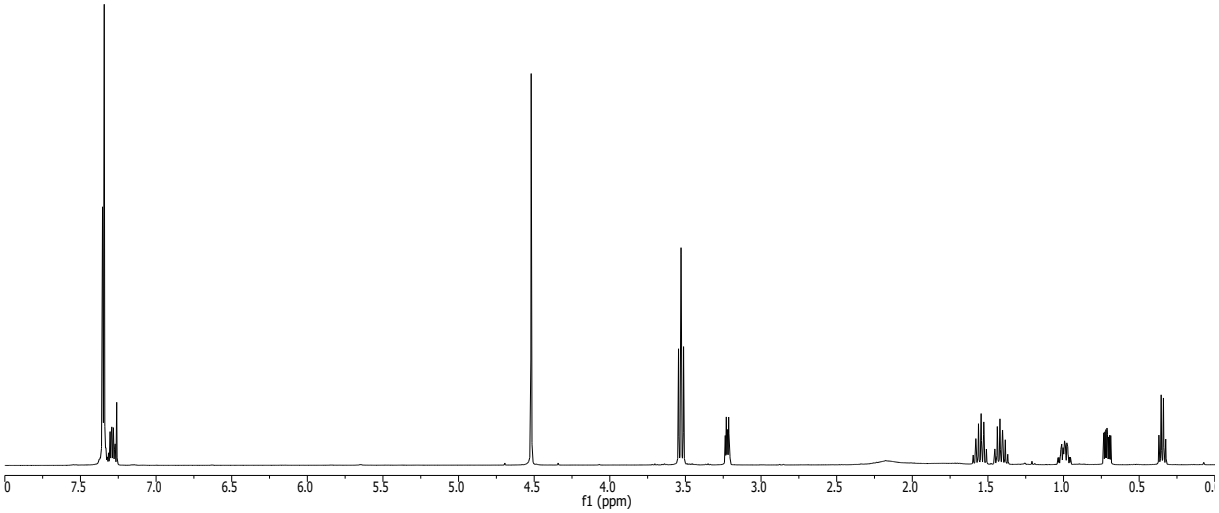

Figure S67. ^{1}H NMR spectrum (400 MHz, $CDCl_3$) for compound **12**.

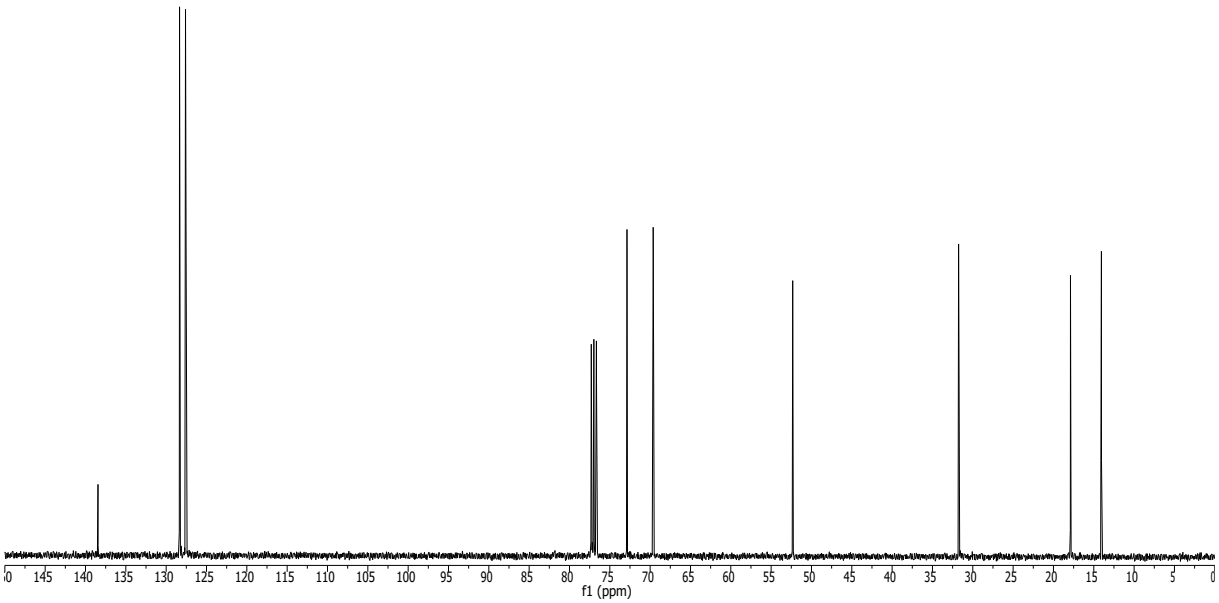

Figure S68. ^{13}C NMR spectrum (100 MHz, $CDCl_3$) for compound **12**.

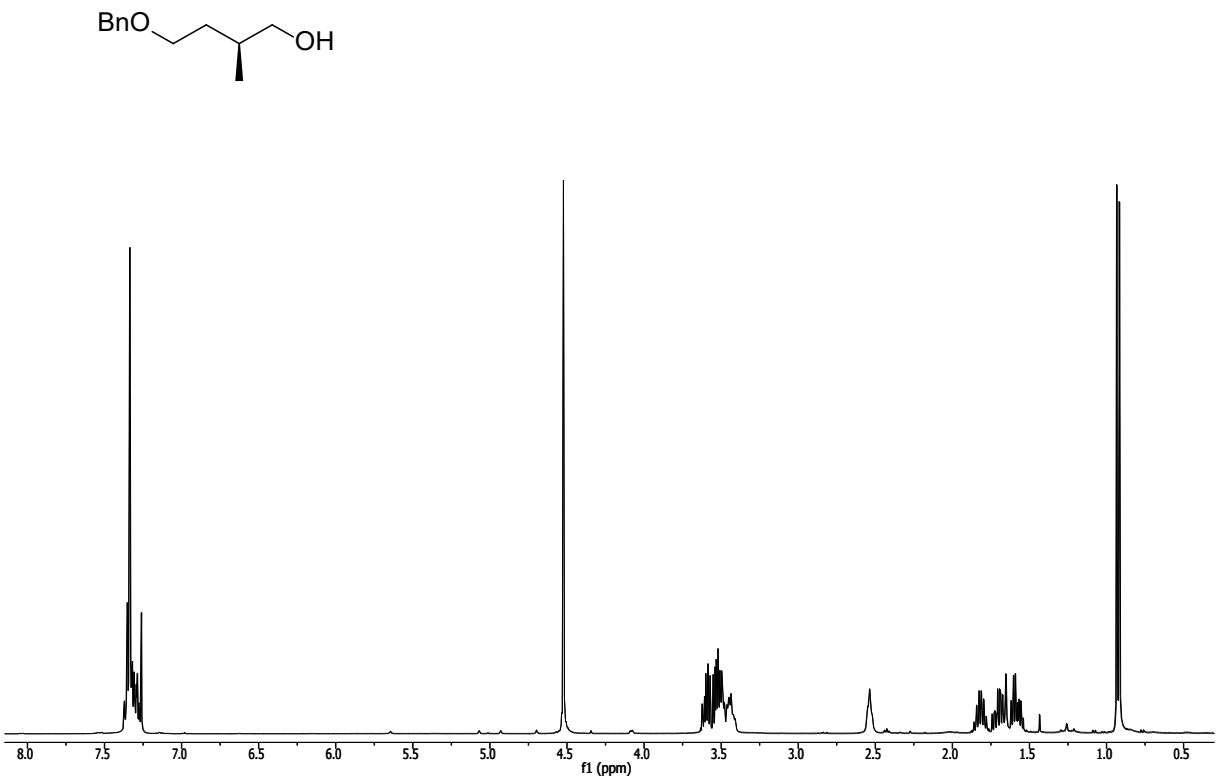

Figure S69. ^{1}H NMR spectrum (400 MHz, $CDCl_3$) for compound **S7**.

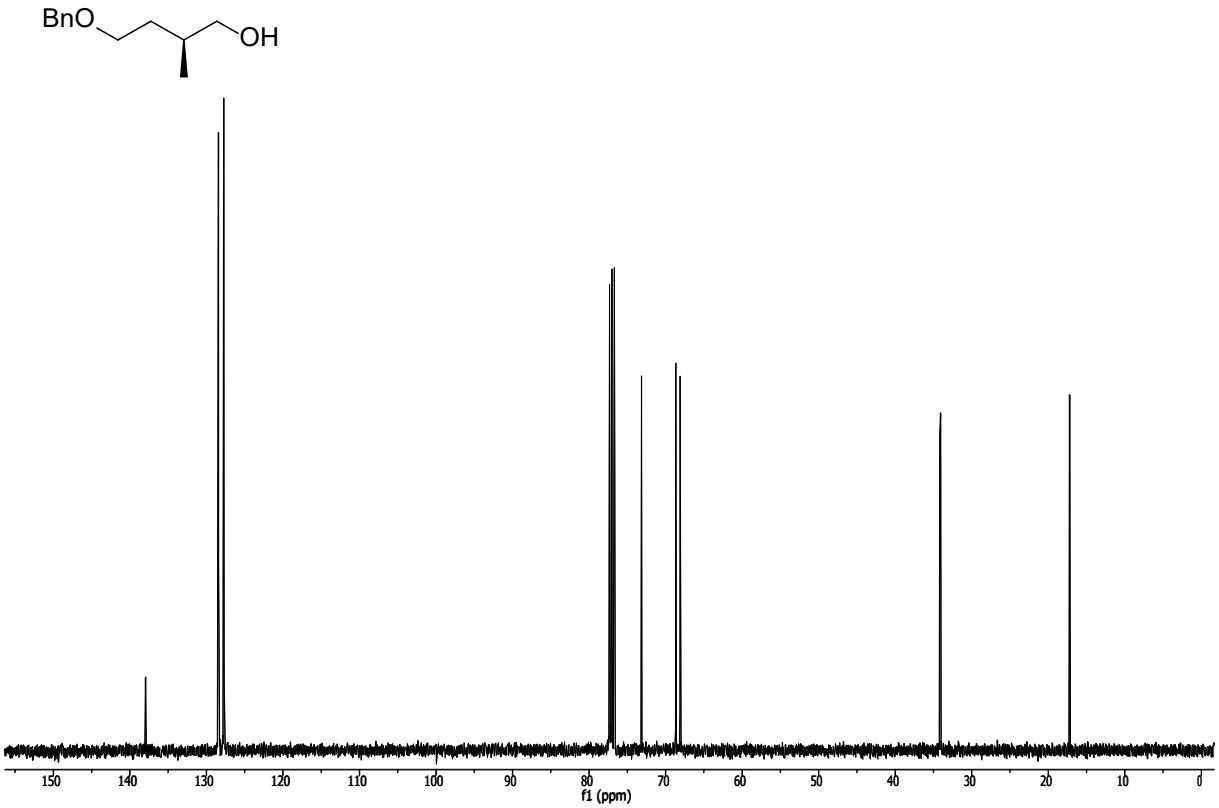

Figure S70. ^{13}C NMR spectrum (100 MHz, $CDCl_3$) for compound **S7**.

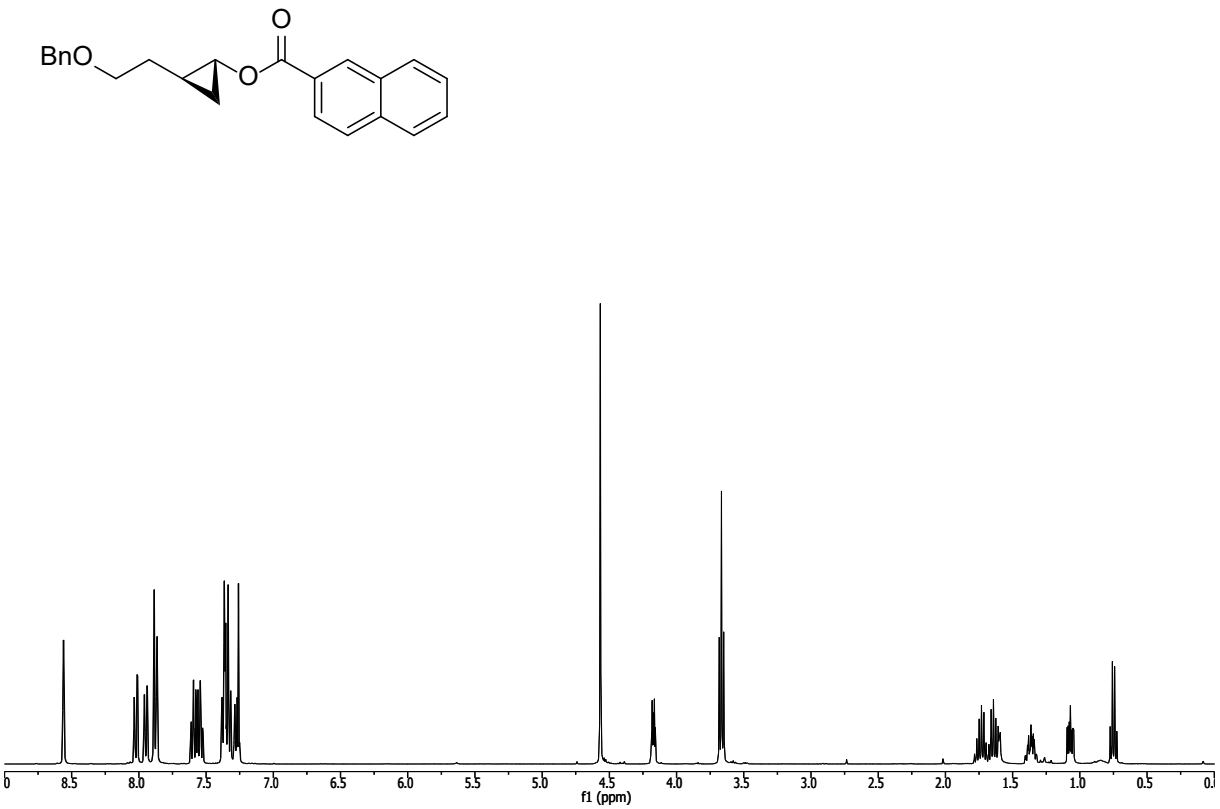

Figure S71. ^{1}H NMR spectrum (400 MHz, $CDCl_3$) for compound **S6**.

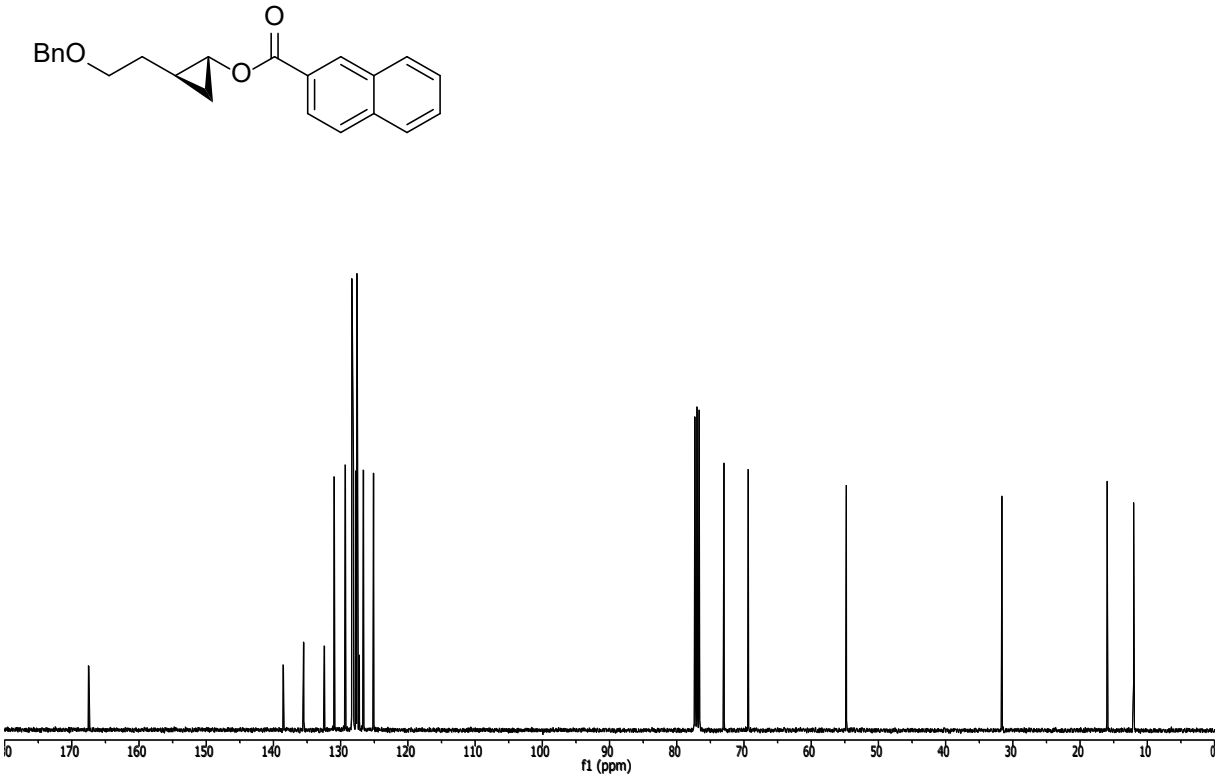

Figure S72. ^{13}C NMR spectrum (100 MHz, $CDCl_3$) for compound **S6**.

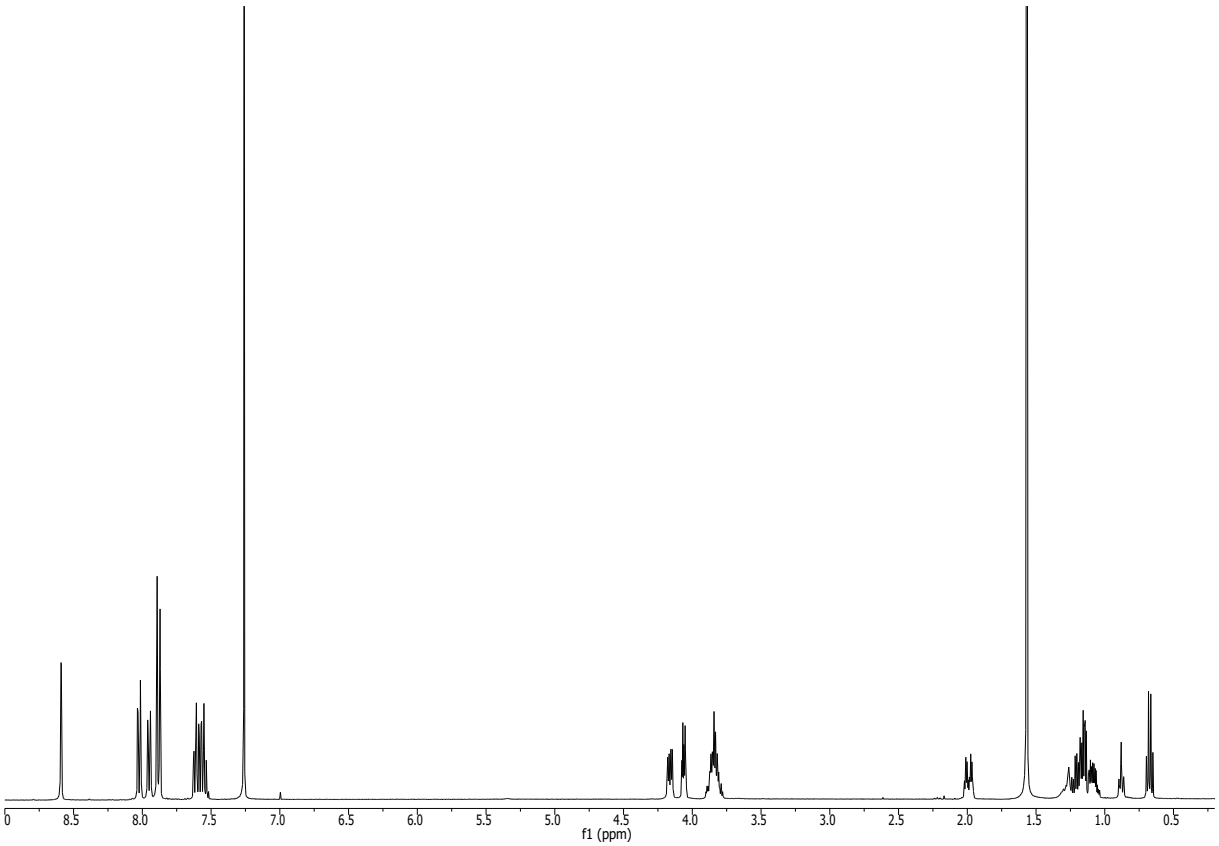

Figure S73. ^{1}H NMR spectrum (400 MHz, $CDCl_3$) for compound **10**.

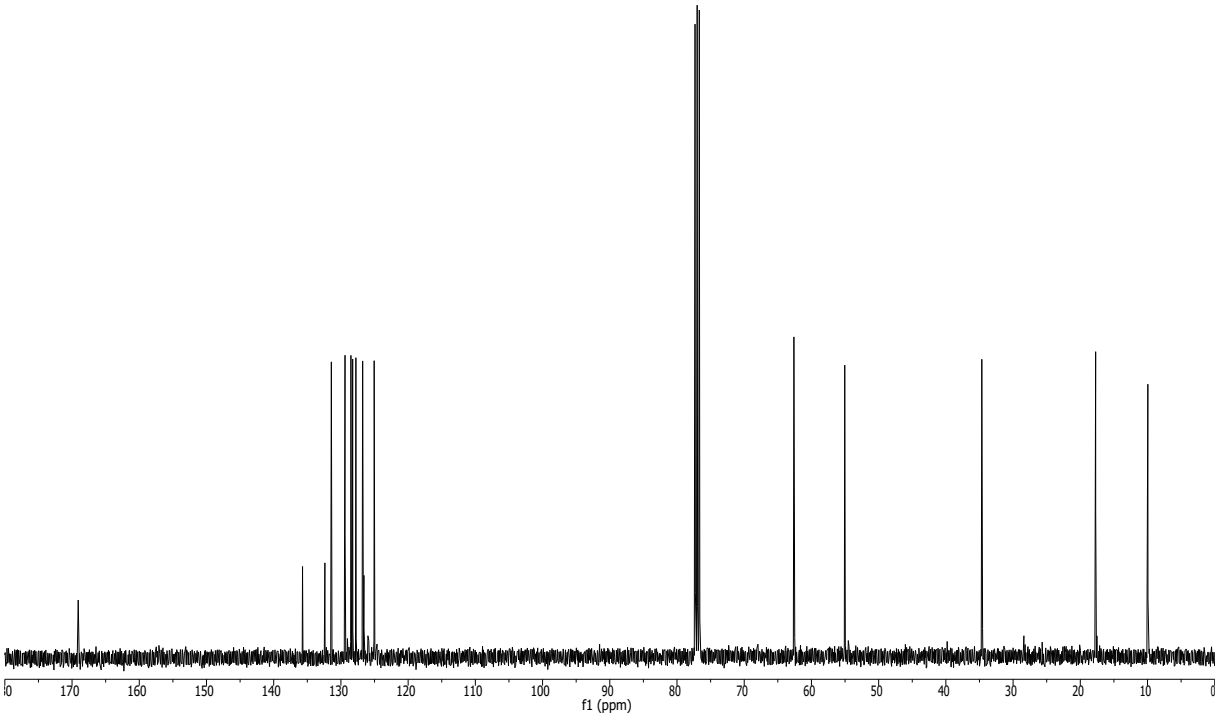

Figure S74. ^{13}C NMR spectrum (100 MHz, $CDCl_3$) for compound **10**.

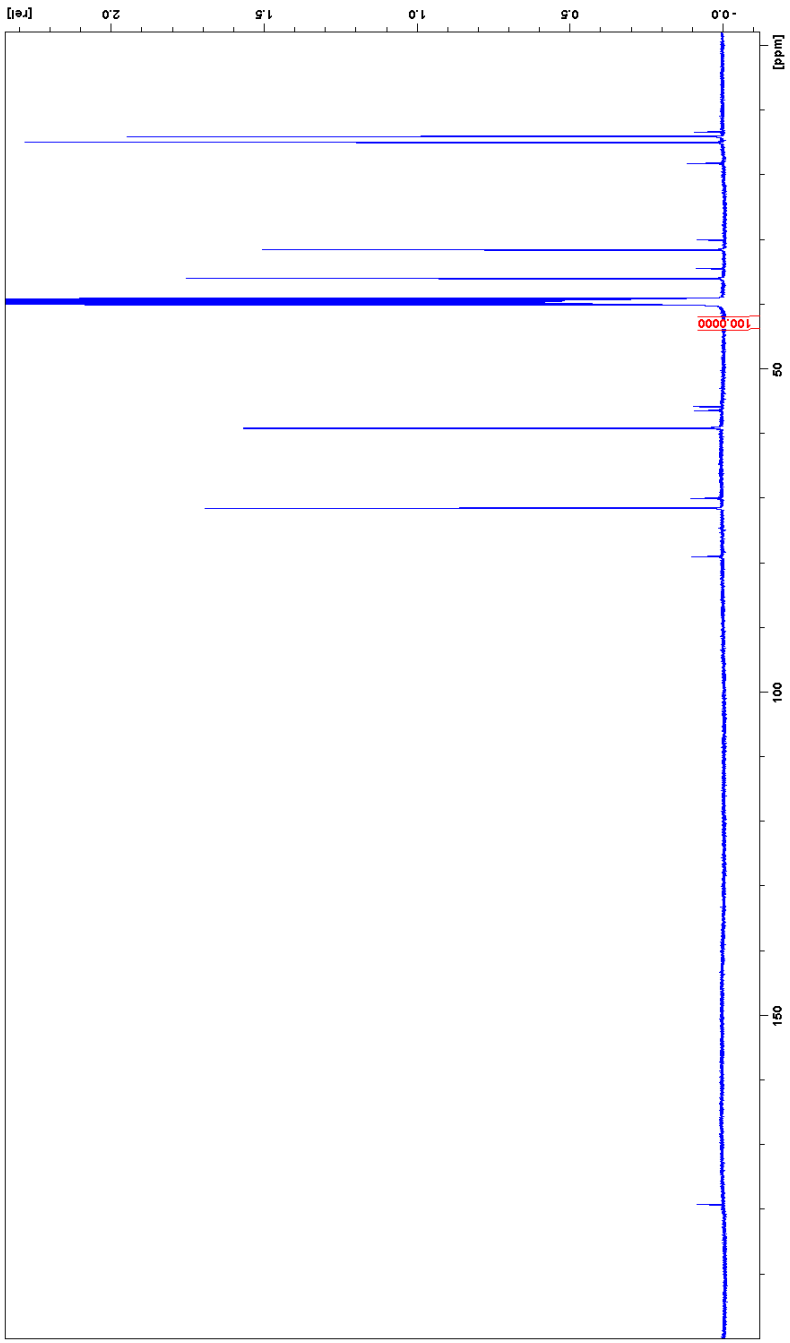

Figure S75. ^{13}C NMR spectrum of toblerol D (**4**) fed with 2-$^{13}C_1$ sodium acetate in DMSO-d_6.

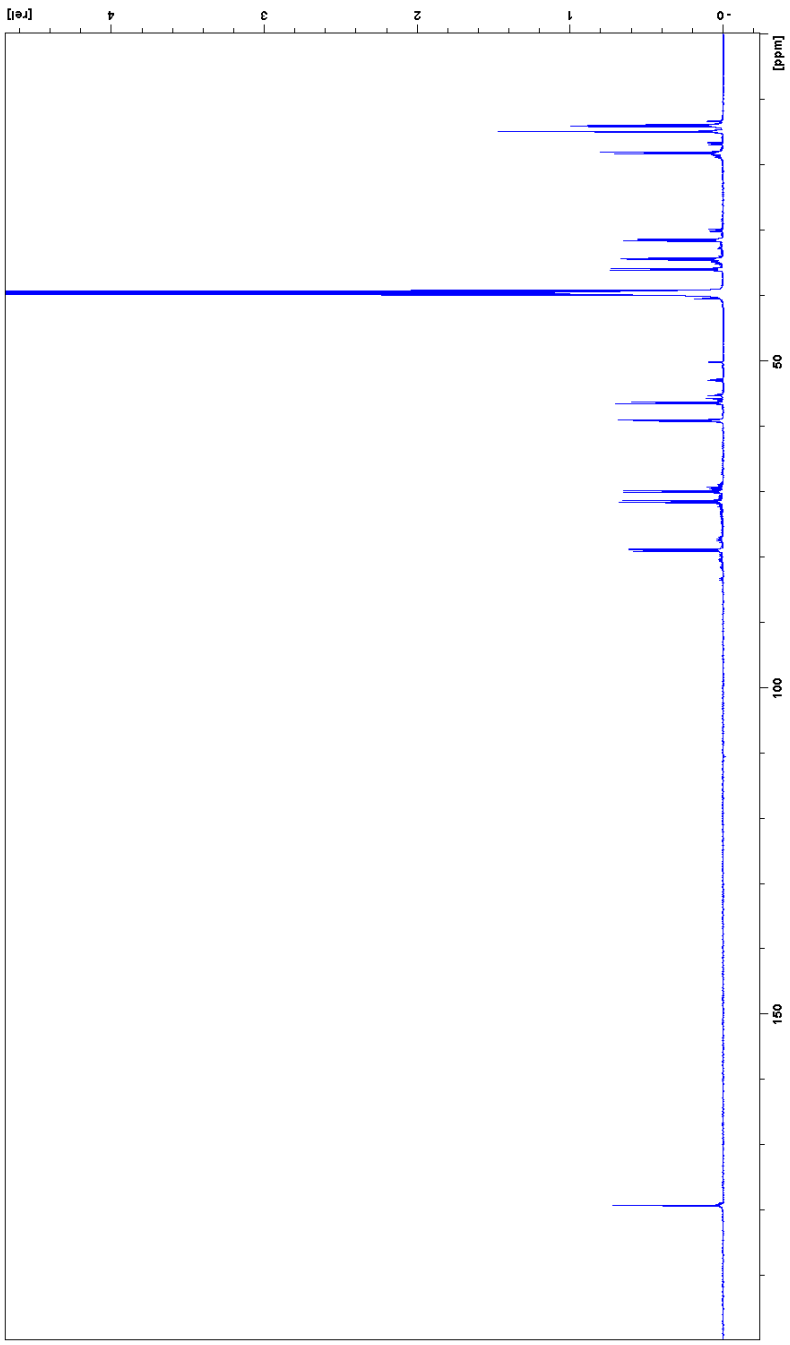

Figure S76. ^{13}C NMR spectrum of toblerol D (**4**) fed with 1,2-$^{13}C_2$ sodium acetate in DMSO-d_6.

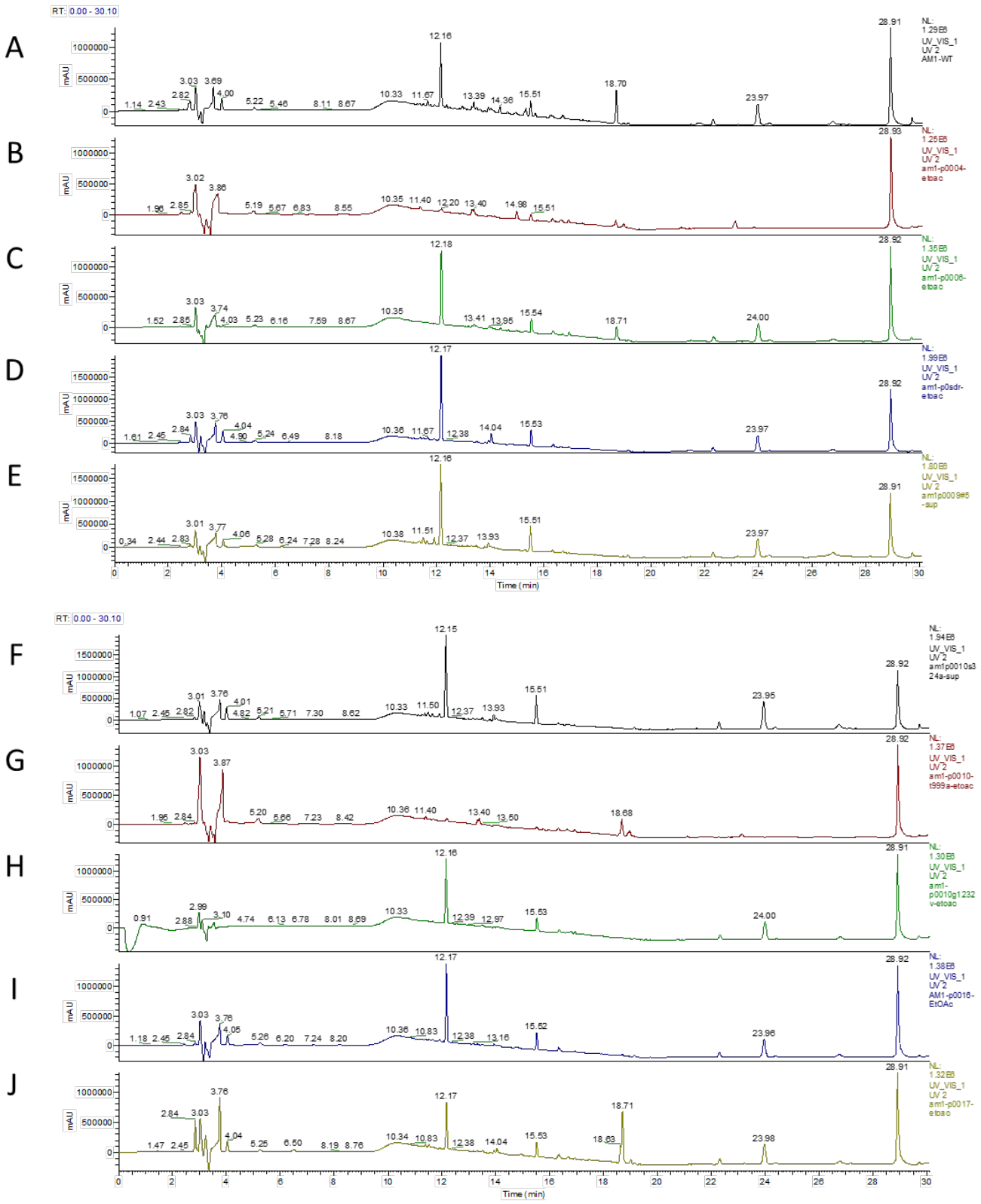

Figure S77. HPLC charts of the supernatant extracts of WT (A), mutant strains of upstream1 (B), upstream2 (C), *tobB* (D), *tobD* (E), *tobE*-HY (F), *tobE*-PX (G), *tobE*-FAD (H), *tobK* (I), and *tobL* (J) at 200 nm. Peaks at 18.7 min in A, B, C, G,and J are for toblerol C.

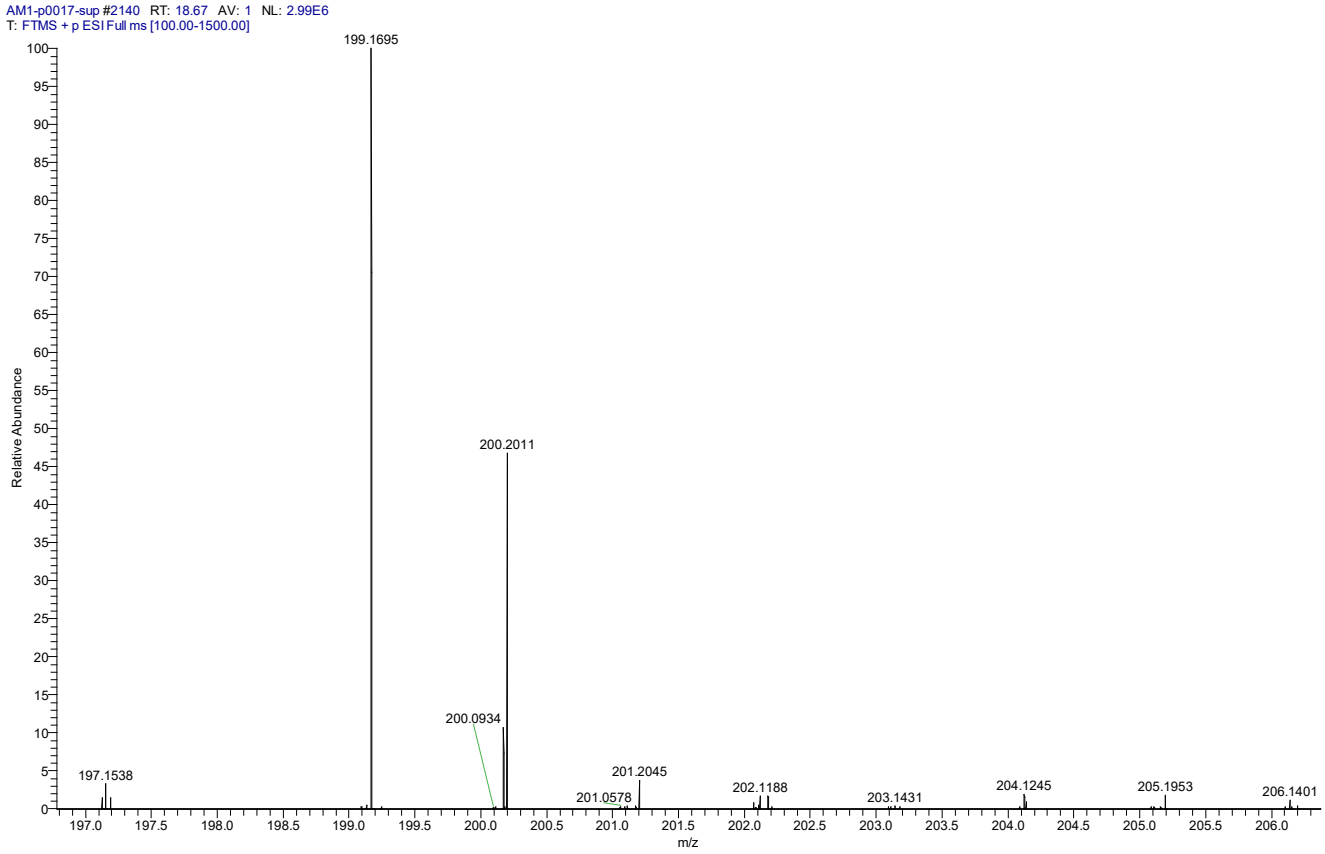

Figure S78: HR-LC-ESIMS data of **13**. Mass spectrum of the peak at 18.67 min (*m/z* 199.1695 $[M+H]^+$).

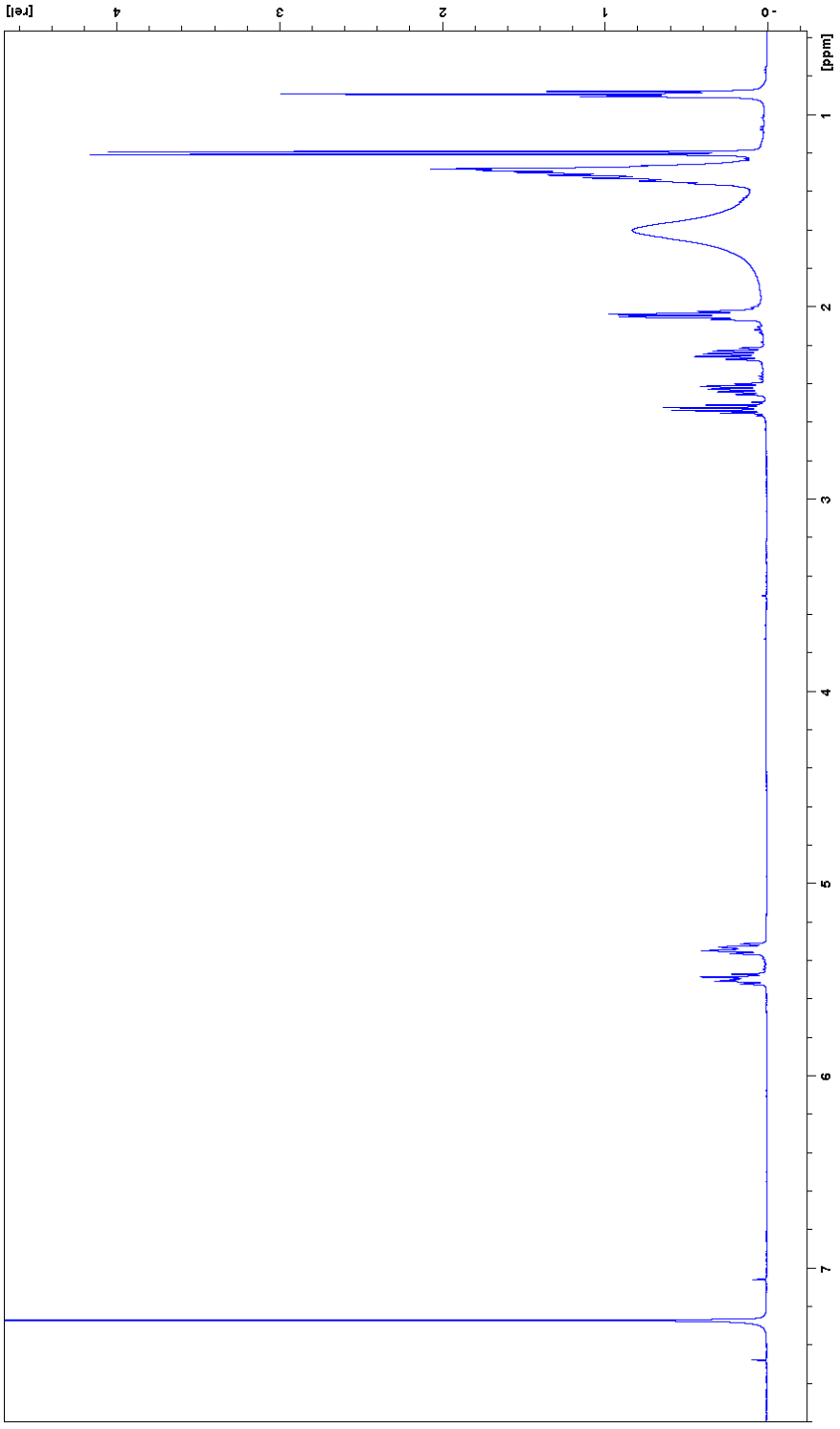

Figure S79. ^{1}H NMR spectrum of **13** in chloroform-*d*.

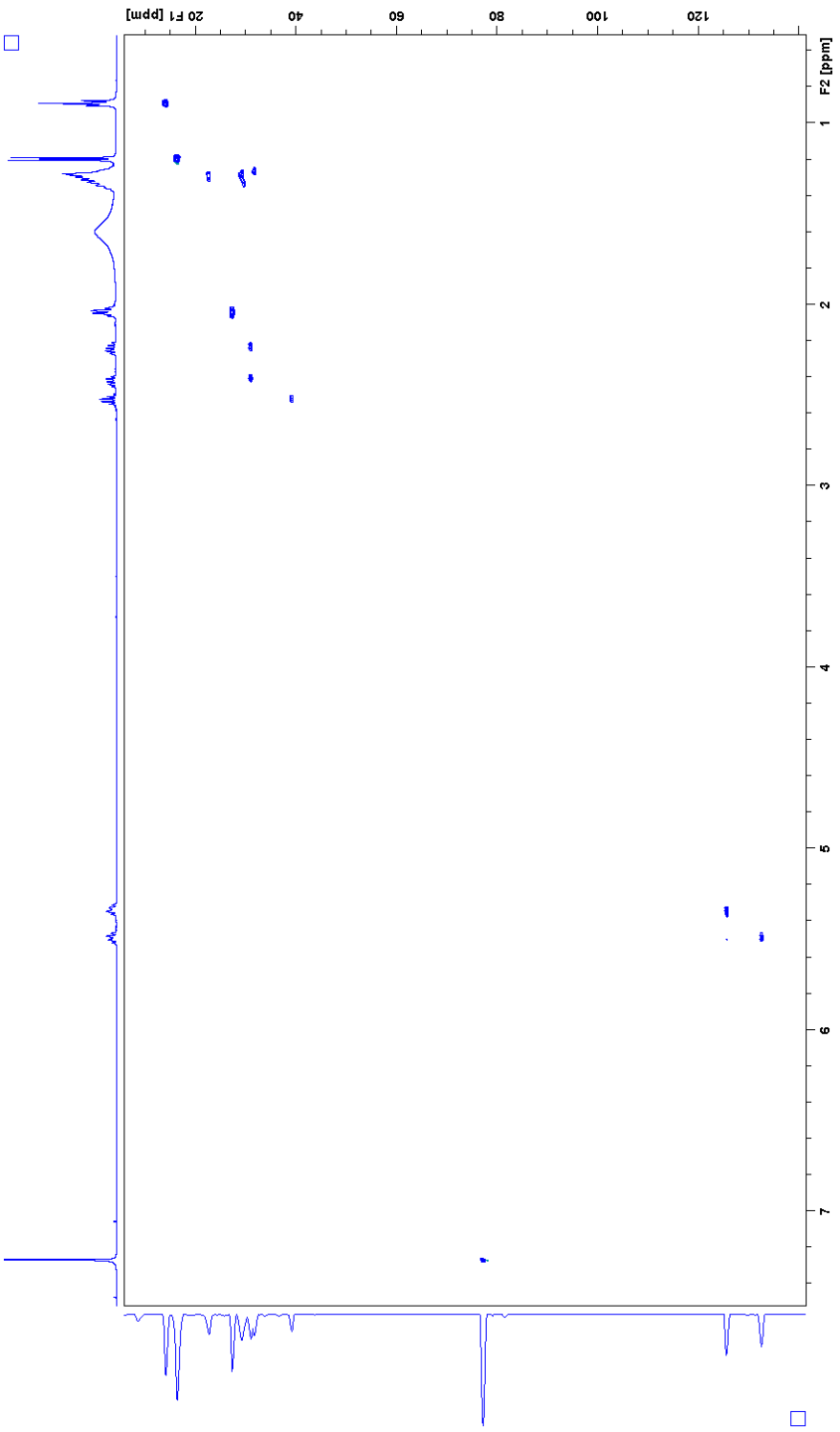

Figure S80. HSQC spectrum of **13** in chloroform-*d*.

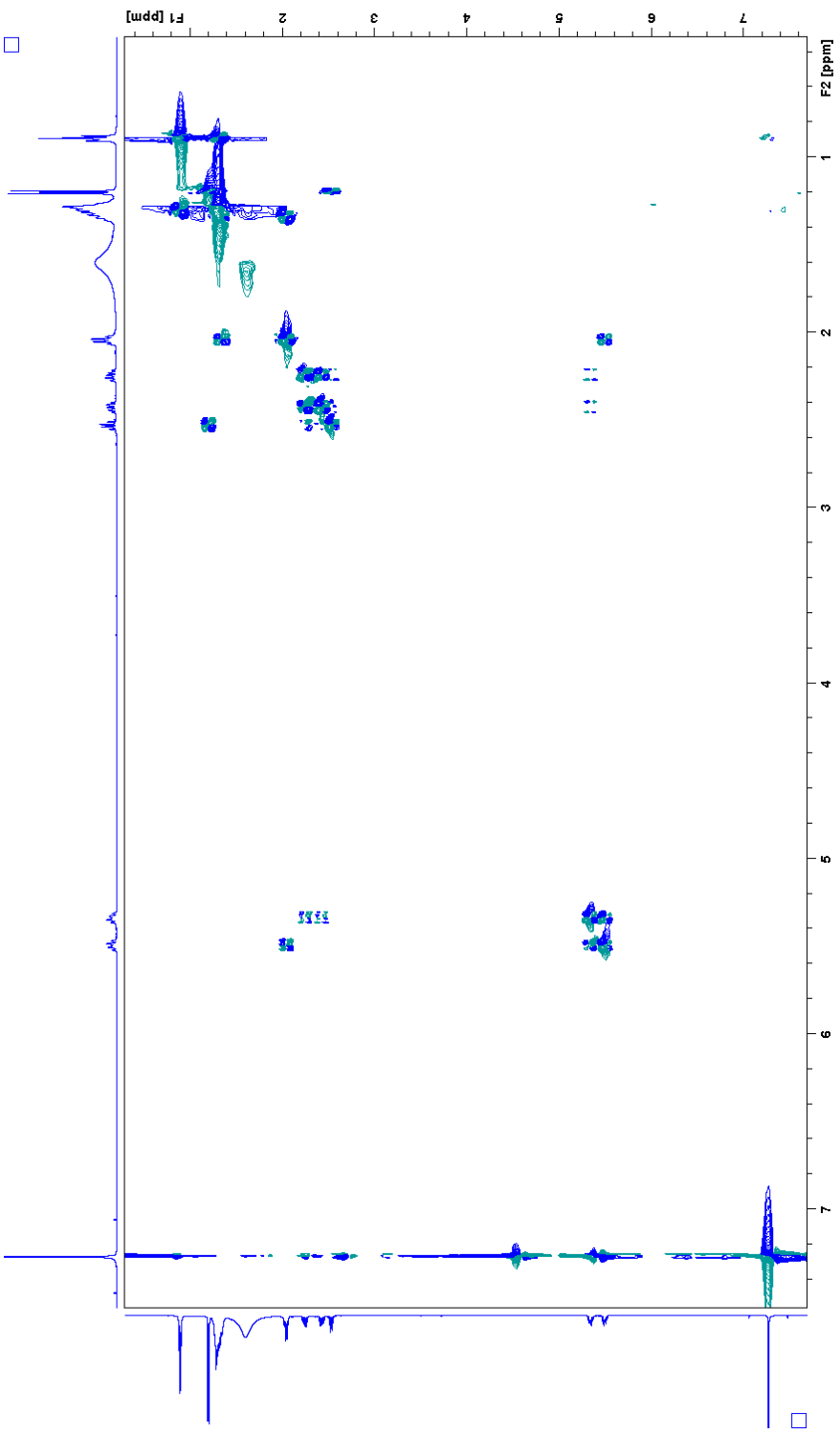

Figure S81. COSY spectrum of **13** in chloroform-*d*.

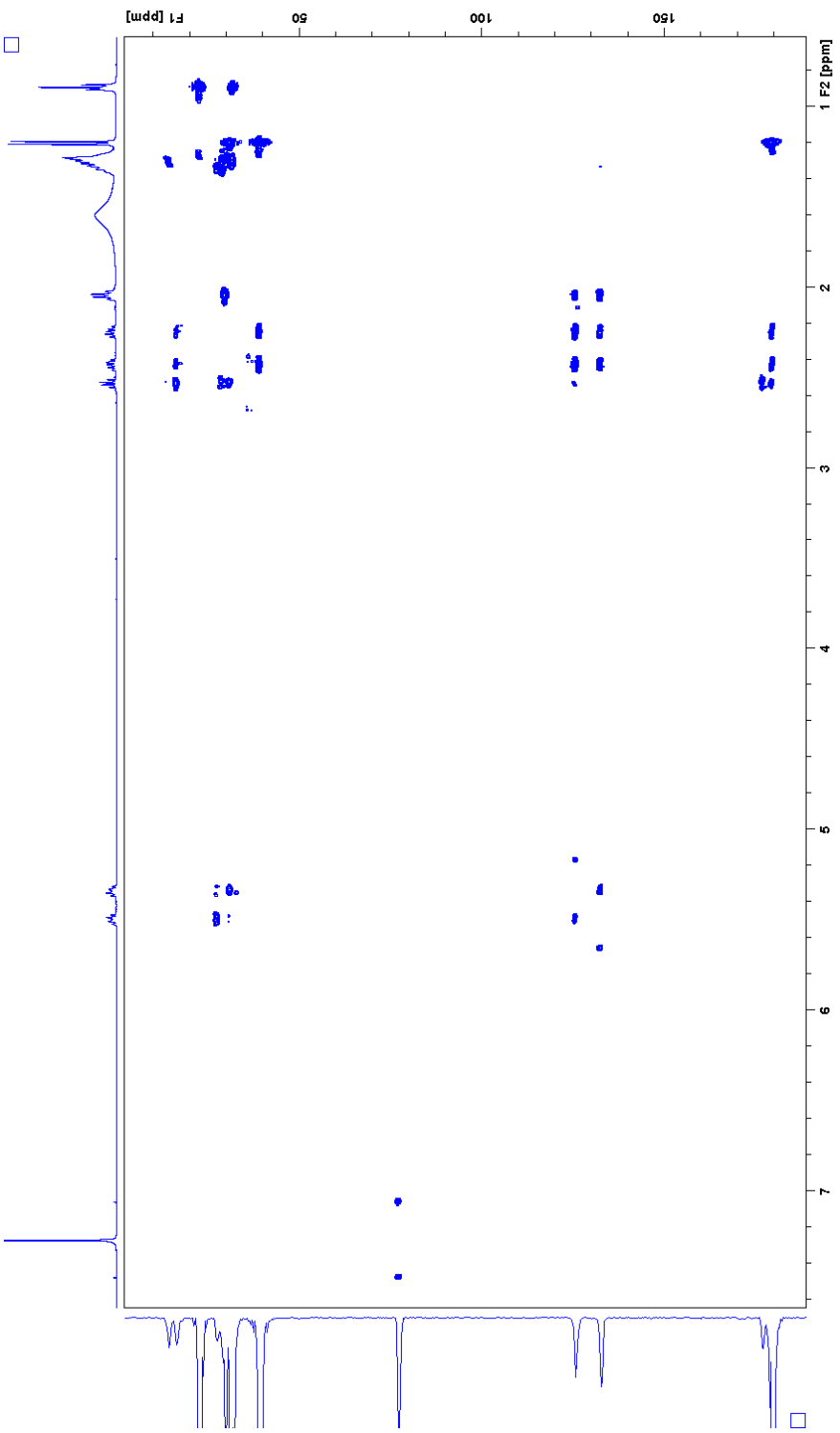

Figure S82. HMBC spectrum of **13** in chloroform-*d*.

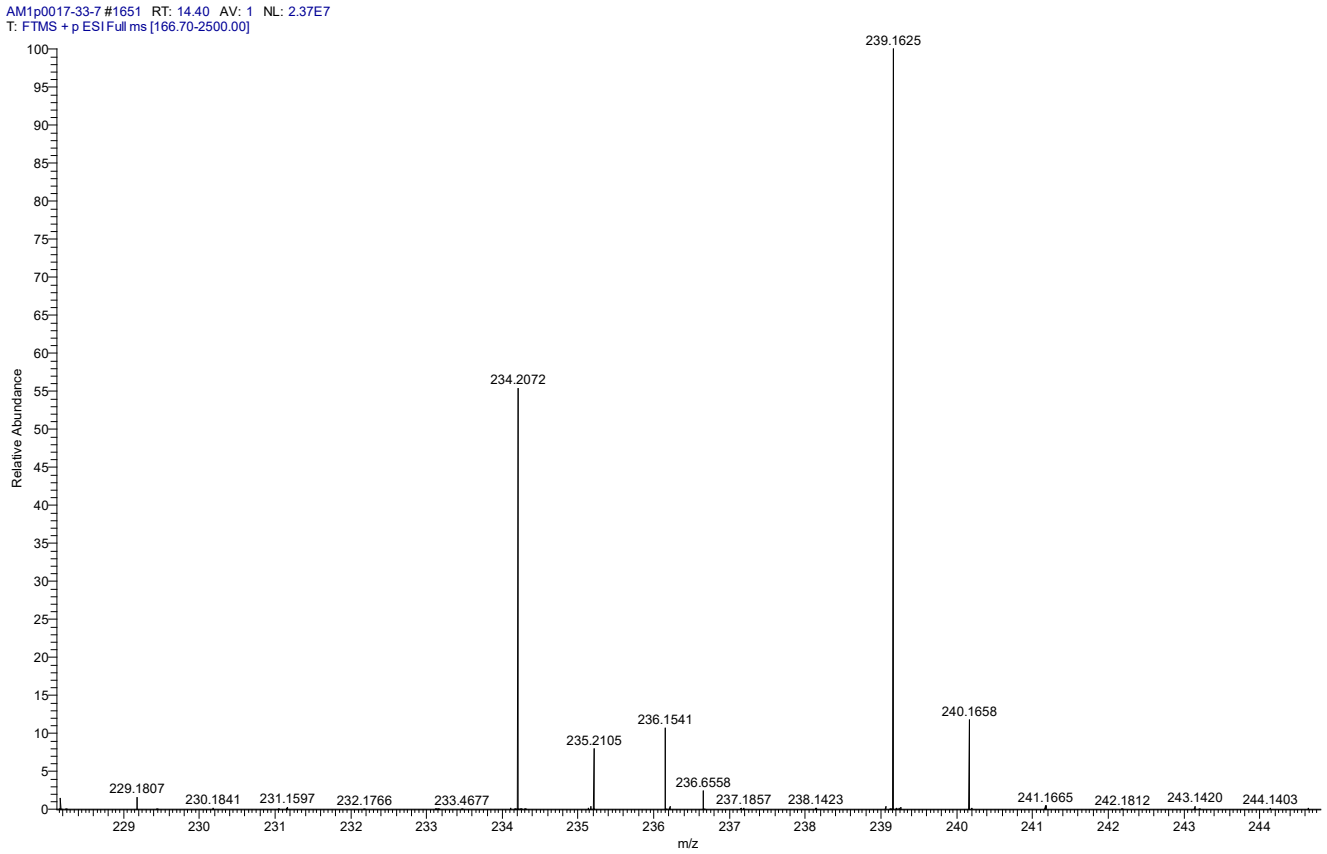

Figure S83: HR-LC-ESIMS data of **14**. Mass spectrum of the peak at 14.40 min (*m/z* 234.2072 $[M+NH_4]^+$ and *m/z* 239.1625 $[M+Na]^+$).

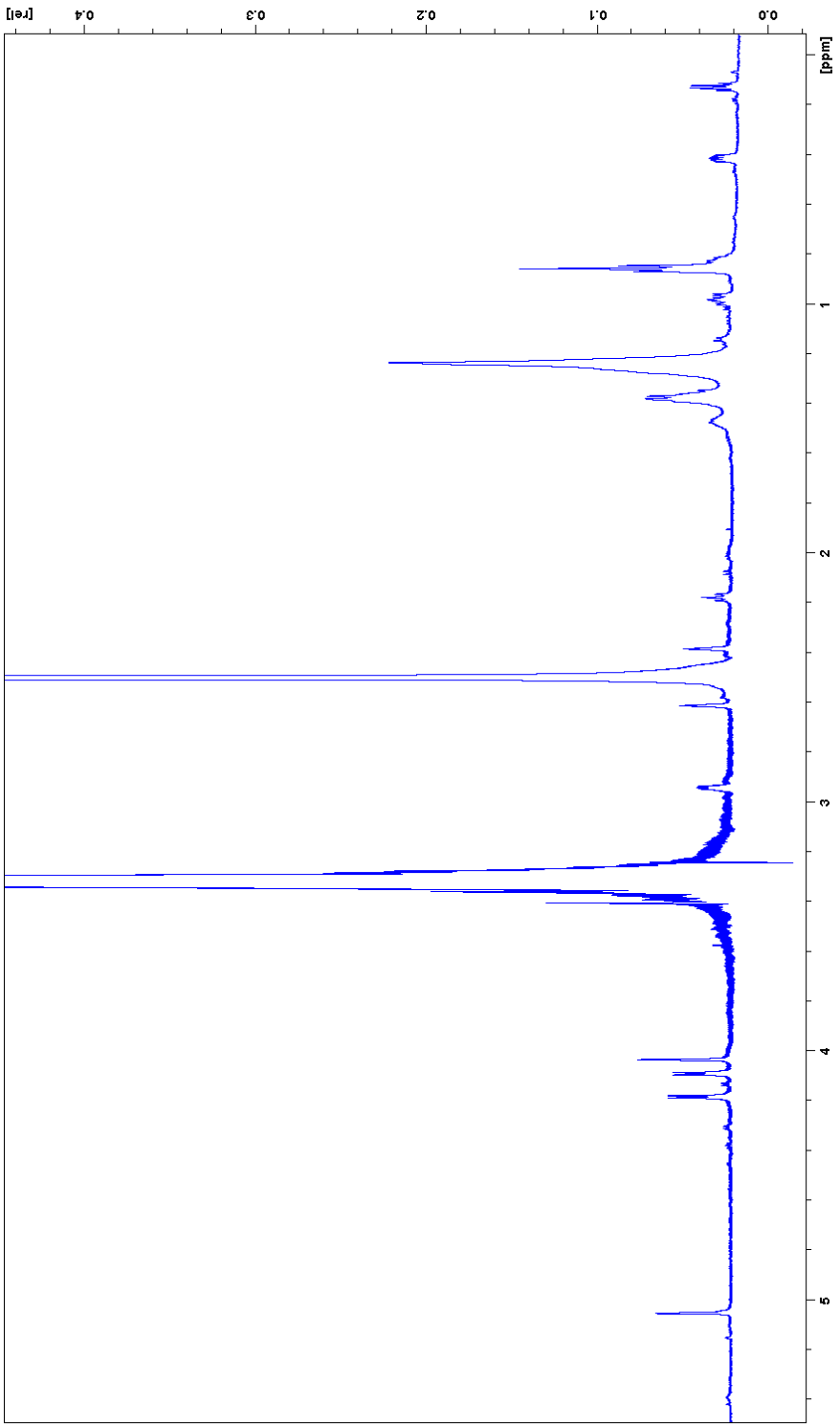

Figure S84. ^{1}H NMR spectrum of **14** in DMSO-d_6.

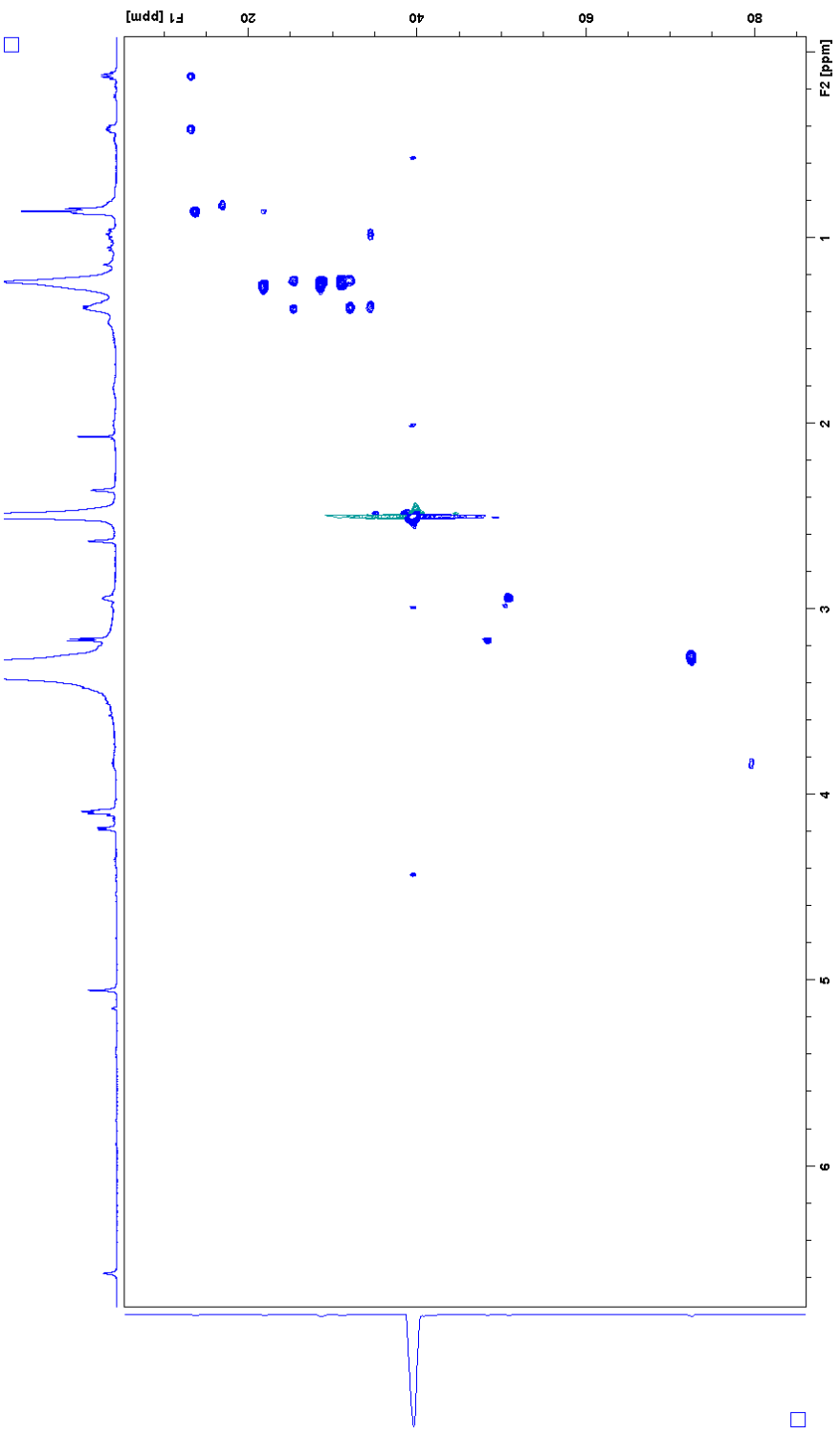

Figure S85. HSQC spectrum of **14** in DMSO-d_6.

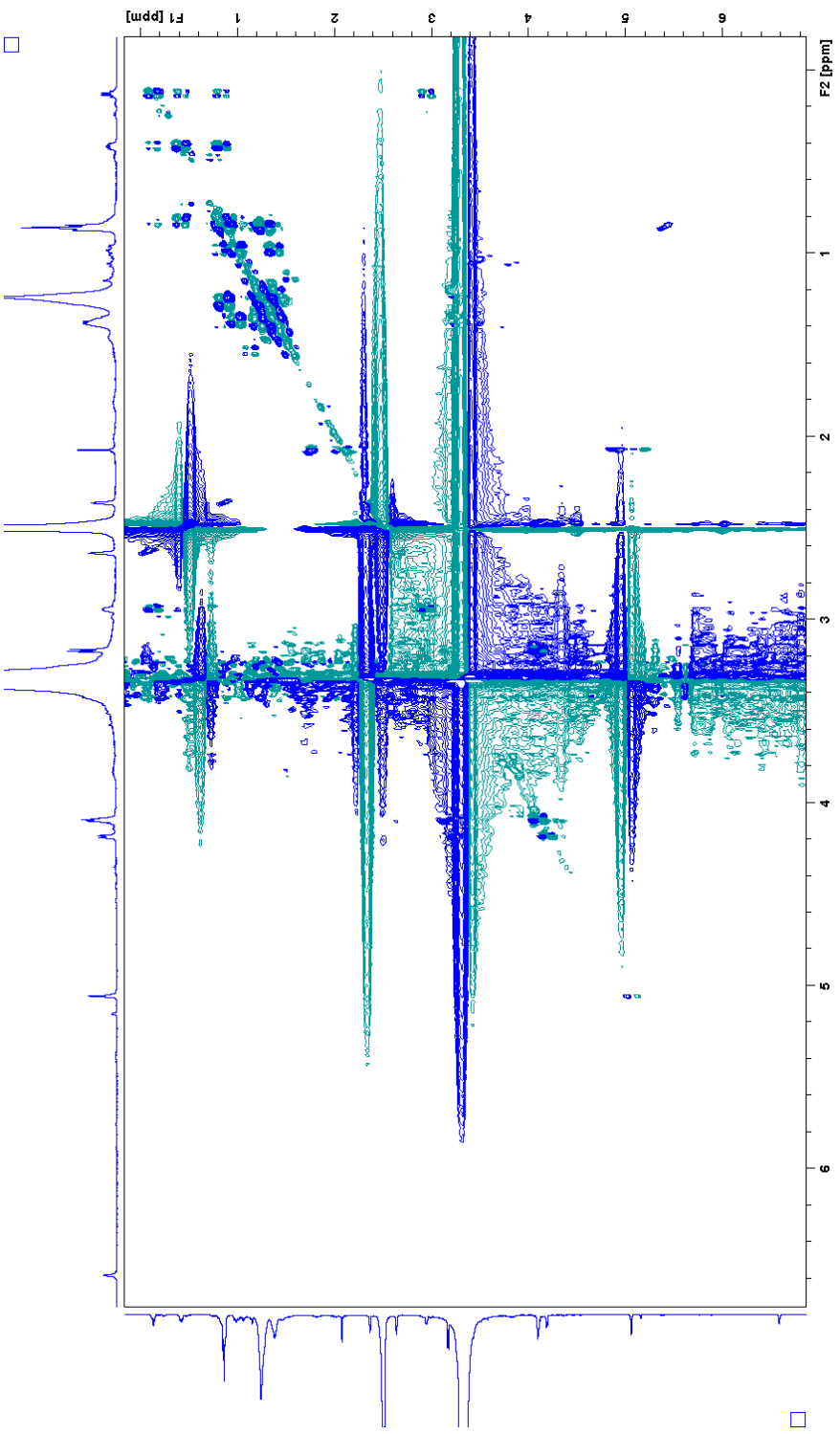

Figure S86. COSY spectrum of **14** in DMSO-d_6.

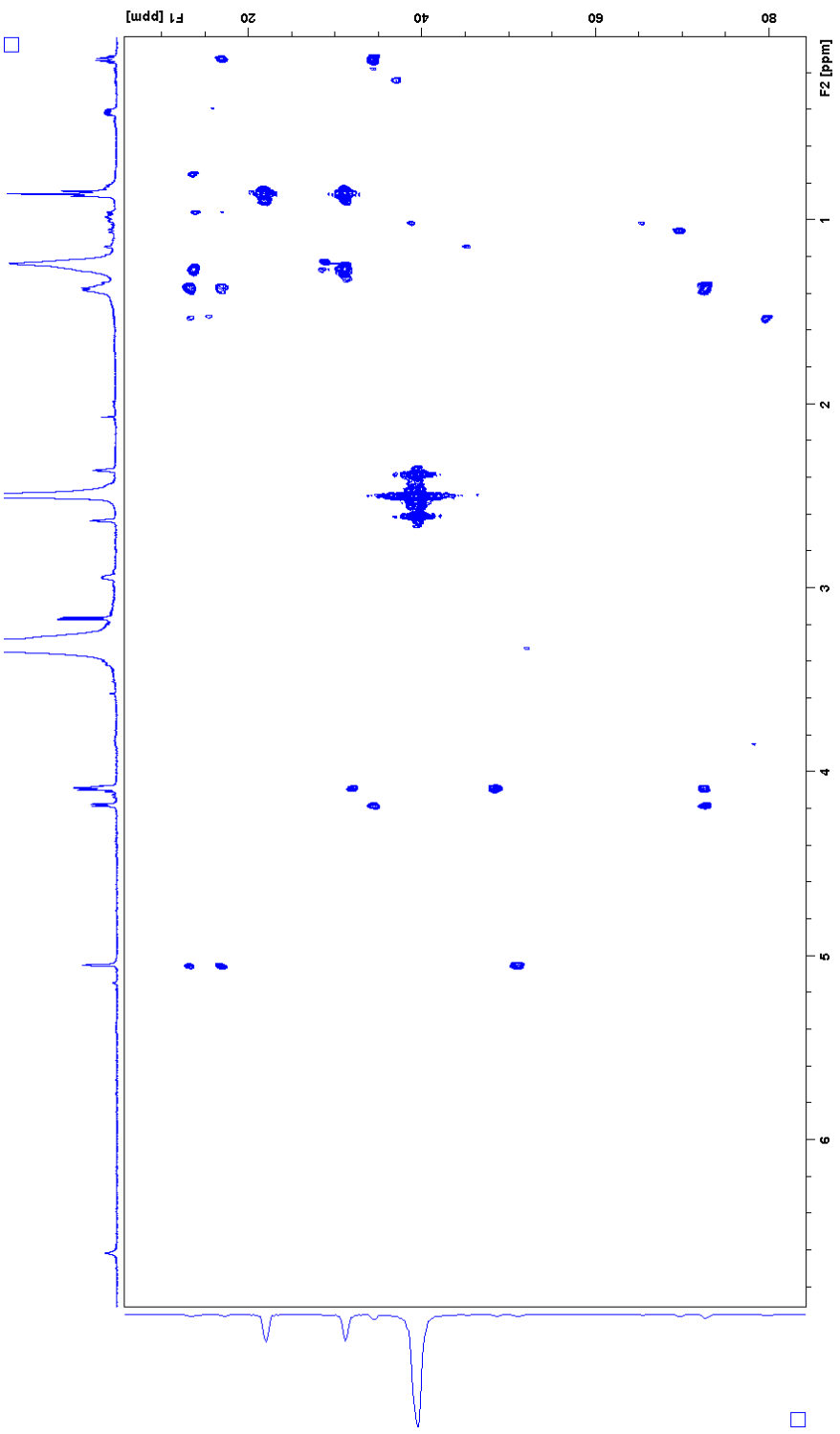

Figure S87. HMBC spectrum of **14** in DMSO-d_6.

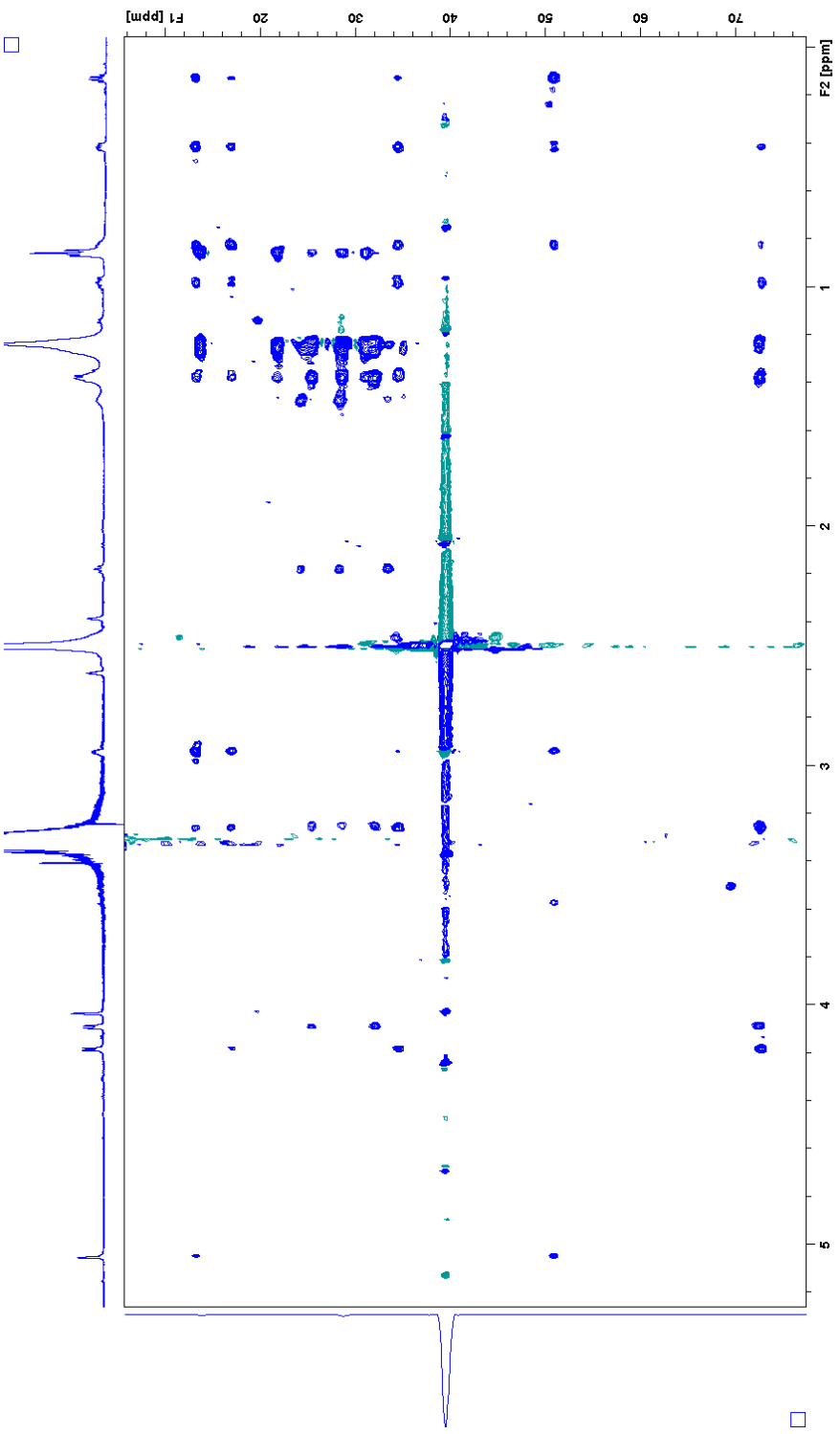

Figure S88. HSQC-TOCSY spectrum of **14** in DMSO-d_6.

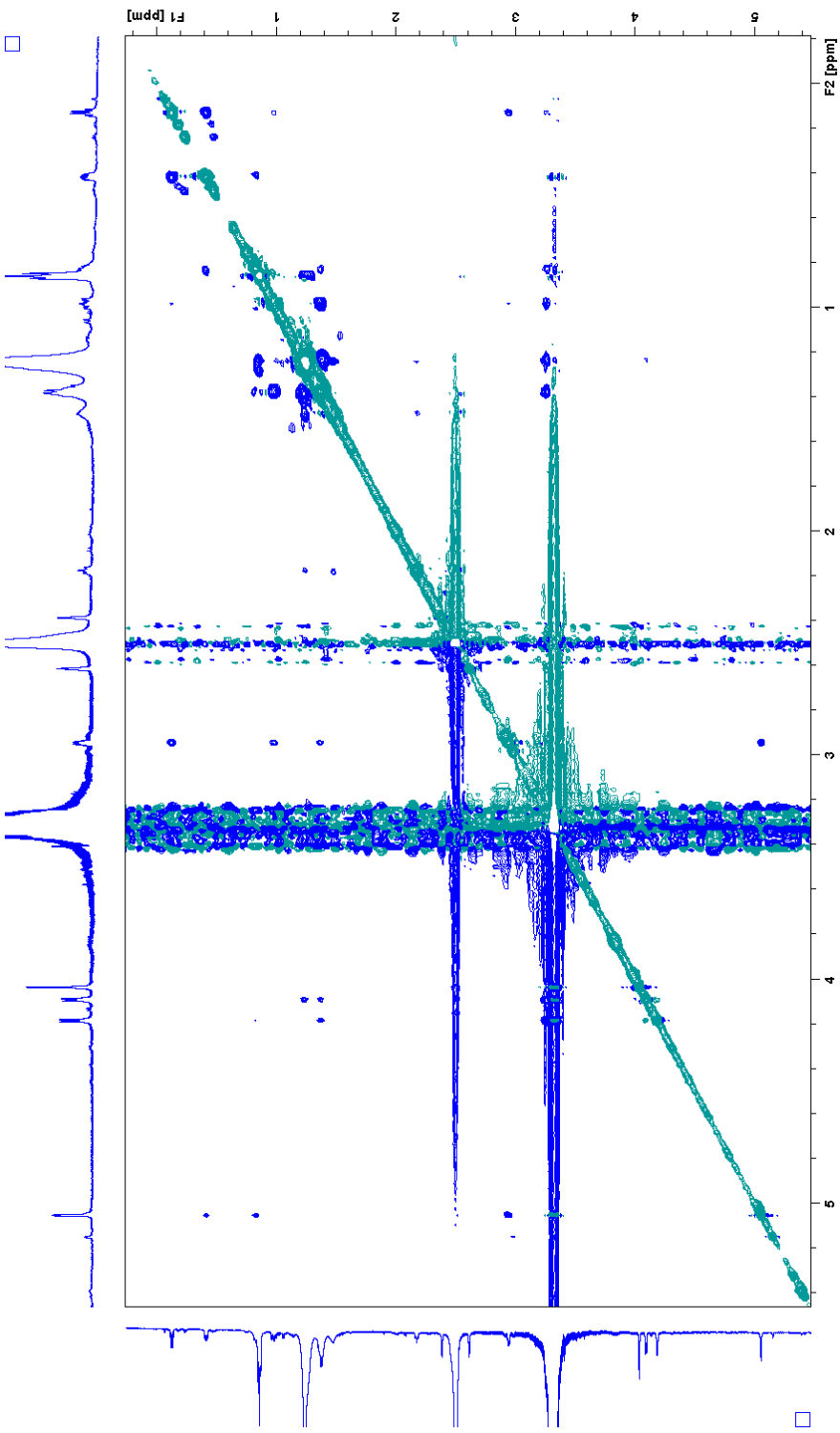

Figure S89. NOESY spectrum of **14** in DMSO-d_6.

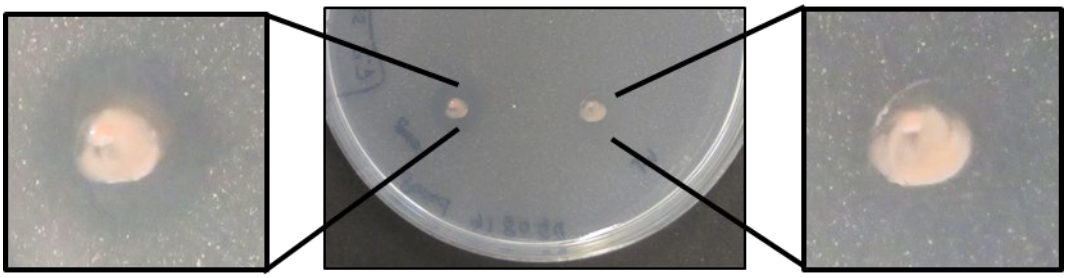

Figure S90. Complementation assay with extracts from WT strain (right) and Δ*tobC* strain (left).

Table S1. ORFs detected on the *Methylobacteria extorquens* AM1 *tob* locus and their putative functions.

ORF (GenBank accession number)	Protein size [aa]	Proposed protein function	Closest protein homologue [source organism]	Identity [%]	GenBank accession number
p0004 (WP_012753524.1)	135	Hypothetical protein	hypothetical protein MetexDRAFT_1542 [*Methylobacterium extorquens* DSM 13060]	100	EHP93549.1
p0005 (WP_003598531.1)	329	Arabinose-binding domain and DNA-binding transcriptional activator containing hypothetical protein	AraC family transcriptional regulator [*Methylobacterium populi*]	99	WP_082911923.1
p0006 (WP_012753525.1)	192	DUF3280 containing hypothetical protein	hypothetical protein MetexDRAFT_1544 [*Methylobacterium extorquens* DSM 13060]	100	EHP93551.1
tobA (WP_003598533.1)	107	HTH-XRE containing hypothetical protein; transcriptional regulator	hypothetical protein AX289_28195 [*Methylobacterium populi*]	96	OAH40909.1
tobB (WP_003598534.1)	246	SDR	short-chain dehydrogenase [*Synechococcus sp.* PCC 7502]	45	WP_015169838.1
tobC (WP_003598535.1)	2281	ACP-KS-DH-ACP-KS	beta-ketoacyl synthase [*Pseudomonas sp.* 1239]	44	WP_088515203.1
tobD (WP_003598536.1)	430	FAD binding monooxygenase	monooxygenase [*Pseudomonas japonica*]	58	WP_042129471.1
tobE (WP_003598537.1)	1647	ACP-HY-PX-FAD	hypothetical protein [*Methyloversatilis discipulorum*]	46	WP_019918767.1

tobF (WP_012753526.1)	993	KS	polyketide synthase [*Pseudomonas japonica*]	50	WP_042129466.1
tobG (ACS42953.1)	656	AT-ER	hypothetical protein AX289_23200 [*Methylobacterium populi*]	99	OAH29620.1
tobH (WP_003598542.1)	87	ACP	phosphopantetheine-binding protein [*Methylobacterium populi*]	99	WP_063987476.1
tobI (WP_003598544.1)	597	AL	fatty acid-CoA ligase [*Methylobacterium populi*]	99	WP_063987475.1
tobJ (WP_003598546.1)	266	TE	thioesterase [*Methylobacterium populi*]	99	WP_063987474.1
tobK (WP_003598549.1)	234	DUF3047 containing hypothetical protein	DUF3047 domain-containing protein [*Nevskia soli*]	52	WP_084182804.1
tobL (WP_003598550.1)	607	P450	cytochrome P450 [*Methylobacterium populi*]	99	WP_063987473.1
ORF1 (ACS42959.1)	1019	Ribonucleotide reductase	ribonucleoside-diphosphate reductase, adenosylcobalamin-dependent [*Methylobacterium extorquens*]	99	WP_082222837.1

Table S2. Distribution of *tob*-like genes in other bacteria.

Strain	*tobA*	*tobB*	*tobC*	*tobD*	*tobE*	*tobF*
Derxia gummosa			X	X	X[a]	X[b]
Derxia lacustris				X		
Methyloligella halotolerans		X[d]	X[e]	X	X[e]	X[e]
Methyloversatilis discipulorum RZ94			X	X	X	X
Methyloversatilis discipulorum FAM1			X	X	X	X
Methyloversatilis universalis EHg5			X	X	X	X
Methyloversatilis universalis Fam500			X	X	X	X
Pseudomonas putida UASWS0946			X	X	X	X
Pseudomonas putida ABAC8			X	X	X[g]	X
Pseudomonas sp. MF6396			X	X	X	X
Pseudomonas sp. NBRC 111117			X	X	X	X
Pseudomonas japonica	Δ[h]		X	X	X[g]	X[e]

Strain	*tobG*	*tobH*	*tobI*	*tobJ*	*tobK*	*tobL*
Derxia gummosa	X	X	Δ[c]	X		
Derxia lacustris						
Methyloligella halotolerans	X	X	X	X		
Methyloversatilis discipulorum RZ94	X	X	X	X	Δ[f]	Δ[f]
Methyloversatilis discipulorum FAM1	X	X	X	X	Δ[f]	Δ[f]
Methyloversatilis universalis EHg5	X	X	X	X	Δ[f]	
Methyloversatilis universalis Fam500	X	X	X	X	Δ[f]	
Pseudomonas putida UASWS0946	X	X	X	X		
Pseudomonas putida ABAC8	X	X	X	X		
Pseudomonas sp. MF6396	X	X	X	X		
Pseudomonas sp. NBRC 111117	X	X	X	X		
Pseudomonas japonica	X	X	X	X		

X, gene for homologus protein present; Δ, gene replaced by other gene; [a]ACP + low-homology region; [b]KS-ACP-?-KR; [c]transporter; [d]other position; [e]pseudogene; [f]additional hypothetical gene; [g]split gene; [h]chemotaxis protein

Table S3. DNA primers used in this study.

Primer Name	DNA Sequence: 5' to 3'
p0004- XbaI UP Fwd	TATATCTAGAGCACTCCGTCTGGTTCCTTC
p0004- UP Rev	TGACGAGTACCCTTGCCATGGTCAGCGGC
p0004- DO Fwd	CATGGCAAGG GTACTCGTCAGTCCCTGACGC
p0004- EcoRI DO Rev	TATAGAATTCTTCCTCGGTCTGGACCGTGG
topA- XbaI UP Fwd	TATATCTAGACTGCAGGCCCGTCCAAGTCG
topA- UP Rev	CCTTCGCTTCATTCCGCATGCATTCCTCCC
topA- DO Fwd	CATGCGGAATGAAGCGAAGGGGCCTTGATAAGAC
topA- HindIII DO Rev	TATAAAGCTTGAACCGGACTGCATCCCGTC
topB- XbaI UP Fwd	TATATCTAGAATGTACCTATTTGGCATGTG
topB- UP Rev	CAAACTGGCGAATCTCCATGTGCGACCTGATC
topB- DO Fwd	CATGGAGATT CGCCAGTTTGCGTCATTATAC
topB- HindIII DO Rev	TATAAAGCTTCTGGATCGATTCCCTCGGCG
topC- XbaI UP Fwd	TATATCTAGACTCCTCCAGCGTTTCCTCAG
topC- UP Rev	CATGGCAAGCAGCATCCGCATTGGCAGCATGTC
topC- DO Fwd	AATGCGGATGCTGCTTGCCATGCGCTGAGG
topC- HindIII DO Rev	ATATAAGCTTGACCACTAGAACCCGCTTGC
topD- XbaI UP Fwd	TATATCTAGATCACCGCCTCGCGATCATAG
topD- UP Rev	GGAGCTTCGCCTGCCTCATCTCAGATCCACTTC
topD- DO Fwd	GATGAGGCAG GCGAAGCTCCGGCAATGATC
topD- HindIII DO Rev	TATAAAGCTTGCGAAGGGCGAACGTGTTTC
tobE S324A XbaI UP Fwd	TATATCTAGATCCTCGATTGAGGCACTCTG
tobE S324A UP Rev	CCCGAAAGCGTAGCCGAGG
tobE S324A DO Fwd	TCCTCGGCTACGCTTTCGGG
tobE S324A HindIII DO Rev	TATAAAGCTTAGCGGACGTATTCCGATAGG
tobE T999A XbaI UP Fwd	TATATCTAGAAGCGCGACTACAATGCGGAC
tobE T999A UP Rev	TCAAAGCAGCACCGAGGACC
tobE T999A DO Fwd	GTCCTCGGTGCTGCTTTGAC
tobE T999A HindIII DO Rev	TATAAAGCTTCAATAGGTCGCGCAGTCGCG
tobE G1232V XbaI UP Fwd	TATATCTAGACGCGCACGAACGGAATCTAC
tobE G1232V UP Rev	CCATCGAGATGACGGCGACG
tobE G1232V DO Fwd	CGTCGCCGTCATCTCGATGG
tobE G1232V HindIII DO Rev	TATAAAGCTTATCTGAGAGCCGCTGTTGCC

topK- XbaI UP Fwd	TATATCTAGACCATGAGCAGGGACGGTACG
topK- UP Rev	CGACCTCGACCATCGGCATGGGCGGGACATC
topK- DO Fwd	CATGCCGATGGTCGAGGTCGGGCCCTAGC
topK- HindIII DO Rev	TATAAAGCTTCTATCGGCCAGGGCGCGTAC
topL- XbaI UP Fwd	TATATCTAGAAATTCGAG
topL- UP Rev	CCAAACGCACAATGAACATTGCTCTCTCCTATTCG
topL- DO Fwd	AATGTTCATT GTGCGTTTGGGAGCGTGATCC
topL- HindIII DO Rev	TATAAAGCTTGACAGGCGCTTCTTGCCAGC

Table S4. NMR data for toblerols A and B (**1** and **2**).

	toblerol A (**1**)		toblerol B (**2**)	
	δ_H, mult.	δ_C	δ_H, mult.	δ_C
1	0.87 (t, 6.7)	13.7	0.86 (t, 6.9)	13.6
2	1.30 m	17.9	1.30 m	17.9
	1.39 m		1.37 m	
3	1.40 m	35.7	1.39 m	35.6
4	3.27 m	69.2	3.25 br	69.1
5	2.91 (dd, 2.2, 5.7)	58.7	2.91 (dd, 2.3, 5.8)	58.6
6	2.82 (dd, 2.2, 7.4)	52.6	2.85 (dd, 2.3, 7.2)	52.5
7	2.66 (dd, 4.4, 7.4)	55.5	2.69 (dd, 4.4, 7.2)	55.4
8	3.05 m	55.0	3.13 (ddd, 4.4, 6.0, 6.9)	54.6
9a	1.46 m	29.7	1.61 m	28.8
9b				
10	0.83 m	16.5	1.16 m	15.1
11a	0.33 (ddd, 5.2, 5.8, 5.8)	13.0	0.74 (ddd, 6.5, 6.5, 6.5)	10.9
11b	0.55 (ddd, 3.1, 5.2, 9.6)		0.92 (ddd, 3.2, 6.5, 10.2)	
12	3.03 m	49.9	3.97 (ddd, 2.8, 3.2, 6.5)	52.4
13				
4-OH	4.85 (d, 5.7)		4.87 brd	
5-OH				
6-OH				
7-OH				
8-OH				
12-OH	5.21 (d, 1.8)			
formate			8.22 s	162.5

Table S5. NMR data for toblerols C and D (**3** and **4**).

	toblerol C (**3**)		toblerol D (**4**)	
	δ_H, mult.	δ_C	δ_H, mult.	δ_C
1	0.85 (t, 6.9)	13.5	0.86 (t, 7.1)	14.0
2	1.26 m	21.7	1.31 m	18.1
			1.40 m	
3	1.26 m	30.6	1.39 m	35.9
4	1.26 m	28.1	3.21 (ddt, 5.7, 6.0, 6.0)	69.9
5	1.30 m	28.8	2.86 (dd, 2.4, 6.0)	59.1
6	1.98 (dt, 6.5, 6.5)	26.3	2.90 (dd, 2.4, 6.0)	56.4
7	5.39 (ddd, 6.0, 6.5, 11.4)	130.3	3.27 (ddd, 4.5, 6.0, 6.2)	71.5
8	5.36 (ddd, 6.0, 6.4, 11.4)	127.0	4.37 (ddd, 4.5, 6.1, 10.3)	78.9
9a	2.01 m	29.0	1.75 (ddd, 10.3, 11.8, 12.0)	31.5
9b	2.05 m		2.31 (ddd, 6.1, 9.0, 12.0)	
10	1.22 m	21.5	2.76 m	34.4
11a	0.73 (ddd, 3.8, 6.3, 8.2)	13.8	1.12 (d, 7.2)	14.9
11b	0.94 br			
12	1.31 m	18.7		179.2
13		174.8		
4-OH			4.81 (d, 5.7)	
5-OH				
6-OH				
7-OH			5.46 (d, 6.2)	
8-OH				
12-OH				
formate				

Table S6. NMR data for toblerols E and F (**5** and **6**).

	toblerol E (**5**)		toblerol F (**6**)	
	δ_H, mult.	δ_C	δ_H, mult.	δ_C
1	0.88 (t, 7.3)	13.7	0.85 (t, 7.3)	13.7
2	1.29 m	18.4	1.26 m	18.4
	1.51 m		1.43 m	
3	1.41 m	32.3	1.18 m	33.7
			1.35 m	
4	3.98 m	68.5	3.32 m	72.4
5	4.17 (dd, 3.2, 9.7)	66.8	3.86 (dd, 5.2, 10.8)	73.2
6	3.47 (ddd, 1.4, 8.5, 9.7)	70.7	5.86 (dd, 5.2, 15.8)	134.9
7	3.69 (ddd, 1.4, 6.8, 7.8)	72.2	5.68 (dd, 7.4, 15.8)	127.6
8	4.38 (ddd, 5.5, 7.8, 10.7)	80.1	4.84 m	77.8
9a	1.47 m	32.3	1.58 (ddd, 10.4, 12.1, 12.1)	36.8
9b	2.39 (ddd, 5.5, 8.5, 12.2)		2.47 m	
10	2.77 m	34.7	2.77 m	34.7
11a	1.11 (d, 7.0)	14.4	1.12 (d, 7.1)	14.4
11b				
12		178.9		178.9
13				
4-OH	4.79 (d, 6.0)		4.45 (d, 5.4)	
5-OH			4.82 (d, 5.0)	
6-OH	5.12 (d, 8.5)			
7-OH	5.36 (d, 6.8)			
8-OH				
12-OH				
formate				

Table S7. NMR data for toblerols G and H (**7** and **8**).

	toblerol G (**7**)		toblerol H (**8**)	
	δ_H, mult.	δ_C	δ_H, mult.	δ_C
1	0.88 (t, 7.1)	13.8	0.88 (t, 7.1)	13.8
2	1.30 m	18.0	1.30 m	18.7
	1.36 m		1.36 m	
3	1.38 m	35.6	1.36 m	36.9
	1.46 m		1.50 m	
4	3.72 m	68.8	3.92 m	76.9
5	3.58 (ddd, 1.7, 7.8, 9.2)	73.4	1.47 m	41.4
			1.71 m	
6	4.10 (dd, 5.1, 7.8)	62.3	4.05 br	71.8
7	3.87 (ddd, 5.1, 5.2, 5.4)	72.9	3.53 (dd, 3.3, 3.3)	88.2
8	4.70 (ddd, 5.2, 5.2, 10.0)	78.6	3.46 m	70.1
9a	1.74 m	31.6	1.18 m	35.6
9b	2.38 (ddd, 6.0, 8.8, 12.1)		1.25 m	
10	2.75 m	34.4	0.81 m	16.6
11a	1.12 (d, 7.2)	14.5	0.20 (ddd, 5.1, 5.7, 5.7)	13.5
11b			0.46 (ddd, 2.9, 5.1, 9.7)	
12		178.9	2.92 (dddd, 2.6, 2.9, 2.9, 5.7)	50.6
13				
4-OH	4.52 (d, 7.2)			
5-OH	5.07 (d, 9.2)			
6-OH			4.75 (d, 4.4)	
7-OH	5.79 (d, 5.4)			
8-OH			4.14 (d, 6.3)	
12-OH			5.06 (d, 2.9)	
formate				

Table S8. NMR data for **13** and **14**.

	toblerol I (**13**)		toblerol J (**14**)	
	δ_H, mult.	δ_C	δ_H, mult.	δ_C
1	0.89 (t, 6.9)	14.1	0.86 (t, 6.9)	13.7
2	1.30 m	22.6	1.26 m	21.8
3	1.27 m	31.7	1.24 m	31.1
4	1.29 m	29.1	1.24 m	28.7
5	1.33 m	29.7	1.23 m	25.5
			1.38 m	
6	2.04 (dt, 6.9, 7.8)	27.3	3.25 m	72.4
7	5.49 (dddt, 1.4, 7.3, 7.8, 11.0)	132.6	1.23 m	32.1
			1.38 m	
8	5.34 (dddt, 1.4, 7.3, 8.2, 11.0)	125.7	3.26 m	72.5
9a	2.24 (ddd, 7.3, 7.7, 14.3)	31.0	0.98 m	34.5
9b	2.43 (ddd, 6.9, 7.3, 14.3)		1.37 m	
10	2.53 (qdd, 7.0, 7.0, 7.0)	39.1	0.83 m	17.0
11a	1.20 (d, 7.1)	16.4	0.13 (ddd, 5.2, 5.7, 6.2)	13.2
11b			0.41 (ddd, 2.6, 5.2, 9.5)	
12		179.7	2.94 m	50.9
13				
4-OH				
5-OH				
6-OH			4.09 (d, 5.5)	
7-OH				
8-OH			4.18 (d, 5.6)	
12-OH			5.05 (d, 1.7)	

References

[1] R. Peyraud, P. Kiefer, P. Christen, S. Massou, J. C. Portais, J. A. Vorholt, *Proc. Natl. Acad. Sci.* **2009**, *106*, 4846-4851.

[2] A. Schäfer, A. Tauch, W. Jager, J. Kalinowski, G. Thierbach, A. Pühler, *Gene* **1994**, *145*, 69–73.

[3] J. Sambrook, D. Russell, Molecular Cloning: A Laboratory Manual (Third Edition): Cold Spring Harbor Laboratory Press; 2001.

[4] S. Vuilleumier, L. Chistoserdova, M. C. Lee, F. Bringel, A. Lajus, Y. Zhou, B. Gourion, V. Barbe, J. Chang, S. Cruveiller, C. Dossat, W. Gillett, C. Gruffaz, E. Haugen, E. Hourcade, R. Levy, S. Mangenot, E. Muller, T. Nadalig, M. Pagni, C. Penny, R. Peyraud, D. G. Robinson, D. Roche, Z. Rouy, C. Saenampechek, G. Salvignol, D. Vallent, Z. Wu, C. J. Marx, J. A. Vorholt, M. V. Olson, R. Kaul, J. Weissenbach, C. Medigue, M. E. Lidstrom, *PLoS ONE* **2009**, *4*, E5584.

[5] Y. Bai, D. B. Müller, G. Srinivas, R. Garrido-Oter, E. Potthoff, M. Rott, N. Dombrowski, P. C. Münch, S. Spaepen, M. Remus-Emsermann, B. Hüttel, A. C. McHardy, J. A. Vorholt, P. Schulze-Lefert, *Nature* **2015**, *528*, 364–369.

[6] J. Schmidt, B. Eschgfaeller, S. A. Benner, *Helv. Chim. Acta* **2003**, *86*, 2937 – 2958.

[7] K. Shirakawa, A. Arase, M. Hoshi, *Synthesis* **2004**, 1814 – 1820.

[8] Z. Yang, J. C. Lorenz, and Y. Shi, *Tet. Lett.* **1998**, *39*, 8621 – 8624.

[9] J. Pietruszka, A. C. M. Rieche, T. Wilhelm, A. Witt, *Adv. Synth. Catal* **2003**, *345*, 1273 – 1286.

[10] T. Imai, H. Mineta, S. Nishida, *J. Org. Chem.* **1990**, *55*, 4988 – 4989.

[11] T. Eguchi, K. Arakawa, T. Terachi, K. Kakinuma, *J. Org. Chem.* **1997**, *62*, 1924 – 1923.

Author Contributions

All authors designed the research and wrote the manuscript; JP performed bioinformatic analyses; RU and BIM did structural elucidation; MBM generated all knock-out strains; MBM and RU did bioassays; BIM performed the synthesis.

[i] The alkenyl carbon bonded to the boron was not observed. For other examples see. K. Shirakawa, A. Arase, M. Hoshi Synthesis 1814-1820 (2004).